



NTNU – Trondheim
Norwegian University of
Science and Technology

Seismic Interpretation of the Messinian Salinity Crisis in the Levant Basin, Eastern Mediterranean Sea

Heidrun Breiset Solem

Petroleum Geoscience and Engineering

Submission date: June 2014

Supervisor: Ståle Emil Johansen, IPT

Co-supervisor: John Comstock, PGS

Norwegian University of Science and Technology

Department of Petroleum Engineering and Applied Geophysics

Abstract

Kilometer-thick sequences of evaporites were deposited in the Mediterranean Sea during the Late Miocene ($\sim 5.96 - 5.33Ma$). The event is known as the Messinian Salinity Crisis and was a result of progressive restriction of the marine gateways between the Mediterranean Sea and the Atlantic Ocean. The event lasted for approximately 600,000 years until normal marine conditions were re-established.

Three-dimensional, depth converted seismic data from the northeastern Levant Basin (offshore Lebanon, eastern Mediterranean Sea) has been interpreted. A regional interpretation study was conducted, which shows that the Levant Basin is a rift-basin with a passive margin to the east. The first part of the deep basin is filled with sediments of Late Cretaceous to Late Miocene age that have been accumulated by massive subsidence of the basin. The second part of the sedimentary infill consists of sediments from Late Miocene-present time. This is marked by the deposition of a thick sequence of Messinian evaporites, underlying deep-marine sediments of Pliocene-Pleistocene age. Interpretation of the seismic data has revealed the occurrence of a well-imaged, relatively high-amplitude sedimentary layer deposited between the Messinian evaporites and the deep-marine deposits. The unknown layer, referred to as the Transition layer, has different characteristics than the evaporites deposited below and the deep-marine sediments deposited above. A detailed seismic interpretation study of the Messinian and younger sediments has been conducted in order to investigate evidence for the origin of the Transition layer.

The results show that the thick sequence of evaporites in the northern Levant Basin is bounded by two erosional surfaces. The base erosion surface marks an important sea-level fall at the beginning of the Messinian Salinity Crisis. The top is an erosional surface of subaerial origin that marks a period of desiccation at the end of the salinity crisis. Two major phases of deformation related to salt tectonics can be observed in the seismic data. The first phase took place in the Late Messinian between deposition of the evaporites and the erosion event that marks the top of the evaporites. The second phase has affected the entire Pliocene-Pleistocene succession, including the top of the evaporites and the

seabed. This phase is linked to gravity-driven, thin-skinned deformation. The seismic characteristics of the Transition layer and the analogy with other coeval deposits in the Mediterranean area favor two possible deposition scenarios for the Transition layer. The layer could have been deposited subaerially by fluvial channels, in similar settings as what can be observed in the Death Valley, USA, today. The other scenario suggests that the sedimentary layer can be fresh to brackish water deposits, known as the "Lago Mare", which can be observed other places in the eastern Mediterranean. Due to the lack of well data from the northeastern Levant Basin, an exact conclusion for the origin of the layer cannot be drawn.

The Levant Basin is an under-explored area, and the evaporite deposition in the eastern Mediterranean is different from that of the more explored western Mediterranean. With available well data, a correlation between the different parts of the Mediterranean Sea would be possible to make. The origin and depositional history of the Transition layer could then be determined with more accuracy. Having correct knowledge about the geological history of the Levant Basin is very important for the understanding of the petroleum systems in the area.

Sammendrag

Flere kilometer tykke evaporittsekvenser ble avsatt i Middelhavet i sen miocen tid ($\sim 5.96 - 5.33Ma$). Denne hendelsen er kjent som den Messinianske salinitetskrisen og var et resultat av at åpningen mellom Middelhavet og Atlanterhavet ble gradvis stengt. Hendelsen varte i omtrent 600,000 år frem til normale marine forhold ble gjenopprettet.

Tre-dimensjonale, dybdekonverterte seismiske data fra den nordøstlige delen av Levantbassenget (offshore Libanon, østlige Middelhavet) har blitt tolket. Et regionalt tolkningsstudie ble utført, og viser at Levantbassenget er et rift-basseng med en passiv margin i øst. De første sedimentene som fyller bassenget er av sen kritt til sen miocen alder, og har blitt akkumulert ved nedsynking av bassenget. Den andre delen av sedimentinnfyllingen består av sedimenter fra sen miocen tid til nå. Dette er markert med en tykk sekvens av messinianske evaporitter, som er avsatt før et lag med dypmarine sedimenter fra pliocen-pleistocen tid. Tolkning av de seismiske dataene viser tydelig forekomsten av et lag med relativt høye amplituder som er avsatt mellom de messinianske evaporittene og de dypmarine avsetningene. Det ukjente laget, som her vil bli omtalt som overgangslaget, virker å være relativt tynt. Laget har helt andre kjennetegn og egenskaper enn evaporittene som er avsatt under og de dypmarine sedimentene som er avsatt over. Et detaljert seismisk tolkningsstudie av avsetningene fra sen miocen tid til nå har blitt utført for å undersøke opprinnelsen til dette overgangslaget. Oppgaven vil spesielt fokusere på avsetningene fra toppen av evaporittene til toppen av overgangslaget.

Resultatene viser at de tykke evaporittsekvensene som ble avsatt i den nordøstlige delen av Levantbassenget er avgrenset av to erosjonsflater. Bunnen av evaporittsekvensen markerer et viktig havnivåfall ved begynnelsen av saltkrisen, mens toppen av sekvensen har blitt erodert på land og viser til en periode med uttørking av området på slutten av saltkrisen. To viktige deformasjonsfaser relatert til salttektonikk kan observeres i de seismiske dataene. Den første fasen skjedde mellom etter avsetning av evaporittene på slutten av messiniansk tid, men før toppen av evaporittlaget ble erodert. Den andre fasen har påvirket alle avsetningene fra pliocen-pleistocen tid, i tillegg til overgangslaget, toppen

av evaporittene og havbunnen. Denne fasen er knyttet til gravitasjonsdrevet tynnskinnet deformasjon. Basert på de seismiske egenskapene til overgangslaget og sammenlikninger med andre avsetninger i Middelhavet, er det to avsetningsscenarier for overgangslaget som favoriseres. Laget kan ha blitt avsatt av fluviale kanaler, i samme type avsetningsmiljø som kan bli observert i Death Valley, USA, i dag. En annen tolkning er at laget kan være ferskvanns- til brakkvannsavsetninger, kjent som "Lago Mare", som er observert flere steder i det østlige Middelhavet. På grunn av mangel på brønndata fra det nordøstlige Levantbassenget er det ikke mulig å trekke en eksakt konklusjon for opprinnelsen av overgangslaget.

Levantbassenget er et lite utforsket område, og evaporittavsetningen i det østlige Middelhavet er forskjellig fra det mer utforsket vestlige Middelhavet. Med tilgang på brønndata vil det være mulig å gjøre en korrelasjon mellom de ulike delene av Middelhavet. Opprinnelsen og avsetningsmiljøet til overgangslaget kan da bestemmes med mer nøyaktighet. Riktig kunnskap om den geologiske historien til Levantbassenget er svært nødvendig for å kunne forstå petroleumssystemet i bassenget.

Preface

This thesis is carried out as a Master Thesis in Applied Petroleum Geophysics (TPG4930) at the Norwegian University of Science and Technology (NTNU) during spring 2014. The thesis is written at the Department of Petroleum Engineering and Applied Geophysics at NTNU, under supervision of Prof. Ståle Emil Johansen. The seismic data used in this thesis is provided by Petroleum Geo-Services (PGS), with approval from the Lebanon petroleum authority. John Comstock, former employee at PGS, has defined the topic for the master thesis. The thesis is written as the final part of my master degree in Petroleum Geosciences.

Trondheim, June 08th 2014

Heidrun Breiset Solem

Acknowledgment

First and foremost I give my acknowledgments to my supervisor at the Department of Petroleum Engineering and Applied Geophysics, Professor Ståle Emil Johansen. His guidance and advice has been very valuable for this thesis. He has expressed enthusiasm for the thesis and has been present when needed. Further, I would like to thank PGS for providing excellent seismic data to use in this thesis. I would also give a special thank to John Comstock, former employer at PGS, for defining the topic for my thesis and for his guidance during this semester.

I would like to thank my family for supporting me throughout all my years of education, which eventually leads to this degree.

An acknowledgement should also go to my study group at "geolabben", especially Dicky Harishidayat who has taken his time to discuss the geology and to help me with Petrel.

Finally, I would like to thank my fellow students for five great years at NTNU and wish you all good luck in the future.

Table of Contents

| | |
|-----------------------------------------------------------------|------------|
| Abstract | i |
| Sammendrag | iii |
| Preface | v |
| Acknowledgment | vii |
| List of Figures | xi |
| List of Tables | xv |
| 1 Introduction | 1 |
| 2 Previous work | 5 |
| 2.1 Consequences | 6 |
| 2.1.1 Termination of the MSC | 6 |
| 2.1.2 Impacts of the MSC | 7 |
| 2.2 Disagreements | 8 |
| 2.2.1 Depth of pre-Messinian basin | 8 |
| 2.2.2 Water depth during onset of MSC | 9 |
| 2.2.3 Timing of the MSC | 9 |
| 2.2.4 Cause of isolation | 10 |
| 2.2.5 Synchronous or Diachronous evaporite deposition | 10 |
| 3 Geological history | 13 |
| 3.1 Shaping the Levant Basin | 13 |
| 3.2 Filling the Levant Basin | 14 |
| 4 Evaporites and Salt Tectonics | 23 |

| | | |
|-----------|---------------------------------------------------------|------------|
| 5 | Data and Methodology | 27 |
| 6 | Regional Seismic Interpretation | 31 |
| 6.1 | Seismic Sections | 34 |
| 6.2 | Units | 39 |
| 6.3 | Interpretation | 50 |
| 7 | Detailed Seismic Interpretation | 55 |
| 7.1 | Evaporites | 55 |
| 7.1.1 | Deposition and deformation | 55 |
| 7.1.2 | Top Evaporite Unconformity | 57 |
| 7.2 | Transition layer | 60 |
| 7.2.1 | Characteristics and observations from seismic | 60 |
| 7.2.2 | Observations from attribute maps | 62 |
| 7.3 | Marine deposits | 70 |
| 7.4 | Scenarios | 73 |
| 8 | Discussion | 75 |
| 8.1 | Salt tectonics | 75 |
| 8.2 | Top salt unconformable surface | 78 |
| 8.3 | Deposition of Transition layer | 80 |
| 8.3.1 | Marine deposition | 80 |
| 8.3.2 | Yafo Sand Member | 82 |
| 8.3.3 | Upper Evaporite Unit | 85 |
| 8.3.4 | Brackish Lago Mare deposit | 85 |
| 8.3.5 | Fluvial deposit | 88 |
| 8.4 | Difficulties | 99 |
| 8.5 | Geological Reconstruction | 99 |
| 9 | Conclusion | 105 |
| 10 | Further Work | 107 |
| | References | 112 |
| | Appendix | 113 |

List of Figures

| | | |
|-----|----------------------------------------------------------------------------------------------|----|
| 1.1 | Map of the Mediterranean Sea | 3 |
| 1.2 | Map of the Levant Basin | 4 |
| 2.1 | Present water salinity at the surface of the ocean | 7 |
| 2.2 | Comparison of the timing of the events in the models proposed | 11 |
| 3.1 | Structural elements in the Eastern Mediterranean Sea | 15 |
| 3.2 | Palaeogeographical reconstruction of the western Mediterranean in the Late Miocene | 16 |
| 3.3 | Geological model proposed for the northern Levant area, part 1 | 17 |
| 3.4 | Geological model proposed for the northern Levant area, part 2 | 18 |
| 3.5 | Geological model proposed for the northern Levant area, part 3 | 19 |
| 3.6 | Geological model proposed for the northern Levant area, Legend | 20 |
| 3.7 | Chronostratigraphic chart of the northern Levant Basin | 21 |
| 4.1 | Evaporated water versus brine concentration and density | 25 |
| 5.1 | Seismic survey legend | 27 |
| 5.2 | Location of 3D seismic survey | 29 |
| 5.3 | Workflow | 30 |
| 6.1 | Map with location of seismic sections | 32 |
| 6.2 | Seismic section 1 | 35 |
| 6.3 | Seismic section 2 | 37 |
| 6.4 | Seismic section 3 | 38 |
| 6.5 | Thinning of SP 1.1 in seismic section 1 | 39 |
| 6.6 | Subsidence of SP 1.1 in section 3 | 40 |
| 6.7 | Close-up of SP 1.2 in section 3 | 41 |
| 6.8 | Faulting of SP 2.3 in section 2 | 43 |
| 6.9 | Close-up of Messinian evaporites (SP 3.1) in section 2 | 44 |

| | | |
|------|-----------------------------------------------------------------------------------------|----|
| 6.10 | Transition layer (SP 3.2) in section 3 | 45 |
| 6.11 | SP 3.3 in section 1 | 46 |
| 6.12 | SP 3.4 from Inline 21660 shows progradation of sediments | 46 |
| 6.13 | Stress domains in SP 3.4, section 3 | 48 |
| 6.14 | Map of structural domains | 49 |
| 6.15 | Interpretation of seismic section 1 | 51 |
| 6.16 | Interpretation of seismic section 2 | 52 |
| 6.17 | Interpretation of seismic section 3 | 53 |
| | | |
| 7.1 | Salt thickness map | 56 |
| 7.2 | Fault zone influences the thickness of the salt body | 57 |
| 7.3 | RMS amplitude map of upper part of the salt | 58 |
| 7.4 | RMS amplitude map of upper part of the salt | 59 |
| 7.5 | Thickness variations within the Transition layer | 61 |
| 7.6 | Transition layer with the same appearance as the upper part of the evaporites | 62 |
| 7.7 | Thickness map of Transition layer | 64 |
| 7.8 | Thickness map of Transition layer with opacity | 65 |
| 7.9 | RMS map of Transition layer | 66 |
| 7.10 | Observation of thick features in thickness map | 67 |
| 7.11 | Minimum amplitude map for top Transition layer | 68 |
| 7.12 | RMS amplitude map for top Transition layer | 69 |
| 7.13 | Maximum amplitude maps of top Transition layer | 70 |
| 7.14 | RMS amplitude maps for Plio-Pleistocene marine sediments | 71 |
| 7.15 | High-amplitude reflections in upper marine layer | 72 |
| 7.16 | Submarine channels | 72 |
| 7.17 | To unconformable surfaces bounding the Transition layer | 73 |
| | | |
| 8.1 | Deformation of evaporites | 76 |
| 8.2 | Asymmetrical Poiseuille flow profile | 77 |
| 8.3 | Intra-evaporite reflectors truncating top salt unconformity | 79 |
| 8.4 | Comparing the Transition layer to the Yafo Sand Member | 83 |
| 8.5 | Regional extent of Yafo Sand Member | 84 |
| 8.6 | Dome-shaped features in the Yafo Sand Member with chaotic core | 84 |
| 8.7 | Seismic section showing the Lago Mare facies in the offshore Sirt Basin | 87 |
| 8.8 | Thickness map of the Transition layer with focus on the channels | 90 |
| 8.9 | Submarine channel system in the Pacific Ocean | 91 |
| 8.10 | Mono Lake, CA, USA | 91 |
| 8.11 | Mono Lake as an analogue to the Transition layer | 92 |

| | | |
|------|--------------------------------------------------------------------------------------------------------|-----|
| 8.12 | Death Valley with water channels on the flat evaporite ground | 94 |
| 8.13 | Sediment distribution | 95 |
| 8.14 | Small canyons in the Death Valley is equal to the observations of the Transition layer | 96 |
| 8.15 | Badwater, Death Valley. Channels traveling on the evaporite ground with- out any gradient | 97 |
| 8.16 | Close-up of figure 8.15 | 98 |
| 8.17 | Geological reconstruction: Legend | 100 |
| 8.18 | Geological reconstruction: Stage 1 | 100 |
| 8.19 | Geological reconstruction: Stage 2 | 101 |
| 8.20 | Geological reconstruction: Stage 3 | 101 |
| 8.21 | Geological reconstruction: Stage 4 and 5 | 102 |
| 8.22 | Geological reconstruction: Stage 6 | 103 |
| 8.23 | Geological reconstruction: Stage 7 | 104 |
| 1 | Surface map of horizon R9 | 114 |
| 2 | Surface map of horizon R8 | 115 |
| 3 | Surface map of horizon R7 | 116 |
| 4 | Surface map of horizon R6 | 117 |
| 5 | Surface map of horizon R5 | 118 |
| 6 | Surface map of horizon R4 | 119 |

List of Tables

| | | |
|-----|-------------------------------------------------------------------------------------------------------------------------------------------------------------------------------------|----|
| 2.1 | Table shows different scenarios that are proposed for the origin and evolution of the Messinian Salinity Crisis | 12 |
| 4.1 | Major groups of evaporite minerals | 23 |
| 5.1 | Overview of seismic attributes that has been used to generate attribute maps. If a certain window length has been used, it will be specified in the figure text of the map. | 28 |
| 6.1 | Overview of interpreted horizons and seismic packages. | 33 |

Chapter 1

Introduction

During the Messinian Salinity Crisis (MSC) in the Late Miocene (5.96-5.33 Ma), thick sequences of evaporites were deposited in the Mediterranean Sea. This was a result of progressive restriction of the marine gateways between the Mediterranean Sea and the Atlantic Ocean, near present day Strait of Gibraltar (Hsü *et al.* , 1973). During the MSC the Mediterranean Sea underwent cyclic hypersaline conditions through partial and possibly complete desiccation. The thick sequence of evaporites (Hsü *et al.* , 1973) and the many canyons incised into the margins of the then drier Mediterranean basin (Druckman *et al.* , 1995), is evidence of at least a partial desiccation of the Mediterranean basin. The MSC is regarded as one of the most dramatic episodes of oceanic change within the past 20 million years (Krijgsman *et al.* , 1999) and probably the most important evaporitic event of Earth's history when considering its very short duration (Rouchy & Caruso, 2006).

After the Deep Sea Drilling Project (DSDP) Leg 42A in 1975 a near-consensus was reached for a scenario proposed by Hsü *et al.* (1973). This scenario involved deposition of evaporites in deep basin and shallow water conditions. The ability of improved age dating in the middle of the 1990s (Krijgsman & Meijer, 2008), by more accurate correlation between Messinian sequences, led to the establishment of many new scenarios (Rouchy & Caruso, 2006). Even with a considerable increase in knowledge, there are still many unresolved and potentially controversial topics related to the MSC. In the previous project (Solem, 2013), I looked into the disagreements that revolve around this event. These include the size and relief of the pre-Messinian Mediterranean basin, the water depth during onset of the MSC, timing of the MSC, synchronous or diachronous evaporite deposition and cause of isolation of the Mediterranean Sea. These disagreements are mainly linked to the fact that most knowledge about the Messinian Salinity Crisis are

based on outcrops that are located onshore and isolated from the deep basins.

In this master thesis, an interpretation study will be conducted. Newly acquired 3D, depth migrated seismic data for the Eastern Mediterranean Sea; the Levant Basin, offshore Lebanon will be interpreted. Studying the Messinian Salinity Crisis in the offshore area allows us to document and interpret a probable continuous record of the entire MSC event. The Levant Basin is an under-explored area where the evaporite deposition is different from that in the more explored western Mediterranean. Only nine exploration wells have been drilled in the southern Levant Basin (*BG - unpublished data*), and not a single well has been drilled in the northern part of the basin, offshore Lebanon.

The good quality of the seismic data reveals an interesting layer with different characteristics than the Messinian evaporites deposited below and the marine sediments above. This layer will be main focus of this thesis. This relatively thin layer is deposited directly above the Messinian evaporites and will be referred to as the Transition layer.

The objective is to understand the depositional history and the characteristics of this transitional layer. First, a regional interpretation of the area will be performed to understand the overall geological history of the Levant Basin, offshore Lebanon. Second, a more detailed interpretation study of the Messinian and younger sediments, with main focus on the Transition layer, will be carried out. The observations from the seismic sections will be compared to results from attribute maps that are generated. Finally, different possible scenarios for the origin of this layer will be discussed. Understanding the fundamental theory of the salinity crisis in the eastern Mediterranean Sea is important to fully obtain the geological history of the Mediterranean area. The Levant Basin is an under-explored area with a lot of hydrocarbon potential. Understanding the geological history is therefore crucial.

A map of the Mediterranean Sea can be found in figure 1.1. The Levant Basin is located offshore Lebanon and Israel, in the eastern Mediterranean Sea. See location map in figure 1.2. The Levant Basin is a deep-marine basin with water depths of 1500-2000 m and covers an area of $83,000\text{km}^2$ (Lie *et al.* , 2011).



Figure 1.1: Map of the Mediterranean Sea where the salinity crisis took place in the Messinian time, Late Miocene. Source: worldatlas.com

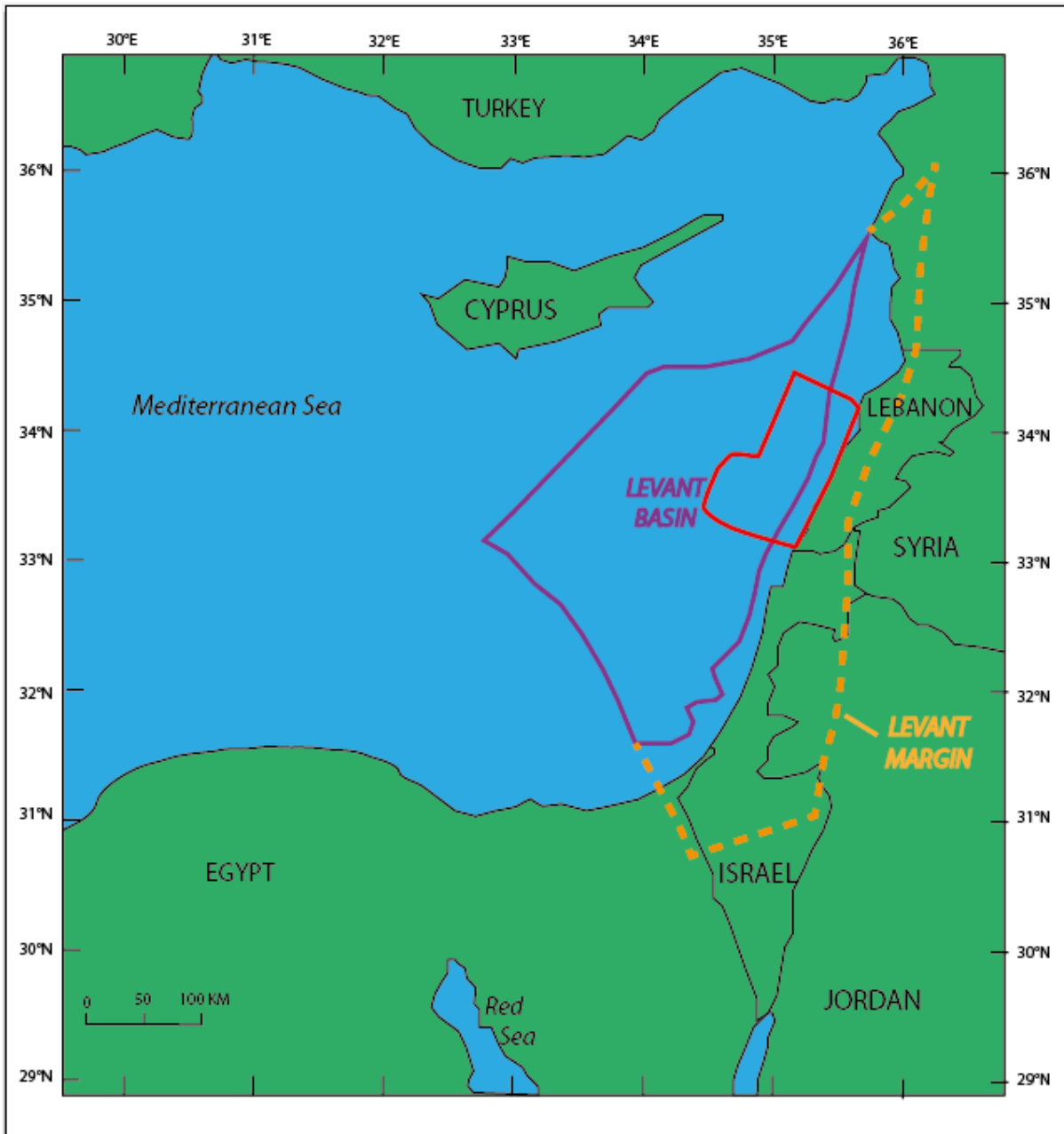


Figure 1.2: Map showing the location of the Levant Basin in the eastern Mediterranean Sea. The Levant Basin is located offshore Lebanon and Israel. The area marked with red is the study area for this thesis. The Levant Basin is marked in purple and the extension of the Levant Margin is marked by yellow dashed line. The x- and y-axis show the coordinates for the Levant Basin.

Chapter 2

Previous work

The following chapter contains a modified summary of a literature study on the Messinian Salinity Crisis (MSC) that I did last semester (Solem, 2013). This study was carried out in order to get an overview of the present state of knowledge and to highlight the disagreements that revolve around the salinity crisis.

The MSC occurred at the end of the Miocene epoch during the Messinian age (5.96 to 5.33 million years ago) in the Mediterranean Sea. The initiation of the MSC resulted from a complex combination of tectonic and glacio-eustatic processes (Krijgsman *et al.*, 1999). These processes progressively restricted the gateways between the Mediterranean Sea and the Atlantic Ocean, causing the Mediterranean to become isolated and hypersaline (Hsü *et al.* (1977); Hsü *et al.* (1973); Hsü (1974)). The change from normal marine conditions to evaporite-forming conditions was a sudden change (Hsü *et al.*, 1977) and is regarded as one of the most dramatic episodes of oceanic change of the past 20 million years (Krijgsman *et al.*, 1999). During the Messinian time the western opening to the Atlantic, present day Strait of Gibraltar, was acting as a floodgate. Several episodes of flooding and isolation led to the deposition of more than 1 km thick sequence of evaporites (Hsü *et al.* (1973); Hsü (1974)). The deposit covers an area more than $10^6 km^2$ and includes dolomite, anhydrite, gypsum, halite and more soluble salts. Based on seismic records, the evaporite succession is divided into two parts (Hsü *et al.* (1977), Krijgsman & Meijer (2008), Rouchy & Caruso (2006), Clauzon *et al.* (1996)). The Lower Unit consists of gypsum, evaporitic limestone and halite (Krijgsman & Meijer, 2008) and is often separated into the Main Salt and Lower Evaporite sequence. The section is up to a thousand meters thick and the salt is seismically homogeneous (Hsü *et al.*, 1973). The Upper Unit consists of gypsum and marls and is referred to as the Upper Evaporites (Krijgsman & Meijer, 2008). This sequence has numerous reflectors and is up to several

hundred meters thick (Hsü *et al.* , 1973). An unconformity is separating the Lower Unit from the Upper Unit (Hsü *et al.* (1973), Krijgsman & Meijer (2008)). The presence of a Messinian evaporite sequence under the Mediterranean Sea was first discovered by the Deep Sea Drilling Project (DSDP) in the 1970s (Hsü *et al.* , 1973). The Messinian salinity crisis is a complex geological event and many models have been proposed in order to interpret and gain understanding of the origin of the Messinian evaporites.

2.1 Consequences

2.1.1 Termination of the MSC

After repeated cycles of isolation and flooding during the Late Miocene, the deposition of the Messinian evaporites terminated at the end of the Messinian Salinity Crisis. The restoration of normal marine conditions may have two possible explanations (Bertoni & Cartwright, 2007b). One possible setting that has been envisaged for this change in sedimentation is that the western gate to the Atlantic was irreparably crushed at the beginning of the Pliocene (Hsü, 1974). Atlantic water flooded the partly desiccated Mediterranean basins and restored normal marine conditions. A second option is a late Messinian-Pliocene gradual refilling of the basin (Riding *et al.* , 1998).

The canyons and gorges that were cut into the desiccated Mediterranean were buried under the sea after the Pliocene deluge. Thick alluvial sediments filled the gorges on land, and those under sea were converted into submarine canyons. The final deluge must have followed a big event that produced a gap deep enough to permit deep-Atlantic bottom faunas to immigrate into the Mediterranean. The opening gradually shoaled during the Pliocene, until the present day situation. As a consequence of the shoaling, the cold Mediterranean benthonic faunas were extinct near the beginning of Pleistocene when the supply of deep-Atlantic waters was cut off. A sill, the Strait of Gibraltar, still exists today. Even though it is shallow, it is still deep enough to permit reflux into the Atlantic of partially evaporated Mediterranean waters. The result of this is that the Mediterranean Sea keeps its salinity only slightly above that of the Atlantic (Hsü, 1974) (figure 2.1).

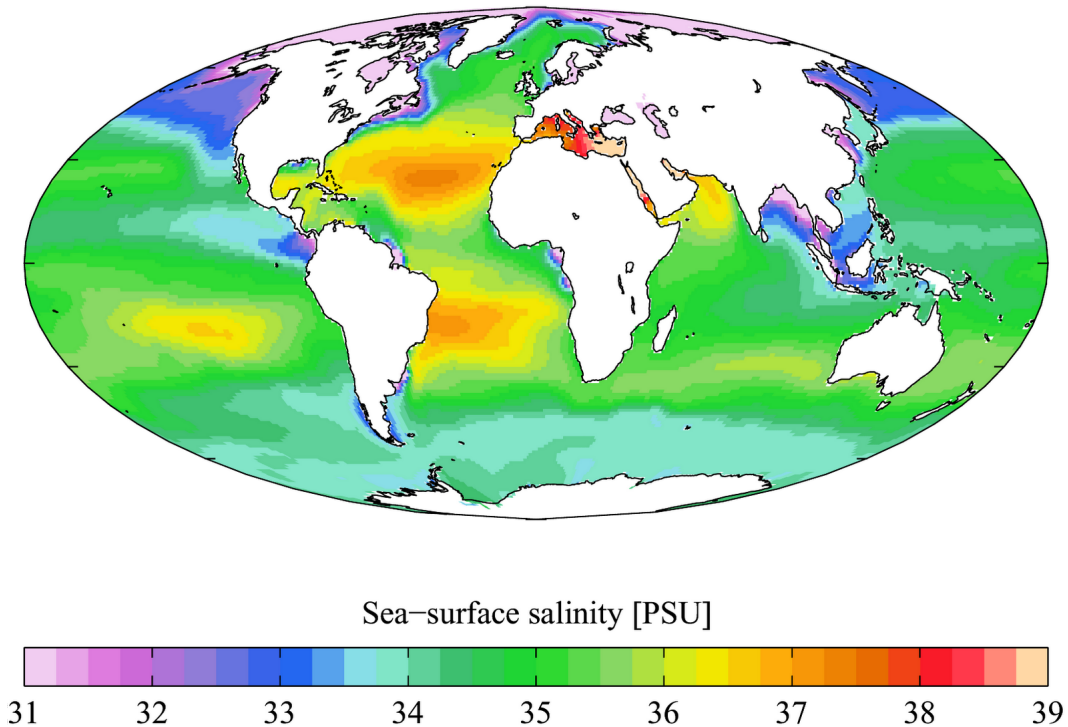


Figure 2.1: Present water salinity at the surface of the ocean, showing higher salinity in the Mediterranean caused by the higher evaporation and isolation of its waters. Source: *World Ocean Atlas, 2005*

2.1.2 Impacts of the MSC

Such a dramatic event as the Messinian salinity crisis had great impact on the surroundings. The event affected the landscape of the circum-Mediterranean, regional and global climates, plants and animals, and have also had impact on the modern world (Hsü *et al.*, 1977). Prior to the Miocene, the Mediterranean was acting as a broad seaway and connected the Indian Ocean with the Atlantic. The communication was cut in the Early Miocene, which deteriorated the climate in the Mediterranean Sea. The Mediterranean became cooler and the circum-Mediterranean lands became drier and colder. The salinity crisis also affected the European climate, which can be seen by fossil floras and fauna. Both flora and fauna that dominated in the Middle and early Late Miocene became rare or disappeared during the late Late Miocene. As the water-level in the Mediterranean Basin lowered, a number of "intermediterranean bridges" were created. These acted as new migrations routes that made it possible for fauna and flora to invade new territories and disappear from others (Hsü, 1974). The present Mediterranean fauna is similar to that of the Pliocene, but very different from that of the Miocene. The change in fauna between the Messinian and Pliocene was due to the sudden Pliocene flooding that stranded animals on islands where they became isolated and developed endemism (Hsü *et al.*

(1977); Hsü (1974)). A partially exposure of the Mediterranean basin floor in the Late Miocene activated movement of groundwater. This might be responsible of the initiation of karst topography in Yugoslavia and other Mediterranean countries (Hsü, 1974).

2.2 Disagreements

The aim of the previous work was to get an overview of the current knowledge and controversies, by conducting a literature review of the MSC. The review shows that there are many unresolved and potentially controversial topics related to the Messinian salinity crisis. These include size and relief of the pre-Messinian basins, water depth during deposition of the evaporites, timing of the onset of the MSC, a synchronous or diachronous evaporite depositions and cause for the isolation of the Mediterranean. A near-consensus was reached after the Deep Sea Drilling Project (DSDP) Leg 42A with a model based on Hsü *et al.* (1973). There was a common agreement about a deep-basin, shallow-water scenario, but differences existed concerning the timing and depositional conditions of the evaporites (Rouchy & Caruso, 2006). The ability of improved age dating in 1995 allowed a direct comparison and correlation of the evaporite sequences (Krijgsman & Meijer, 2008). This resulted in a considerable increase in knowledge after 1995. Several new scenarios were proposed after this. In the following sections, five topics of disagreement will be presented. There will be referred to six different models that are presented in table 2.1.

2.2.1 Depth of pre-Messinian basin

Prior to the DSDP Leg 42A in 1975, controversies revolved around the depth of the pre-Messinian Mediterranean basin. Scenarios with both deep-basin and shallow-basin were proposed (Hsü *et al.* , 1973). Deep-water species were found in biostratigraphical data and geographical studies showed canyon formation at the margins (Krijgsman & Meijer, 2008). This, together with evidence from the drilling project, seismic profiling surveys and geological reconstructions, has convincingly confirmed that a deep Mediterranean basin were in existence before Messinian time.

2.2.2 Water depth during onset of MSC

The depositional environment for the Lower and Upper Evaporite units is still under discussion. The water depth of the Lower Evaporite deposition is widely debated and from the models that has been looked in to, there is a disagreement. A deep water scenario, as proposed in Model 2 (Table 2.1), would imply that no major sea-level lowering took place at the onset of the Messinian Salinity Crisis. The Lower Evaporites were deposited in a deep-water Mediterranean basin. The Atlantic connection must have been modified in such extent that continuous inflow of marine water would compensate for the net water loss in the Mediterranean, but in a way that outflow from the Mediterranean to the Atlantic was restricted (Krijgsman & Meijer, 2008). Continuous inflow with restricted outflow can explain the thick section of evaporites. Other authors (i.e. Hardie and Lowenstein (2004) and Lu and Meyers (2006)) have also proposed a deep-water model. On the other side, Model 1, 3, 4, 5 and 6 (Table 2.1) argue in favor for shallow-water conditions during the onset of the salinity crisis. Model 1, 3 and 5 support a major drawdown in sea-level, while in Model 4 and 6 shallow-water conditions were obtained by only a minor drawdown.

2.2.3 Timing of the MSC

The Messinian Salinity Crisis took place during the Messinian, in the Late Miocene. Most authors agree to date the onset of the MSC to 5.96 ± 0.02 million years, with a duration of $\sim 600,000$ years until it terminated at 5.33 million years ago. However, this dating is highly dependent on what is used as sedimentary marker of the MSC. According to Model 6 (Clauzon *et al.*, 1996), the earliest evaporitic event started ~ 0.1 millions years after the beginning of the third magnetic reversal event (Chron C3r), i.e. at approximately 5.75 Ma. This tie the onset of the MSC to the oxygen isotopic stages (peak glacial stages) TG22 and TG20. This is 210 kyr later than 5.96 Ma. In contrast, Model 3 (Rouchy & Caruso, 2006) claims that the first evidence of evaporitic conditions in some marginal areas of the Sicilian basin can be traced back to around 6.14 Ma, pre-dating the onset at 5.96 Ma with 180 kyr. The transition from the pre-evaporitic unit to the overlying evaporites is usually transitional and very complex. Therefore, the dating will be different depending on whether i.e. the base of the first massive evaporites is chosen or the base of the transitional beds. In addition, Rouchy & Caruso (2006) state that the age of the onset of the MSC in the deeper basins are still completely unknown, which represent 90% of the surface covered by the Messinian evaporites. The time of termination of the MSC at 5.33 Ma has also been discussed. According to Riding *et al.* (1998), the Sorbas

gypsum deposits mark the end of the salinity crisis. This section is overlain by normal marine sediments of latest Messinian age. Model 5 therefore argue that the salinity crisis was completed before the end of the Messinian, and had a duration of $\sim 400,000$ years before it ended at 5.5 Ma.

2.2.4 Cause of isolation

Two possible mechanisms have been discussed to influence the closing of the Late Miocene gateways: (1) glacio-eustatic sea-level drop; (2) tectonic uplift. The models argue in favor for a dominantly tectonic origin of the MSC. However, eustatic fall in sea-level linked with global cooling have also partly affected the isolation. Clauzon *et al.* (1996) in Model 6 relate the isolation and onset of the salinity crisis to a cooling period with weak global sea-level fall that corresponds to the isotopic stages TG22 and TG20. Krijgsman & Meijer (2008) in Model 2 state that stable isotope analyses reveal that the peak glacial stages TG22 and TG20 clearly post-date the initiation of the Messinian evaporites in the Mediterranean, and that there is no evidence for a glacio-eustatic control for the onset of the MSC. Model 3 (Rouchy & Caruso, 2006) argue that even though the isolation of the Mediterranean happened predominately because of tectonic, the MSC was triggered by the interplay of both glacio-eustatic changes and fluctuations of the circum-Mediterranean climate. Altogether, most hypotheses agree that a combination of tectonic processes and glacio-eustatic initiated the MSC and isolated the Mediterranean from the Atlantic Ocean.

2.2.5 Synchronous or Diachronous evaporite deposition

An obvious disagreement in the models proposed is whether the evaporite deposition occurred at the same time in the marginal and deep basins or not. Three different possibilities are proposed. Model 2 argues for a synchronous deposition where deposition of the evaporites took place both in marginal basins and in deep basins at the same time. A good correlation should therefore exist between the marginal and deep-basin evaporites. Model 1 and 3 is partly in agreement with Model 2, but argue for a slightly diachronous deposition chronology. This means that the salinity crisis took place at the same time in both the western and eastern Mediterranean, but with a slight diachronism between the marginal and the deep basins. Still, all of the Lower Evaporites were deposited prior to the Upper Evaporites. In contrast, Model 4, 5 and 6 postulate a complete diachronism where the evaporite deposition occurred in two steps. The models argue that deposition

of evaporites was totally dependent on local basinal settings and happened first in the marginal basins, followed by deposition of evaporites in the deep basins. For Model 4 and 5 a third episode of evaporite deposition occurred in the marginal basins after deposition in the deep basins. A comparison of the timing of the events in the models is shown in figure 2.2.

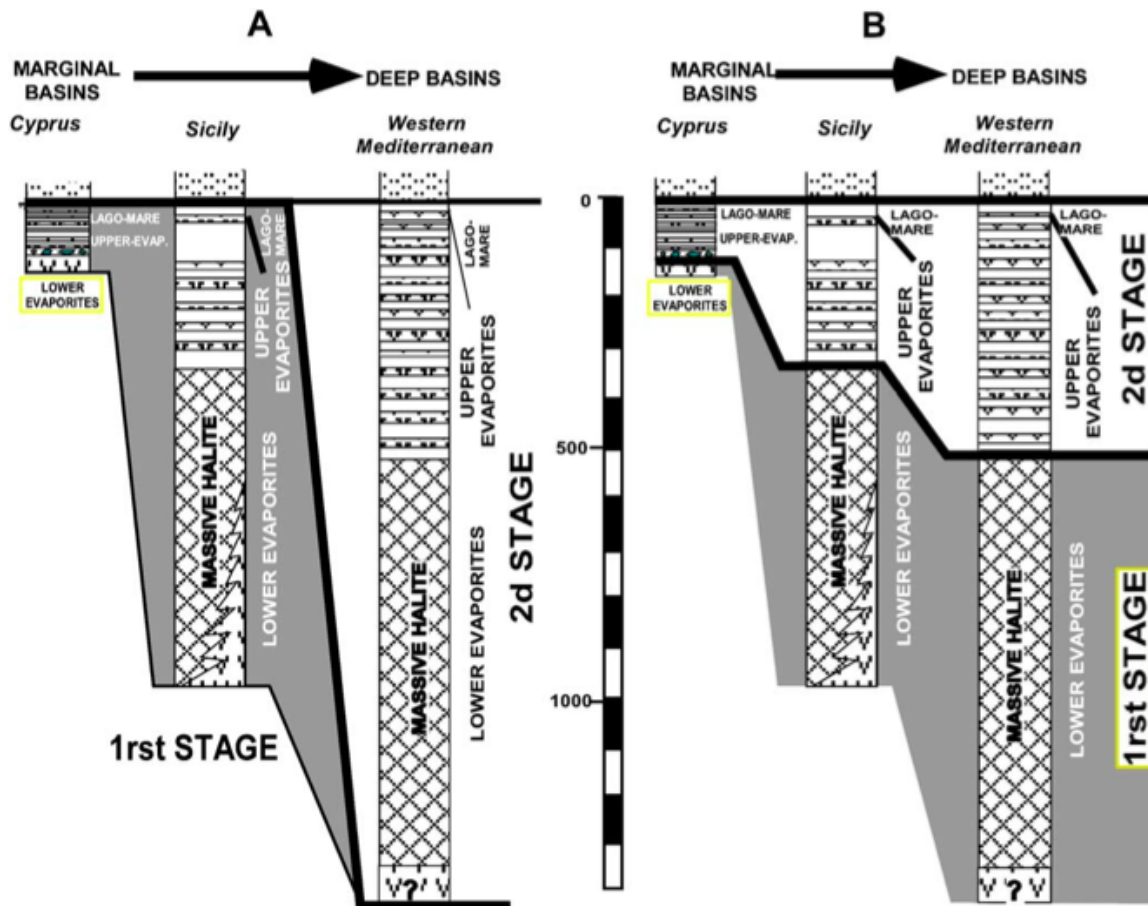


Figure 2.2: Comparison of the timing of the events in the models proposed. (A) Model 6 by Clauzon et al. (1996) implies that a complete duplication of the same sedimentary and hydrological events occurred first in the marginal basins then secondly in the deep basins. This is in agreement with Model 4 (Butler et al., 1999) and Model 5 (Riding et al., 1998). (B) In contrast, Model 1 (Hsü et al., 1973), Model 2 (Krijgsman & Meijer, 2008) and Model 3 (Rouchy & Caruso, 2006) interpret the events to have affected successively the whole Mediterranean. Source: Rouchy & Caruso (2006). **Note:** This figure can only be applied to the western Mediterranean Basin. This cannot be correlated to the northeastern Levant Basin (study area), eastern Mediterranean, since there have not been drilled any wells there yet.

Table 2.1: This table shows different scenarios that are proposed for the origin and evolution of the Messinian Salinity Crisis. For each model 1-6, the table summarizes which authors that have generated the model, the duration of the salinity crisis, whether the evaporite deposition was synchronous or diachronous, and water depth during deposition of the Lower Evaporites. These are three topics that are highly discussed between the models. While a common agreement is that the MSC lasted from 5.96-5.33 Ma, there is a slight disagreement depending on what is used as a marker for the onset of the MSC. With synchronous and slight diachronous deposition, the salinity crisis has affected successively the whole Mediterranean. In contrast, a diachronic deposition implies that a complete duplication of the same sedimentary and hydrological events occurred first in the marginal basins then secondly in the deep basins. In case of diachronous deposition (Model 4-6), only minor sea-level lowering is necessary to obtain shallow-water conditions. Model 1 and 3 favor slight diachronous deposition with shallow water obtained from a major drawdown. In case of Model 2, no sea-level lowering has occurred and the deposition of the Lower Evaporites was synchronous in deep water.

| Model | Paper | Time interval (Ma) | Synchronous vs. Diachronous | Water depth during deposition of LE |
|---------|----------------------------------|-----------------------|--------------------------------------------------------------|-------------------------------------|
| Model 1 | Hsü et al. 1973, 1974 1977 | 5.96 - 5.33 | Slight Diachronous: Marginal and deep basins | Shallow water |
| Model 2 | Krijgsman et al. 1999, 2008 | 5.96 - 5.33 | Synchronous: Whole Mediterranean | Deep water |
| Model 3 | Rouchy and Caruso 2006 | (6.14-5.96) - 5.33 | Slight diachronism: Marginal and deep basins | Shallow water |
| Model 4 | Butler et al. 1999 | 6.13 - 5.3 | Diachronous: Sicilian basin to deep basins | Shallow water |
| Model 5 | Riding et al. 1998 | 5.9- 5.5 | Diachronous SE Spain marginal basins to deep basins | Shallow water |
| Model 6 | Clauzon et al. 1996 | 5.75- 5.32 | Diachronous: Marginal basins to deep basins | Shallow water |

Chapter 3

Geological history

3.1 Shaping the Levant Basin

The Levant region covers the eastern portion of the eastern Mediterranean Sea. The Levant basin and continental margin is situated in a tectonically complex area (figure 3.1) where the Anatolian, African and Arabian plates interact (Bertoni & Cartwright, 2005). The region can be described as a foreland basin on the African Plate (Roberts & Peace, 2007). The area has a long history of rifting, convergence, subsidence and uplift.

The Levant Basin was shaped in three main tectonic phases: a rifting phase, a post-rift, passive margin phase and a convergence phase (Gardosh *et al.* , 2008). The rifting phase occurred in the uppermost Paleozoic and Early Mesozoic and was related to the breakup of the super-continent Gondwana and the formation of the Neo-Tethys Ocean. This rifting resulted in the formation of extensive NE-SW oriented horst and graben systems that extended throughout the Levant onshore and offshore (Gardosh *et al.* , 2006).

Post-rift subsidence and cooling in the Late Jurassic to Middle Cretaceous gradually formed a passive margin in the east subsequent with the development of a deep-marine basin in the west bordered by a shallow-marine shelf. The formation of the passive margin is characterized by stacking of shallow-platform carbonates associated with relative sea-level changes. Deep-water carbonates dominated the slope and basin in west (Gardosh *et al.* , 2008). A paleo-depositional hinge belt developed along the eastern margin of the basin from the Middle Jurassic. Deep wells along the present-day coastline of Israel show that the hinge belt separates the enormous shallow-marine platform to the east from the deep marine basin to the west (Gardosh *et al.* , 2006).

The third tectonic phase in the shaping of the Levant Basin was a convergence phase in the Late Cretaceous and Tertiary. This was related to the closure of the Neo-Tethys Ocean and the collision of the African-Arabian plate with the Eurasian plate. Early Mesozoic structures underwent inversion and extensive contractional structures were formed throughout the Levant basin and margin (Gardosh *et al.*, 2006). Example of this is the formation of the Syrian Arc fold belt that created a series of NE-SW-oriented compressional structures along the Levant continental margin (Bertoni & Cartwright, 2005). The Levant margin experienced regional uplift as Afro-Arabia collided with Eurasia, probably linked to mantle plume activity (Hawie *et al.*, 2013).

In the Late Miocene, the Anatolian Plate moved westward and the Red Sea and Gulf of Aden opened. As a response to this, a large fracture system named the Levant Fracture System emerged and separated Arabia from Africa. This is a N-S sinistral fault system that presents a right bend onshore Lebanon and transpression therefore occurs (Hawie *et al.*, 2013). This tectonic phase has a major influence on the Miocene and younger deposits, and can therefore be thought of as the fourth tectonic event shaping the Levant area.

3.2 Filling the Levant Basin

Late Cretaceous - Late Miocene

The Levant Basin is filled with sediments from the Late Cretaceous to present time. The sediments from Late Cretaceous, Paleocene and Eocene are composed mainly of limestones and appear to be deformed by compressional structures related to the Syrian Arc foldbelt (Bertoni & Cartwright, 2006). Since the Oligocene time, deposition of large volumes of siliciclastic sediments dominated the area. These sediments were sourced from the Red Sea rift shoulders and from the Paleozoic Nubian sandstone (Hawie *et al.*, 2013). Series of incisional features that cut down into the Cretaceous deposits have been observed. This is interpreted as a submarine canyon system that developed during the Oligocene, namely, the El Arish, Afiq and Ashdod Canyons (Bertoni & Cartwright (2005), Bertoni & Cartwright (2006), Bertoni & Cartwright (2007a)). As a consequence of the transpressive movements along the Levant Fracture System, Mount Lebanon was strongly uplifted in the Middle to Late Miocene.

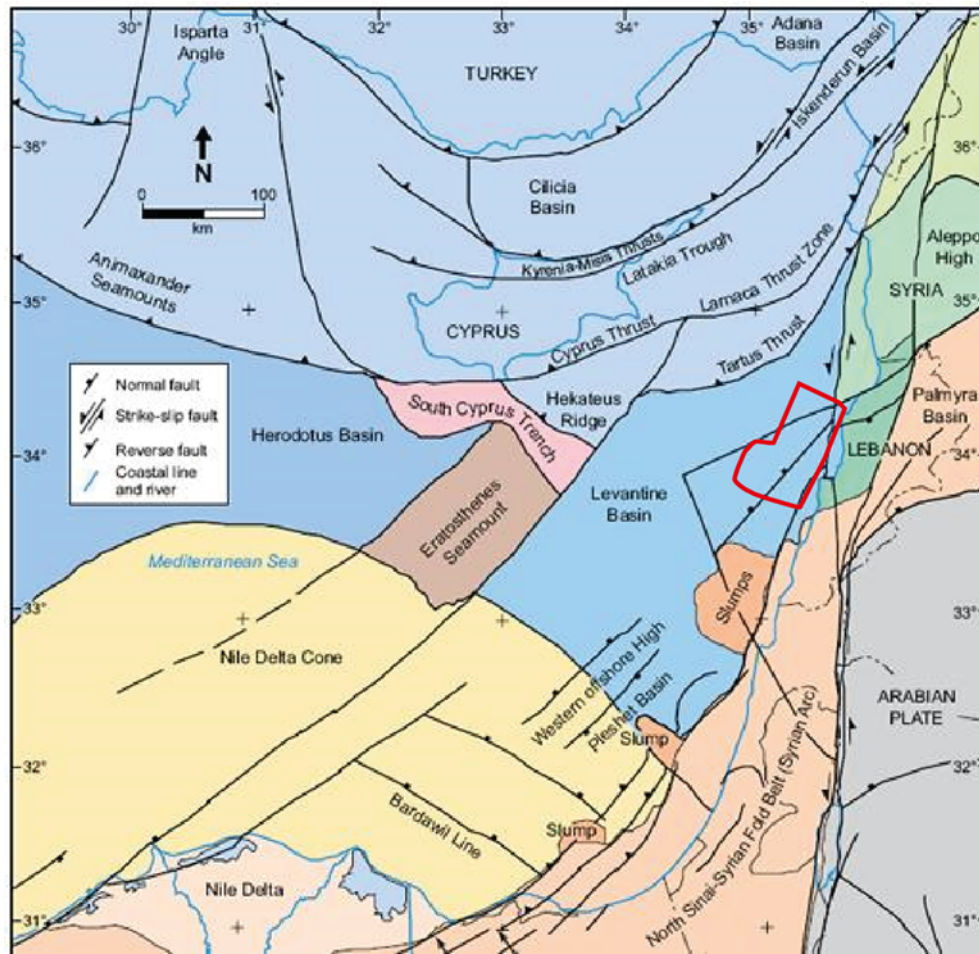


Figure 3.1: Structural elements in the Eastern Mediterranean Sea. The location of the Levant Basin is in blue to the right. The study area for this thesis is approximately marked in red. Source: modified from Breman, 2006.

Late Miocene - Present

A complex combination of tectonic and glacio-eustatic processes (Krijgsman *et al.*, 1999) led to a progressive restriction of the gateways (figure 3.2) between the Mediterranean Sea and the Atlantic Ocean in the Late Miocene. Because of this, the Mediterranean Sea became partially isolated during the Messinian, which caused the onset of the Messinian Salinity Crisis (Bertoni & Cartwright, 2007b). The resulting sea-level fall led to a major erosional phase of the Mediterranean margins and to evaporite deposition in the entire basin (Bertoni & Cartwright, 2005). Thick evaporite sequences up to 2 km were deposited on the seafloor, while meandering coastal streams eroded the margin and formed deeply incised valleys (Bertoni & Cartwright (2007b); Hsü (1974)).

The deposition of evaporites was terminated at the end of the Miocene/beginning of Pliocene due to restoration of normal marine conditions across the Mediterranean Basin

Figure 3.2: A possible palaeogeographical reconstruction of the west end of the Late Miocene Mediterranean, approximately 8 million years ago. A combination of tectonics and glacio-eustatic processes led to a progressive restriction of the gateways between the Mediterranean Sea and the Atlantic Ocean (near present-day Strait of Gibraltar). The present coastline is marked in red. S: Sorbas Basin, B: Betic Corridor, R: Rifean Corridor, G: Strait of Gibraltar, M: Mediterranean Sea. Source: Modified from Duggen *et al.* (2003).



(Bertoni & Cartwright, 2007b). The Pliocene transgression flooded the Upper Miocene shelf (Buchbinder & Zilberman, 1997) and a thick prograding wedge of mainly Nile-derived siliciclastic sediments deposited in the Levant Basin and margin (Yafo Formation) (Bertoni & Cartwright, 2006). The post-Messinian sediments in the Levant margin and basin are affected by thin-skinned deformation. This is due to salt mobilization and to shelf loading that caused the collapse and landward tilt of the Pliocene and Recent deposits (Bertoni & Cartwright, 2006). A simplified sketch (figure 3.3 - figure 3.6) has been made by Hawie *et al.* (2013). This illustrates the geological model that the authors have proposed for the northern Levant distal margin and basin, offshore Lebanon. A chronostratigraphic chart from the northern Levant Basin is given in figure 3.7.

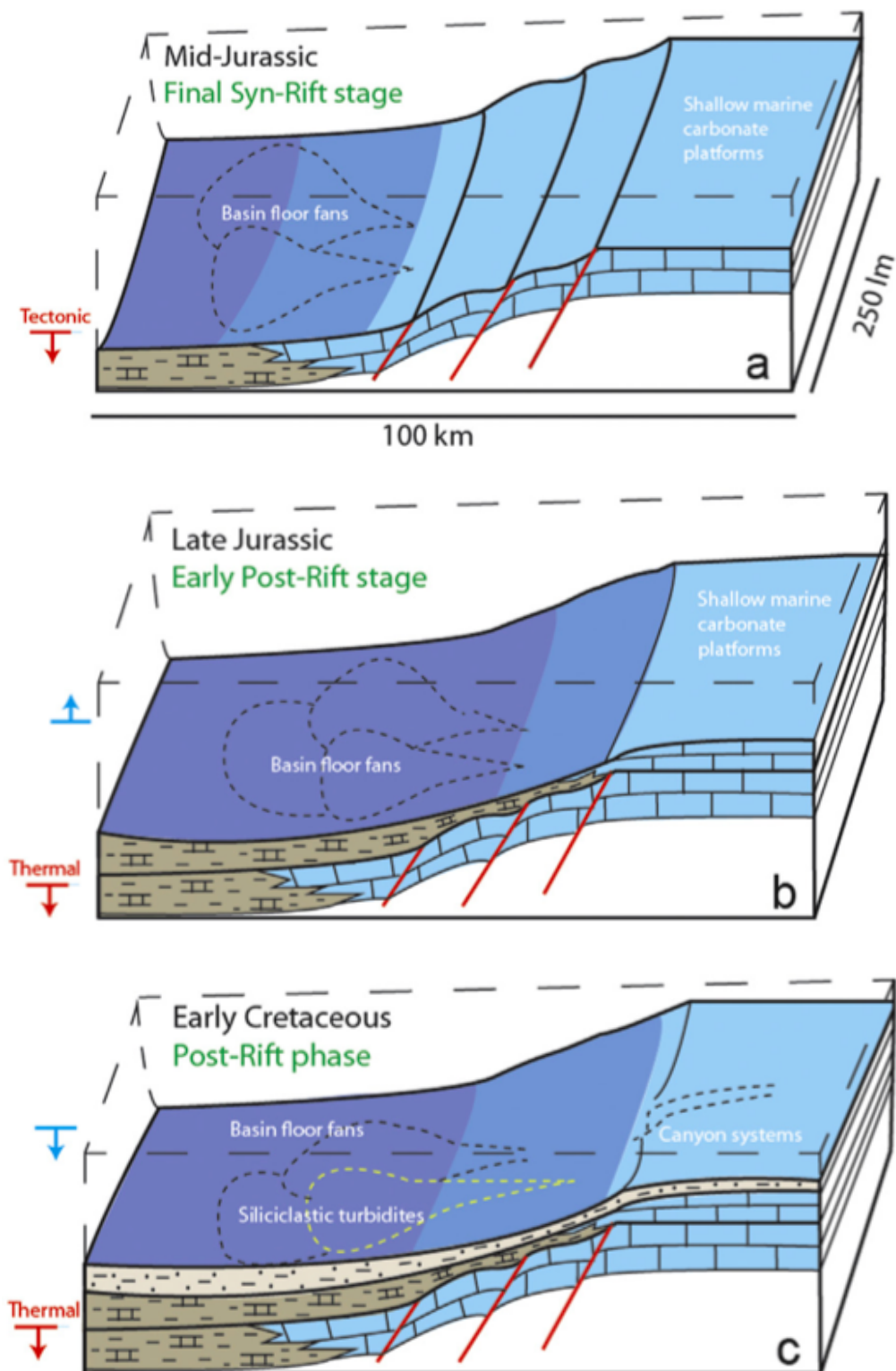


Figure 3.3: The figure presents simplified sketch-diagrams that are proposed for the northern Levant distal margin and basin, offshore Lebanon. This is part 1. Part 2 and 3 follow in figure 3.4 and figure 3.5. See legend in figure 3.6. Source: Hawie et al. (2013).

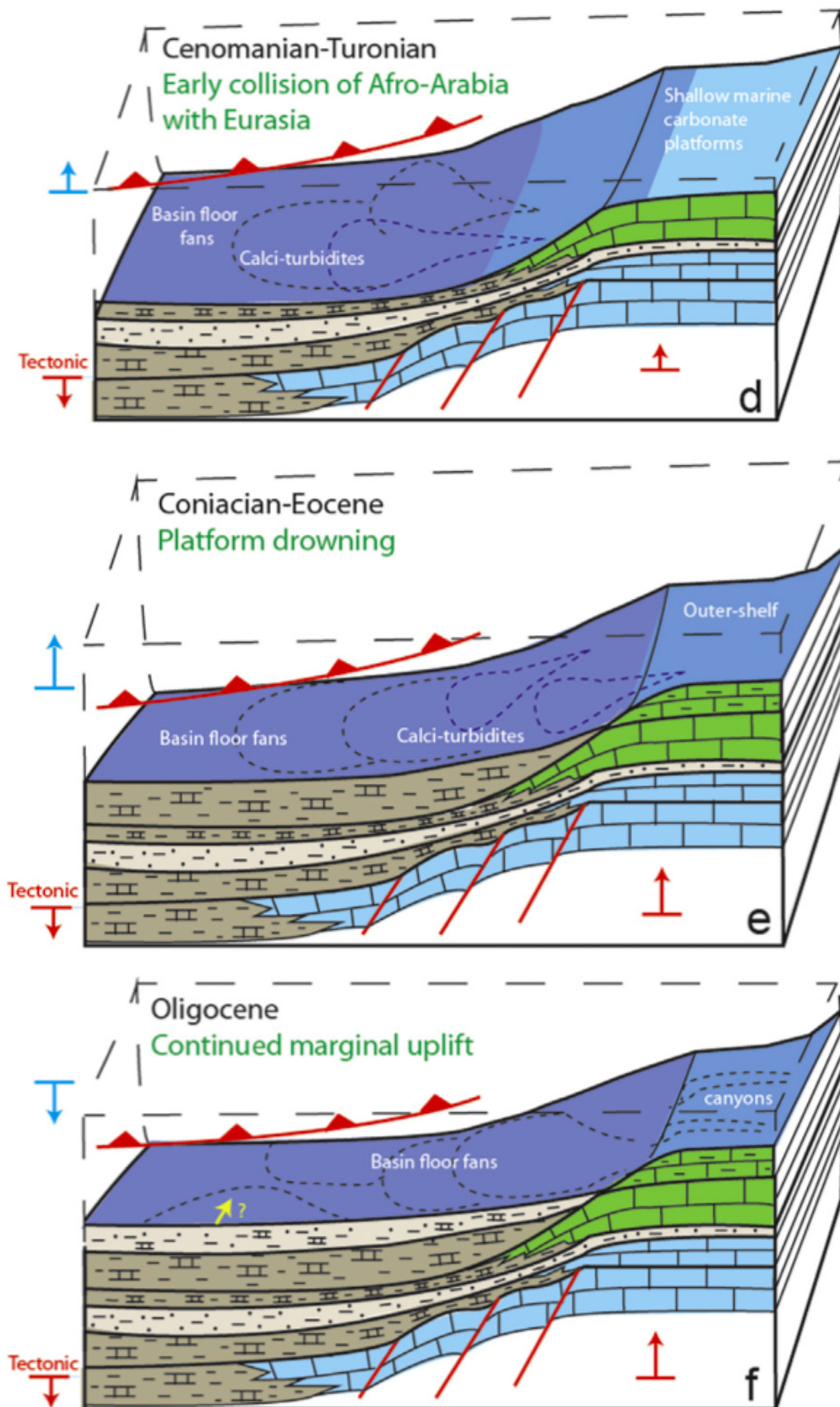


Figure 3.4: The figure presents simplified sketch-diagrams that are proposed for the northern Levant distal margin and basin, offshore Lebanon. This is part 2 and is a continuation of figure 3.3. Part 3 follows in figure 3.5. See legend in figure 3.6. Source: Hawie et al. (2013).

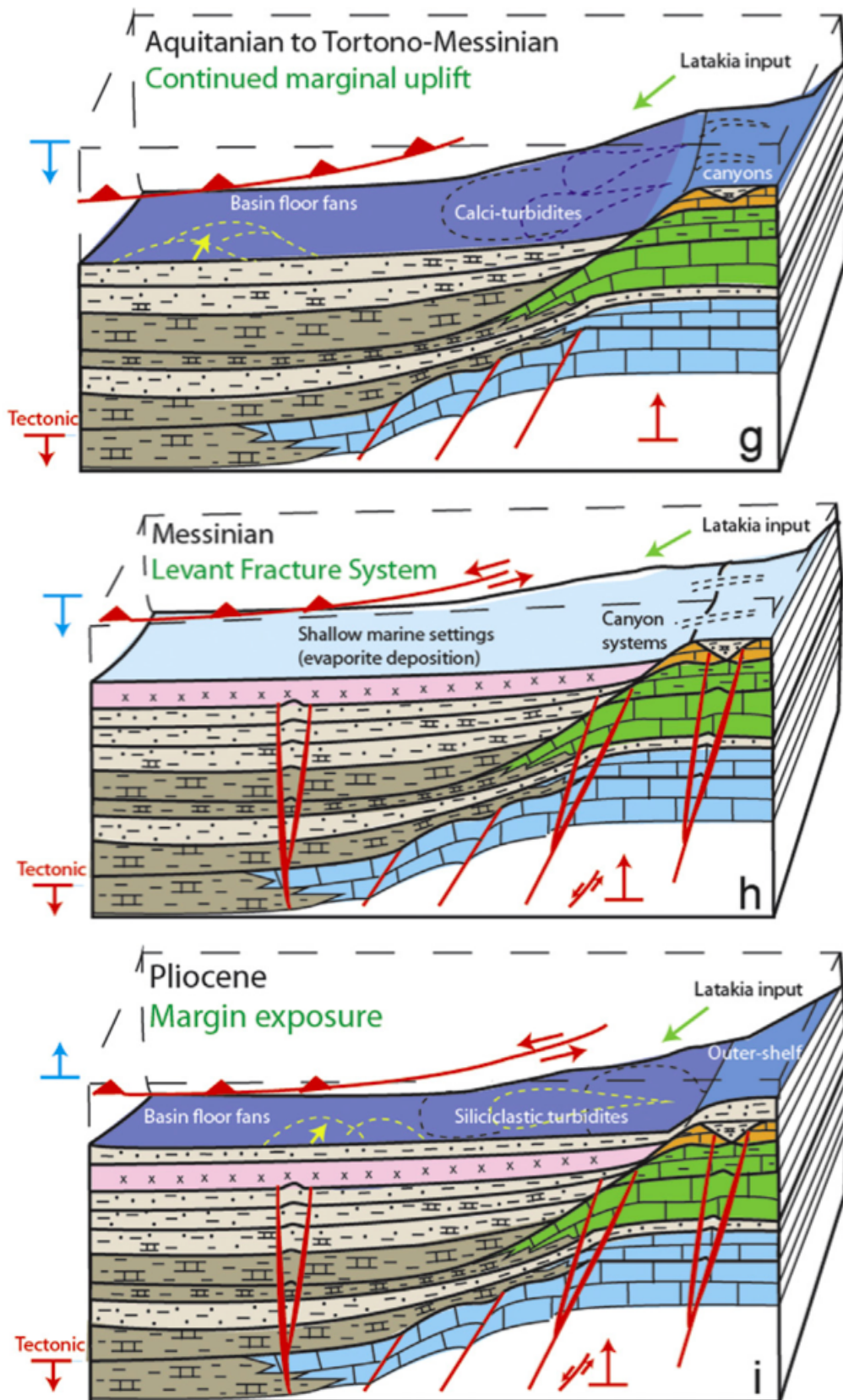


Figure 3.5: The figure presents simplified sketch-diagrams that are proposed for the northern Levant distal margin and basin, offshore Lebanon. This is part 3 and is a continuation of figure 3.3 and figure 3.4. See legend in figure 3.6. Source: Hawie et al. (2013).

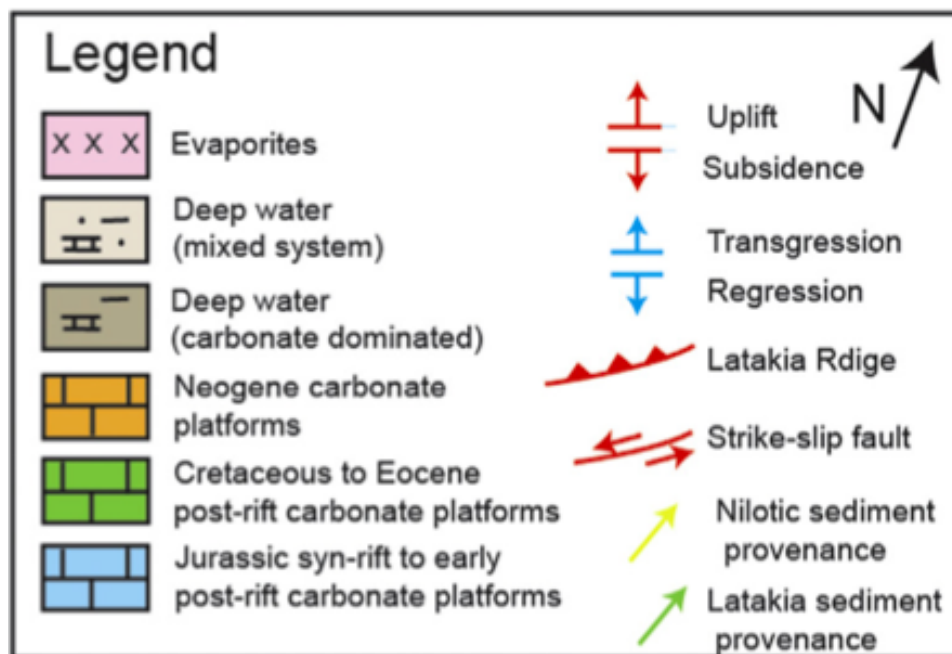


Figure 3.6: The figure presents the legend for the previous three figures (figure 3.3, figure 3.4 and figure 3.5). Source: Hawie et al. (2013).

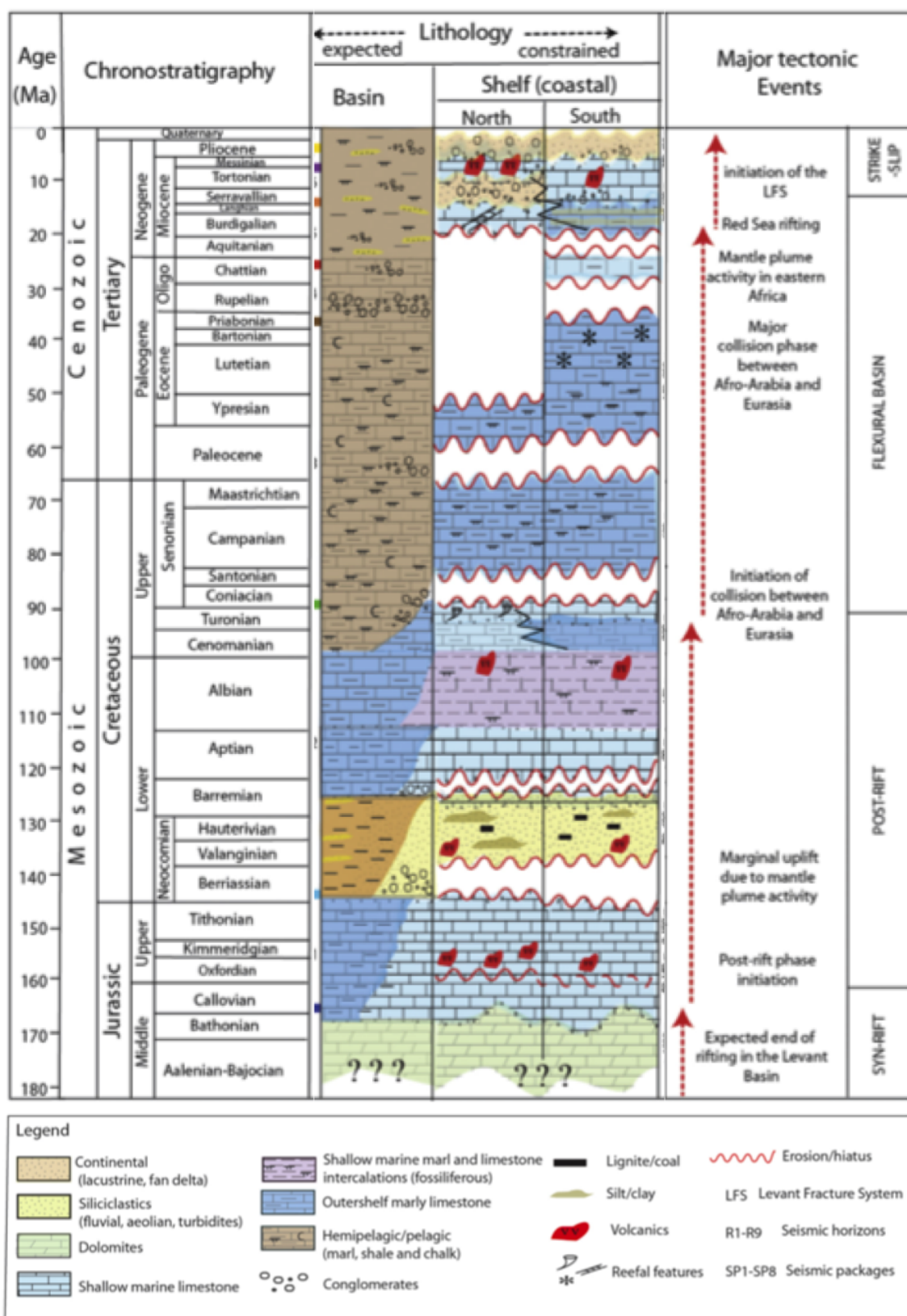


Figure 3.7: A chronostratigraphic chart showing the observed onshore sedimentary facies and their extrapolation into the northern Levant Basin offshore Lebanon. The proposed lithology for the basin and coastal shelf is given in the middle columns. The major tectonic events that has shaped the Levant Basin is given in the column to the right. Source: Hawie et al., 2005.

Chapter 4

Evaporites and Salt Tectonics

Evaporites

Evaporites are sedimentary rocks that form from brines when the amount of water lost by evaporation exceeds the amount of water from rainfall and influx from rivers and streams. The evaporites have a layered crystalline structure, but the mineralogy of the rocks is very complex, giving the origin of more than 100 varieties of evaporites. Volumetrically, less than a dozen species are important. Minerals in evaporite rocks include carbonates, chlorides and sulfates (Schwab, n.d.), as can be seen in table 4.1. Evaporites can be of either marine origin or non-marine origin, and can be precipitated in both shallow- and deep-water settings (Kendall, 1988).

Table 4.1: Major groups of evaporite minerals

| Mineral class | Mineral name | Chemical Composition |
|---------------|--------------|----------------------|
| Carbonates | Dolomite | $CaMg(CO_3)_2$ |
| | Calcite | $CaCO_3$ |
| | Magnesite | $MgCO_3$ |
| Chlorides | Halite | $NaCl$ |
| | Sylvite | KCl |
| | Carnallite | $KMgCl_3 * 6H_2O$ |
| Sulfates | Anhydrite | $CaSO_4$ |
| | Gypsum | $CaSO_4 * 2H_2O$ |
| | Kieserite | $MgSO_4 * H_2O$ |

In addition to aridity, the evaporite basin must be fully or partial isolated from the open ocean in order to precipitate evaporites. Isolated deep-water basins enable the concentra-

tion of salinity to exceed the salinity of normal seawater (3.5 ‰). The hypersaline brine will be concentrated to a point where evaporite mineral precipitation occurs (Schwab, n.d.). The evaporites usually occur in cycles, where each stage of this cycle represents a certain concentration of seawater (Kendall, 1988). Marine evaporites precipitate in a set order, with the more insoluble minerals precipitating first (Schwab, n.d.) (figure 4.1). When 50 ‰ of the original water volume remains, carbonates will begin to form. Gypsum or anhydrite, depending on the temperature, will be formed when the seawater volume is reduced to one-fifth of the original, and more soluble minerals such as halite will form when 10 ‰ of the original volume remains. When the original water volume has been reduced to 1.5 ‰ and exceptionally high levels of concentration has been reached, potassium chlorides like sylvite (KCl), and potassium and magnesium sulphates (K-Mg salts) will precipitate (GeoconservationUK, n.d.). The loss of brine volume and brine level in the basin is called "evaporative drawdown" (Kendall, 1988). From time to time the basin can be refilled by periodic breaching of the barrier, either by crustal down-warping or by sea-level changes. This makes it possible to deposit a thick, regionally extensive evaporite sequence (Schwab, n.d.).

Salt tectonics

The term "salt" are often used for rock bodies composed of mostly halite (NaCl), with varying amounts of other evaporites. Salt is mechanically weak and flows like a fluid. It is hard to compress and is therefore less dense than all moderate to fully compacted siliciclastic rocks and most carbonates. Due to the incompressibility and its fluid rheology, it is unstable under a wide range of geologic conditions. Because of the unique properties of salt, basins having salt tend to deform more easily than basins without salt. Deformation involving flow of salt is referred to as salt tectonics. The primary driving force for salt tectonics is differential loading, which includes gravitational loading, displacement loading and thermal loading. The salt will move if the driving forces overcome the resisting forces (Hudec & Jackson (2007)).

Salt layers are gravitationally unstable under modest differential loading or tilting, so most basins containing salt are spectacularly deformed. It is very difficult to restore a highly deformed salt basin back to its original configuration because of the extreme strains within the salt layer. The knowledge about the early stages of gravitational spreading, in particular initial flow regime of the salt and localization of detachments, is therefore limited. Top and base salt are commonly reasonably well imaged in seismic data, but

internal continuous seismic reflections that act as maskers for deformation within the salt is rare to image due to the reflectivity in the salt. The salt body is therefore usually featureless with incoherent seismic facies (Cartwright *et al.*, 2012).

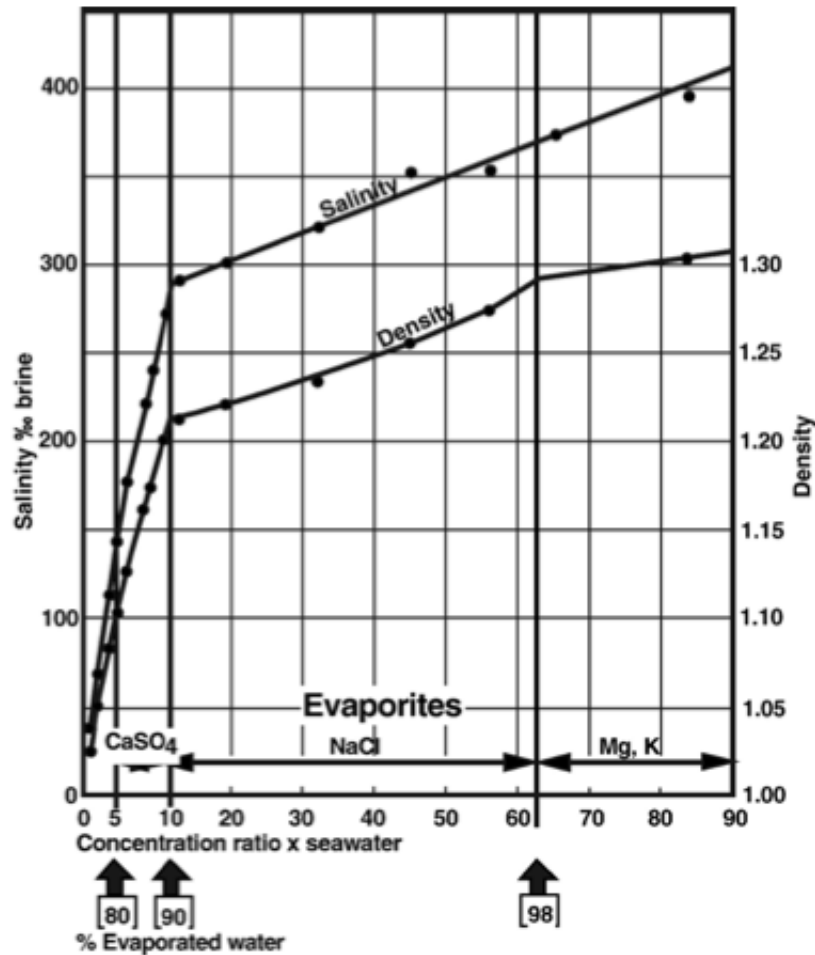


Figure 4.1: The curve presents the evaporated water versus brine concentration and density. Less soluble minerals such as carbonates precipitate before the more soluble salts (Mg, K). The curve of brine concentration and density increases during the processes of evaporation, with indication of water evaporated at each stage. The evaporation rate decreases with increasing concentration because of the activity of water in the solution. Therefore, the evolution towards the highest levels of concentration is progressively slowing down. Left y-axis: Salinity ‰ brine; Right y-axis: Density; x-axis: Concentration ratio x seawater, ranging from 0 to 90. The arrows below the lower x-axis are marking 80, 90 and 95 % of evaporated water. Source: Rouchy and Caruso (2006).

Chapter 5

Data and Methodology

Seismic data

The main dataset used in this study consists of three-dimensional (3D) seismic data that covers an area of approximately 5370 km^2 . The seismic survey is a continuous PGS 3D PSDM MegaSurvey that consists of several seismic surveys that has been matched, merged and depth migrated in 2013 by PGS. The survey consists of 5001 inlines and 3079 crosslines with an interval length of 25 m. In addition, an extra 1870 km^2 of data is used for correlation with the Levant margin.

The dataset is full stack seismic data and kirchhoff pre-stack depth migration (PSDM) has been performed. The seismic data has zero phase polarity and negative amplitudes correspond to increase in acoustic impedance. In this dataset red color represents positive amplitudes and blue color is negative amplitudes (figure 5.1). The seabed has negative amplitude and is blue in color. The quality of the 3D depth migrated data is remarkably good and details that were not possible to see in the time migrated data can now be studied. The location of the area that is covered by the seismic data is represented in figure 5.2.

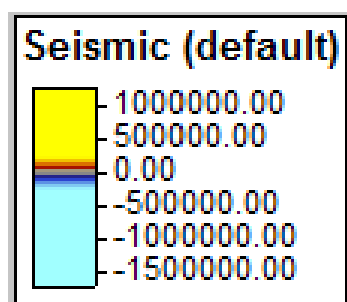


Figure 5.1: Legend of seismic survey. Red color represents positive amplitudes and decrease in acoustic impedance. Blue color represents negative amplitudes and increase in acoustic impedance.

Methodology

The program used to interpret the seismic data in this thesis is Petrel E&P Software Platform 2013 from Schlumberger. Petrel has been used to observe and interpret seismic packages and their bounding surfaces in the Levant Basin. The horizon interpretation has been carried out by tracing reflective events. There are no well data available for me from the northeastern Levant Basin, so the ages proposed for the seismic units are based on character description of the seismic packages from literature studies. The seismic horizons were interpreted using seeded 2D autotracking and guided autotracking. The *Surface* process was used to make surfaces of the mapped horizons. The study area is very big and contains huge amounts of data. The interpretation part of this thesis has therefore taken a lot of time.

Maps based on seismic attributes have been created by extracting data across a surface from the seismic volume. An overview of the attributes that have been used to generate maps can be found in table 5.1.

Table 5.1: Overview of seismic attributes that has been used to generate attribute maps. If a certain window length has been used, it will be specified in the figure text of the map.

| Attribute | Description | Process in Petrel |
|-------------------|---------------------------------------------------------------------------------------------------------|--------------------|
| Thickness | Gives a thickness map in meters by subtracting one surface from another. | Calculator |
| RMS Amplitude | Computes Root Mean Squares on instantaneous trace samples over a specified window. | Surface attributes |
| Maximum Amplitude | Measures reflectivity within a depth window. Returns the maximum positive number in the defined window. | Surface attributes |
| Minimum Amplitude | Measures reflectivity within a depth window. Returns the maximum negative number in the defined window. | Surface attributes |

An overview of the workflow in Petrel and after can be seen in figure 5.3. Adobe Illustrator CSS has been used to create a good presentation of the pictures, by drawing the outline of a shape and then assign it a fill. This gives the reader a better understanding of what is presented.

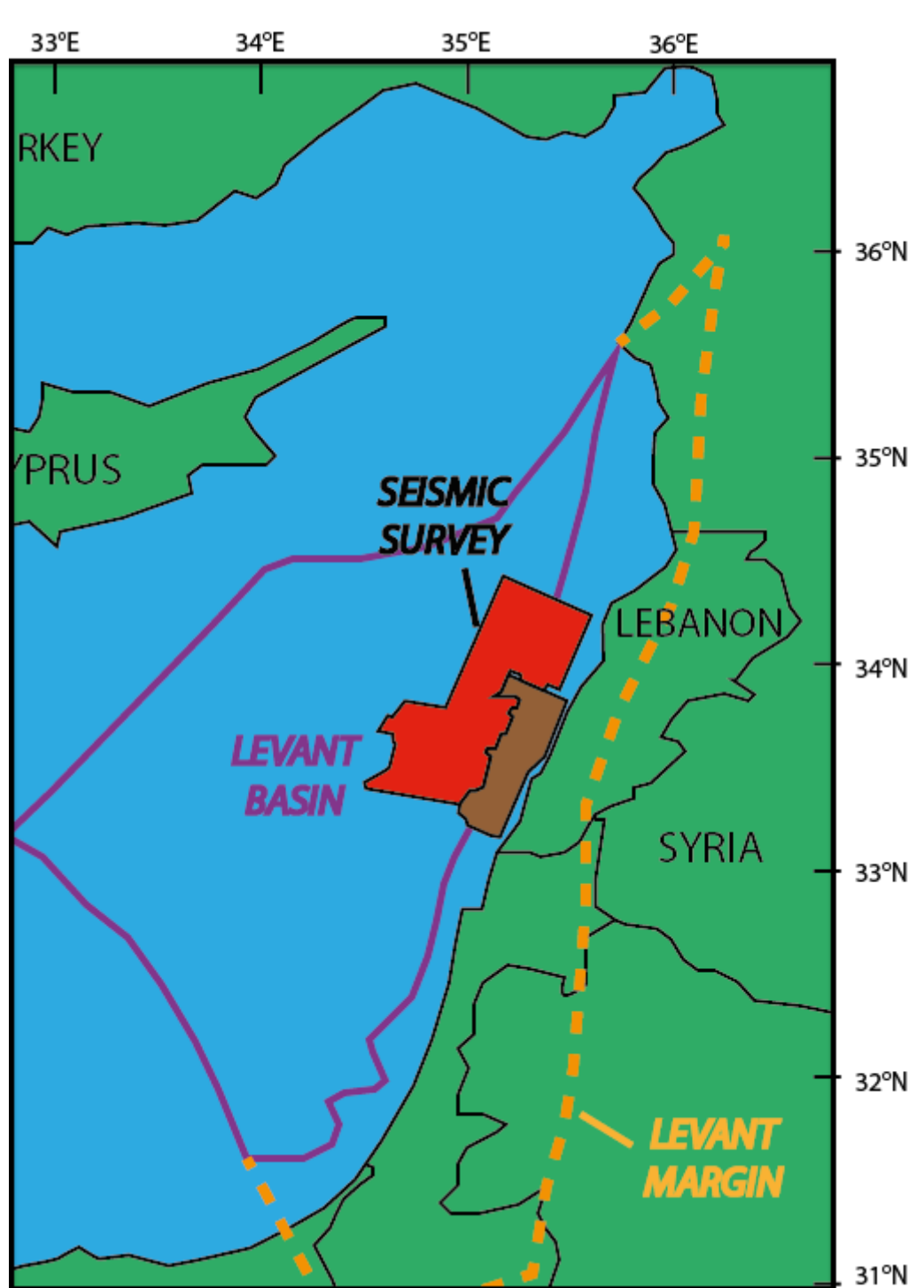


Figure 5.2: Map showing the location of the 3D seismic survey in the Levant Basin. The red area represents the main seismic dataset used in this study. The brown area represents additional data used for correlation of the seismic data from the basin to the margin. A purple line outlines the Levant Basin, and the yellow dashed line marks the Levant Margin. The study area is offshore southern and middle Lebanon.

Workflow

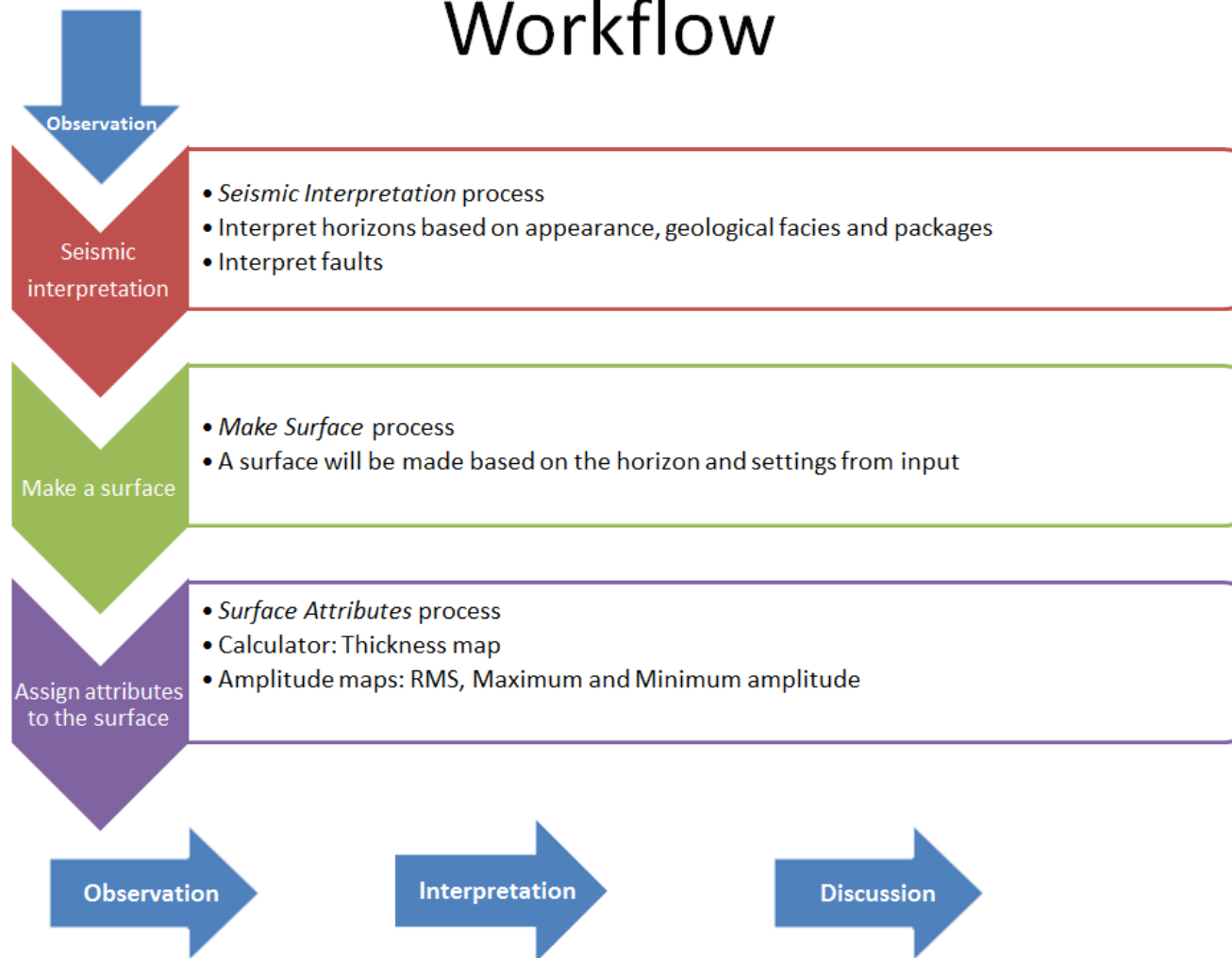


Figure 5.3: The figure presents the workflow in Petrel and the process after. The work started with observation of the seismic data, then horizons and faults were interpreted. The following step was to make surfaces that could be used in attribute analyses. The resulting maps were compared with observations in the seismic sections and then interpreted. The final step in the workflow was to discuss chosen topics from the results.

Chapter 6

Regional Seismic Interpretation

The stratigraphic focus of this chapter extends from the Upper Cretaceous to Recent. Three representative seismic sections have been chosen in order to describe the geological settings in this area based on seismic data (figure 6.1).

Nine horizons (including the seafloor) were identified and interpreted on the 3D seismic profiles and will in this study be referred to as *R1* (oldest) - *R9* (youngest). These horizons have been chosen based on their appearance (i.e. amplitude and continuity) and the way they are separating seismic packages (SP) with different seismic facies and stratigraphic contacts. The Levant Basin can further be separated into three units, based on appearance and depositional history, where each seismic package belongs to one of the units (Table 6.1). A seismic interpretation for each unit will be presented based on the three seismic sections.

Reflectors R1, R2 and R3 were picked in order to get an overview of the geological history. They are, however, not of interest for the main focus of this thesis and have therefore not been interpreted in such a detail. Reflectors R4 - R9 are much more continuous than the lower reflectors, and are more important for the detailed study of the younger sediments. Surface maps of horizons R4-R9 can be seen in the Appendix.

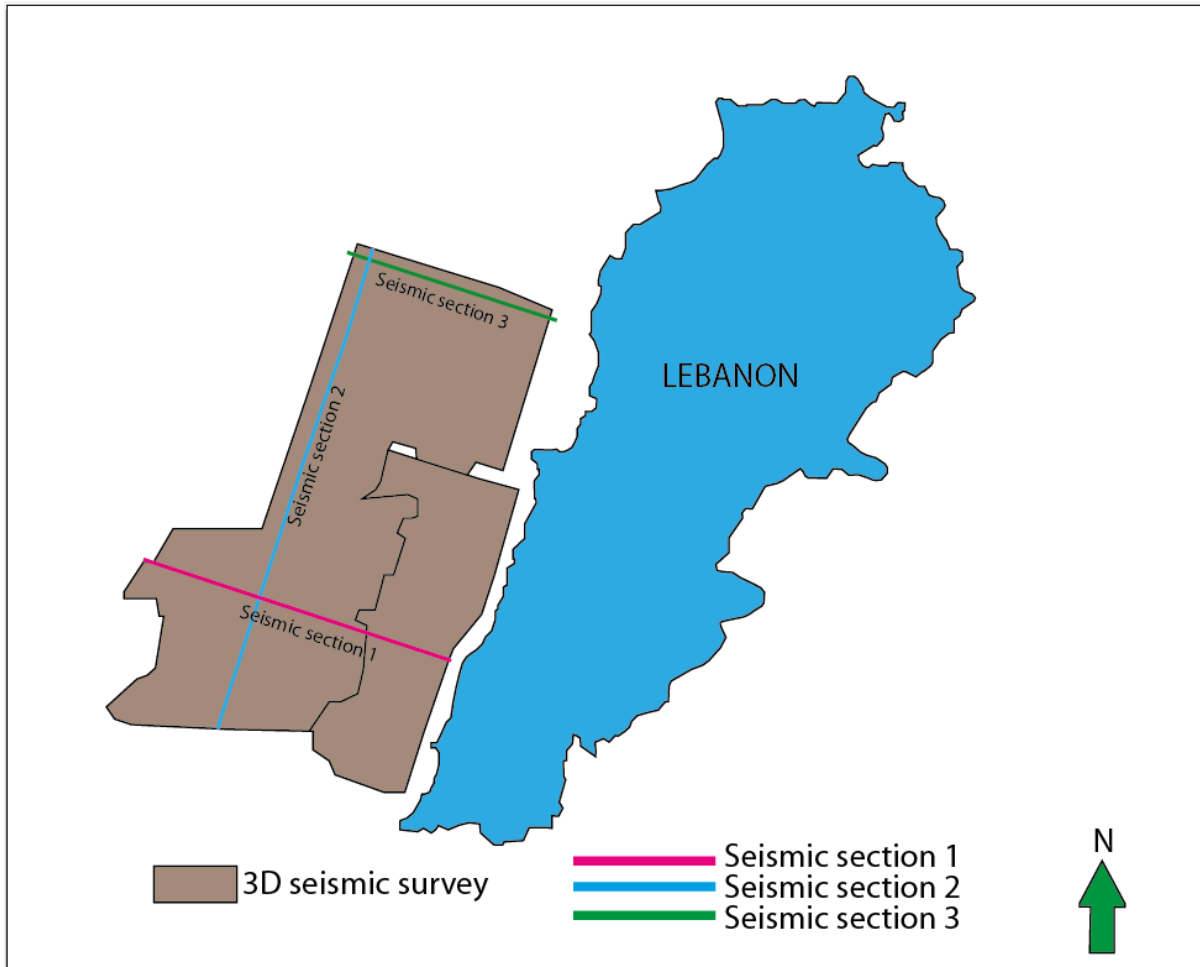


Figure 6.1: Map showing the 3D seismic survey with location of the three representative seismic sections that have been interpreted. Pink line: seismic section 1; Blue line: seismic section 2; Green line: seismic section 3; brown area: area for 3D seismic survey; Blue area: Lebanon; Green arrow: Direction of North.

Table 6.1: The table presents an overview of the interpreted horizons (R1-R9) and the seismic packages (SP) that they are bounding. Based on depositional history, the seismic sections can be divided in three different units (Unit 1-3), where the seismic packages have gotten their names based on which unit they belong to. In addition, the deposition (Dep.) column shows whether the seismic packages were deposited prior to or after salt deposition. The deposits within Unit 1 is older than Unit 3.

| Reflector | Unit | SP | Dep. |
|-----------|------|--------|--------------|
| R9 | 3 | | POST SALT |
| | | SP 3.4 | |
| R8 | | | |
| | | SP 3.3 | |
| R7 | | | |
| | | SP 3.2 | |
| R6 | | | |
| | | SP 3.1 | SALT |
| R5 | 2 | | PRE SALT |
| | | SP 2.3 | |
| R4 | | | |
| | | SP 2.2 | |
| R3 | | | |
| | | SP 2.1 | |
| R2 | 1 | | |
| | | SP 1.2 | |
| R1 | | | |
| | | SP 1.1 | |
| | | | |

6.1 Seismic Sections

The following three sections are chosen in order to give an interpretation of the Levant Basin and its geological history. They are taken from different parts of the basin and will together give a good overview of the northeastern part of the Levant Basin.

Seismic Section 1

Seismic section 1 shows an W(NW)-E(SE) crossing inline from the basin and up to the margin (figure 6.2). Location of the section can be seen in figure 6.1.

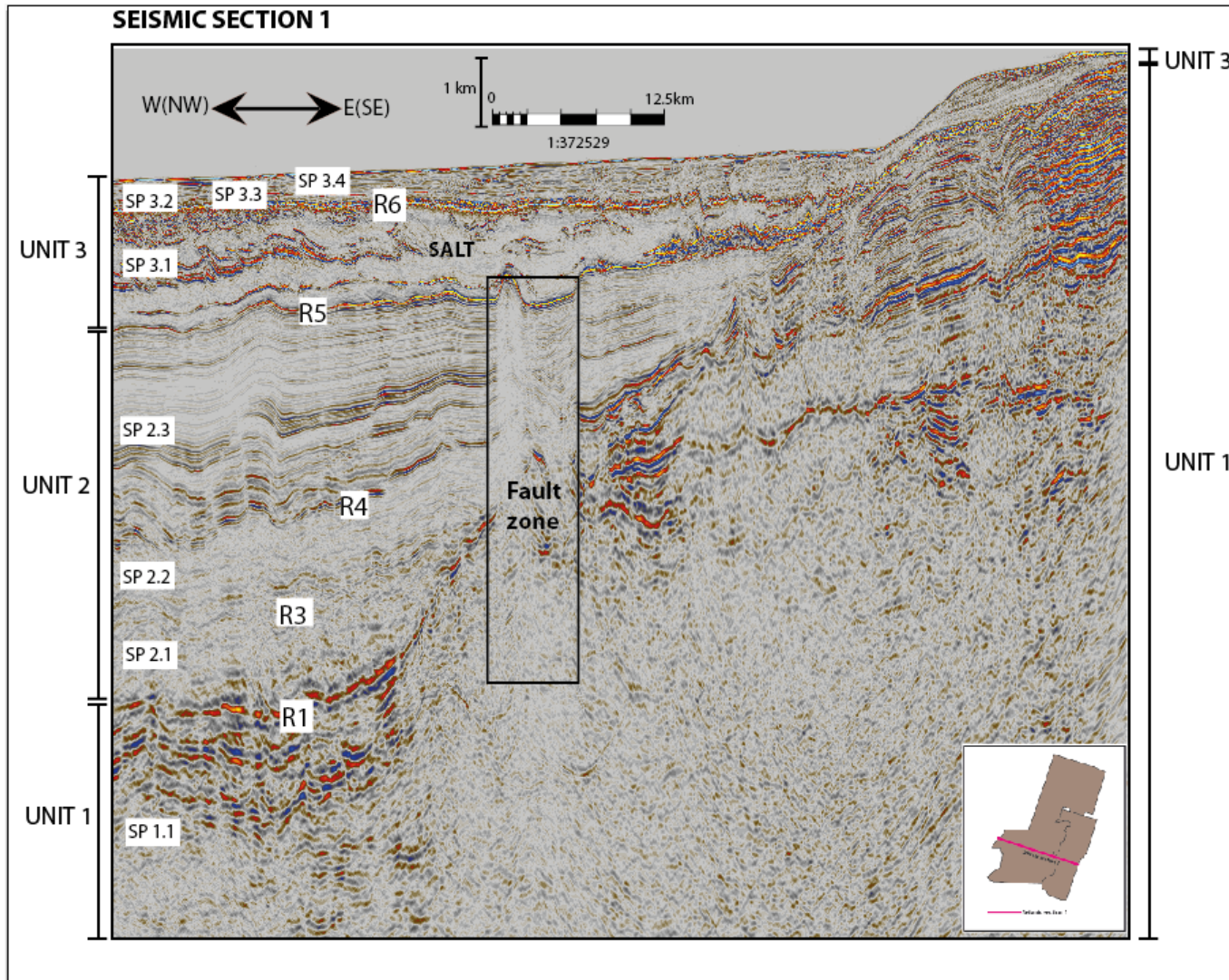


Figure 6.2: Seismic section 1. Inline crossing the area from W(NW) to E(SE). Units 1-3, Seismic packages (SP) 1.1 - 3.4 and Reflectors R1-R9 are marked on the section. These will be further described in section 6.2-Units. A fault zone consisting of many smaller strike-slip faults is marked in the section. The fault zone is influencing Unit 1 and Unit 2, and the base of Unit 3. Location map can be found in the lower right corner of the section, for more details see figure 6.1.

Seismic Section 2

Seismic section 2 shows an S(SW)-N(NE) crossline semi-parallel with the coastline (figure 6.3). Location of the section can be seen in figure 6.1.

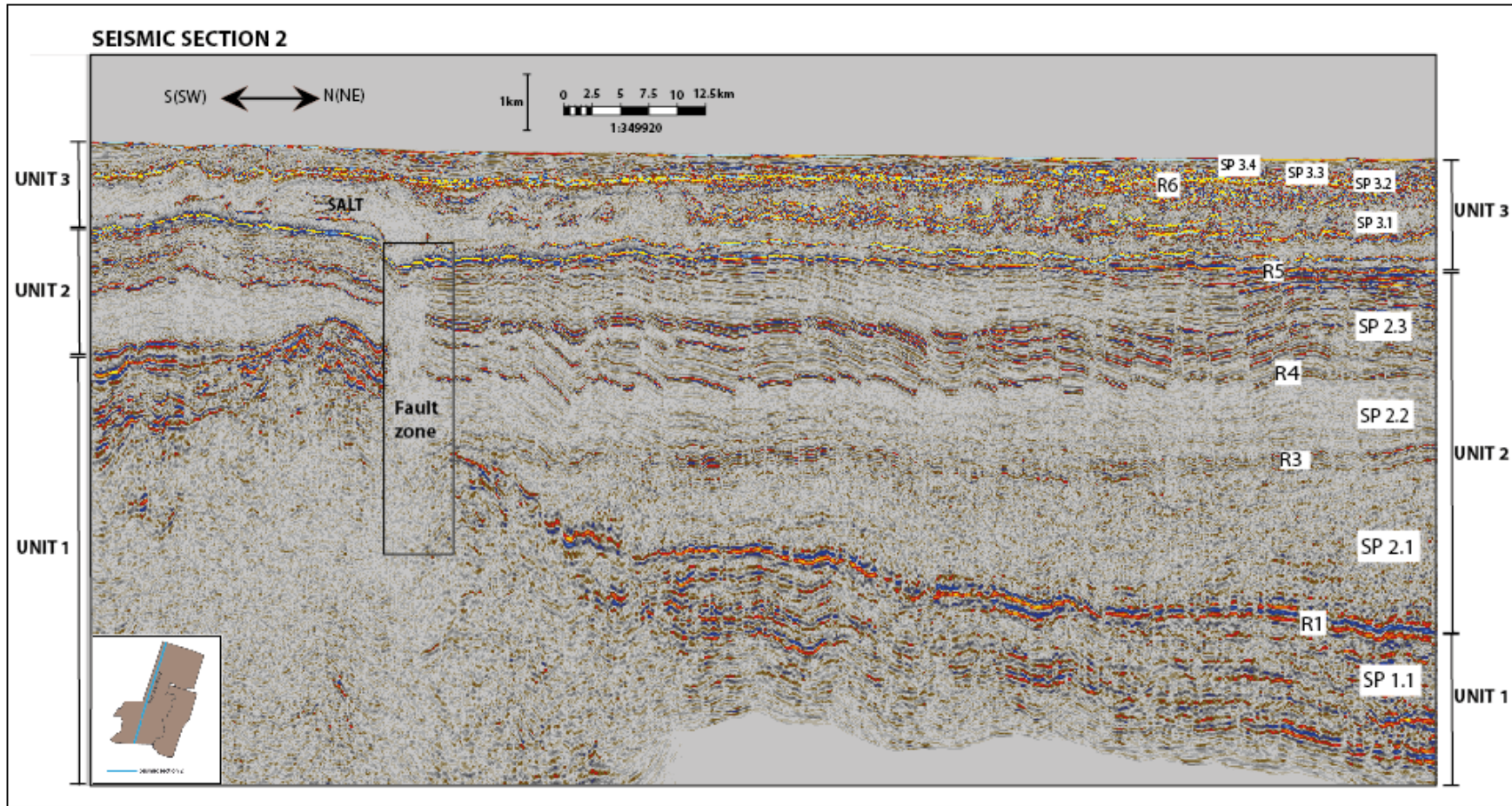


Figure 6.3: Seismic section 2. Crossline crossing the area from S(SW) to N(NE). Units 1-3, Seismic packages (SP) 1.1 - 3.4 and Reflectors R1-R9 are marked on the section. These will be further described in section 6.2-Units. A fault zone consisting of many smaller strike-slip faults is marked in the section. The fault zone is influencing Unit 1 and Unit 2, and the base of Unit 3. Location map can be found in the lower left corner of the section, for more details see figure 6.1

Seismic Section 3

Seismic section 3 shows an W(NW)-E(SE) crossing inline from the basin and up to the margin (figure 6.4). This inline is located further north than Seismic section 1. Location of seismic section 3 can be seen in figure 6.1.

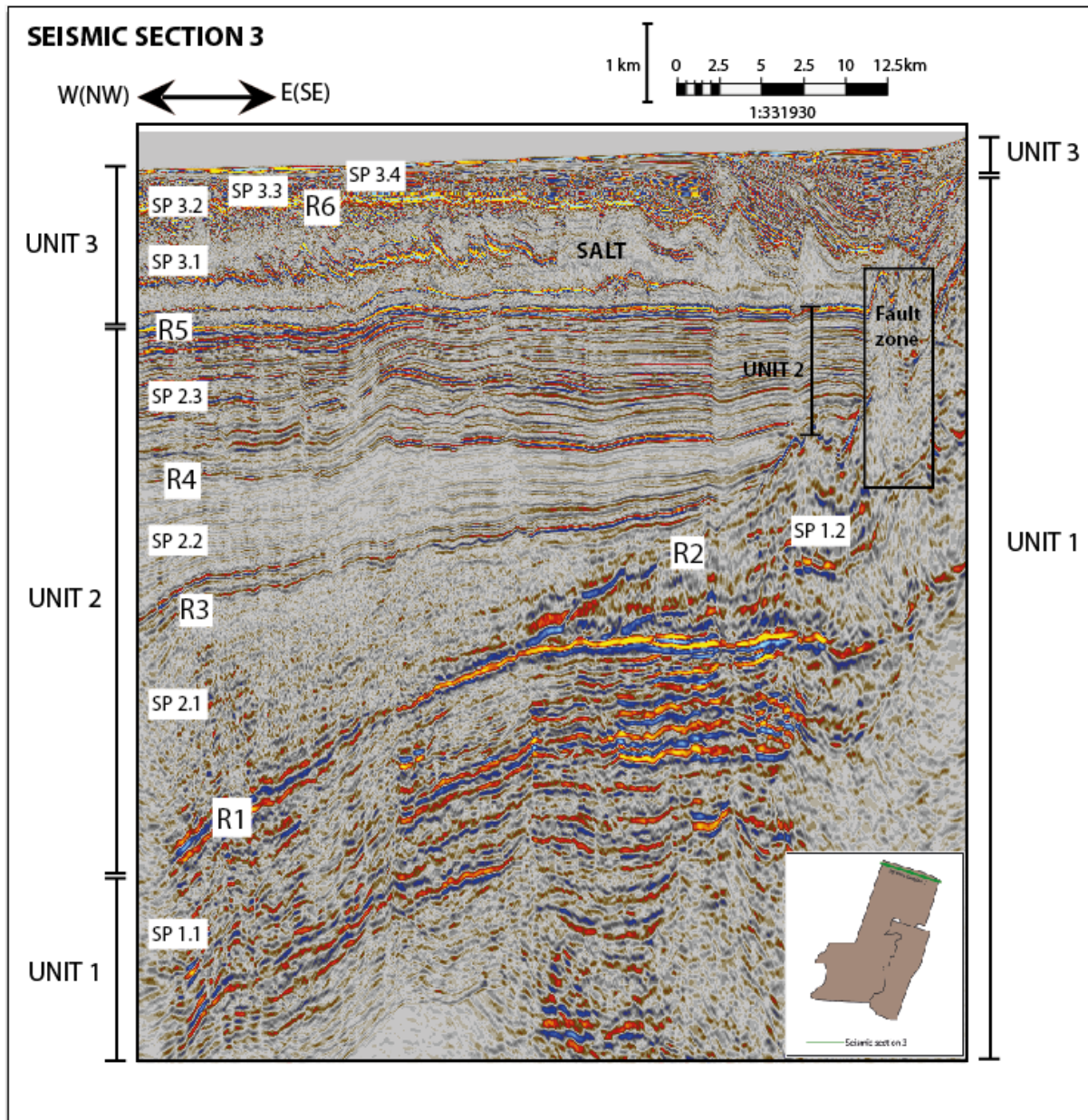


Figure 6.4: Seismic section 3. Inline crossing the northern area from W(NW) to E(SE). Units 1-3, Seismic packages (SP) 1.1 - 3.4 and Reflectors R1-R9 are marked on the section. These will be further described in section 6.2-Units. A fault zone consisting of many smaller strike-slip faults is marked in the section. The fault zone is influencing Unit 1 and Unit 2, and the base of Unit 3. Location map can be found in the lower right corner of the section, for more details see figure 6.1.

6.2 Units

See seismic sections 1-3 (figure 6.2 - figure 6.4) when the units and seismic packages are explained in the following sections.

Unit 1

The top of Unit 1 is marked by horizon R1 in seismic section 1 and 2, and by horizon R2 in section 3. These horizons separate Unit 1 from Unit 2 horizontally. Vertically, Unit 1 is separated from Unit 2 by a major strike-slip fault zone. Many smaller faults can also be observed in this unit. The fault zone is dividing Unit 1 into two parts, where one side is elevated and laterally moved compared to the other side.

SP 1.1

SP 1.1 can be observed in all three seismic sections and is bounded on top by horizon R1, which is the deepest horizon interpreted.

In seismic section 1, SP 1.1 is the only package in Unit 1. High amplitudes can be observed in the upper part of the package. On the eastern side of the fault zone (figure 6.2), the upper strong amplitude reflectors seems to be thinning towards the fault zone (figure 6.5).

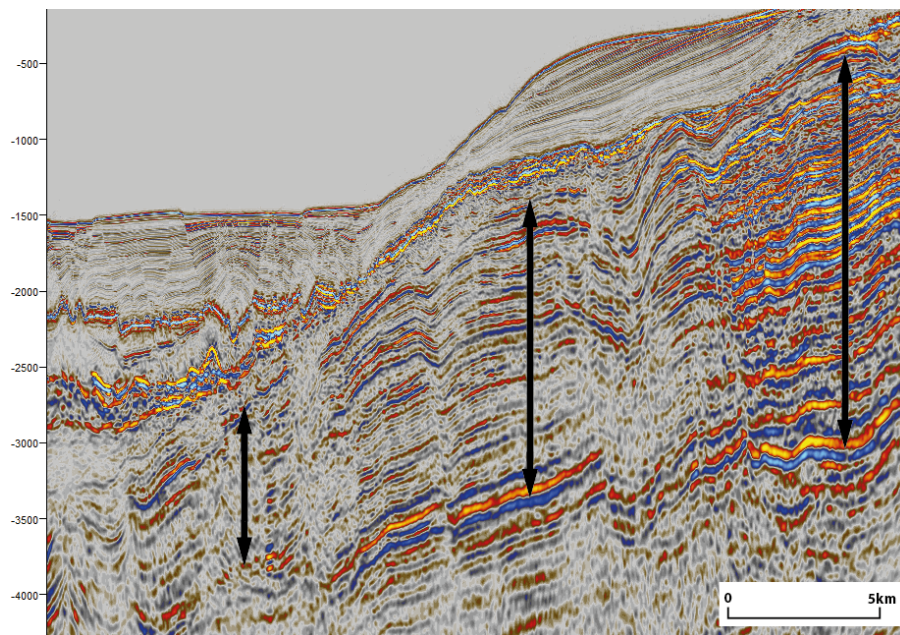


Figure 6.5: The arrows in the figure indicate how seismic package (SP) 1.1 in seismic section 1 (figure 6.2) is thinning towards the fault zone (towards left)

In seismic section 2, the same strong amplitudes can be observed, and the layers are almost stratified and partly continuous in the northern part of the section. A difference of more than 3 km is present between the southern and northern part of the fault zone, and the northern part has subsided.

More distinct subsidence can be observed in section 3, where the layers are dipping. After being deposited flat, the package has subsided more than 3 km (figure 6.6). R1 is interpreted to be a regional unconformity of Late Cretaceous age, and the sediments in SP 1.1 are therefore of Late Cretaceous and older age, and consist mainly of carbonates.

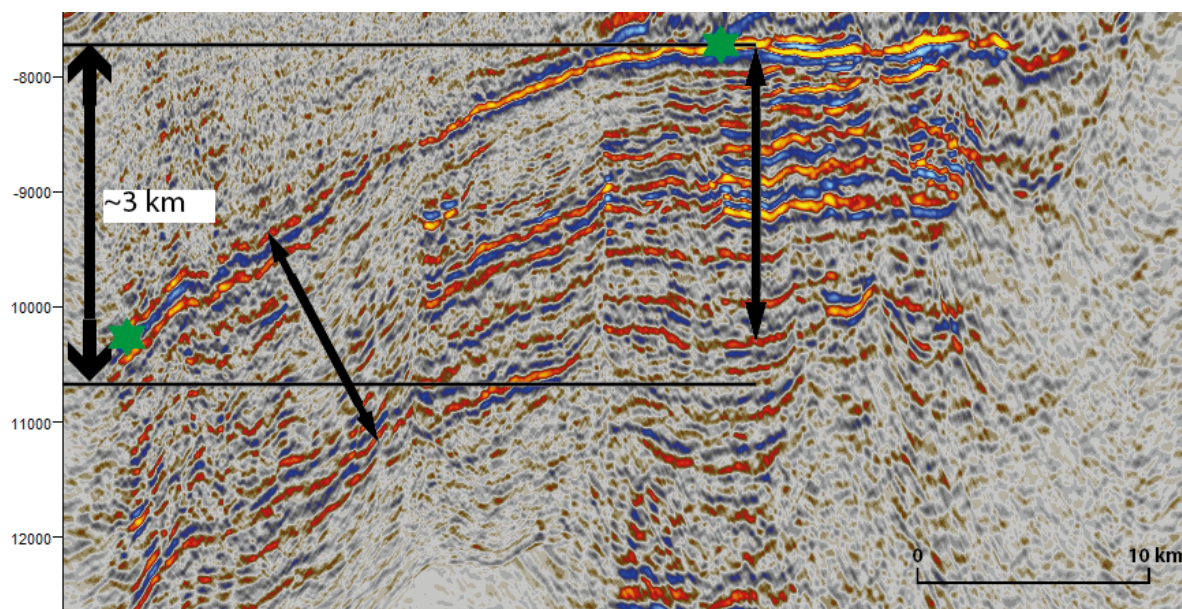


Figure 6.6: A close-up of SP 1.1 in seismic section 3 (figure 6.4). The green stars are marking the top of the package. The depth distance between the two green stars are approximately 3 km. Thin, black arrows show how the package has subsided.

SP 1.2

SP 1.2 is only present in seismic section 3. This package is deposited on top of SP 1.1. Horizon R2 is bounding this build-up, and clearly separate these sediments from the ones to the left of it (figure 6.7). SP 1.2 is interpreted to be a carbonate platform that has been deposited in shallow water. In order to maintain shallow water, this deposition must have been associated with relative sea-level changes.

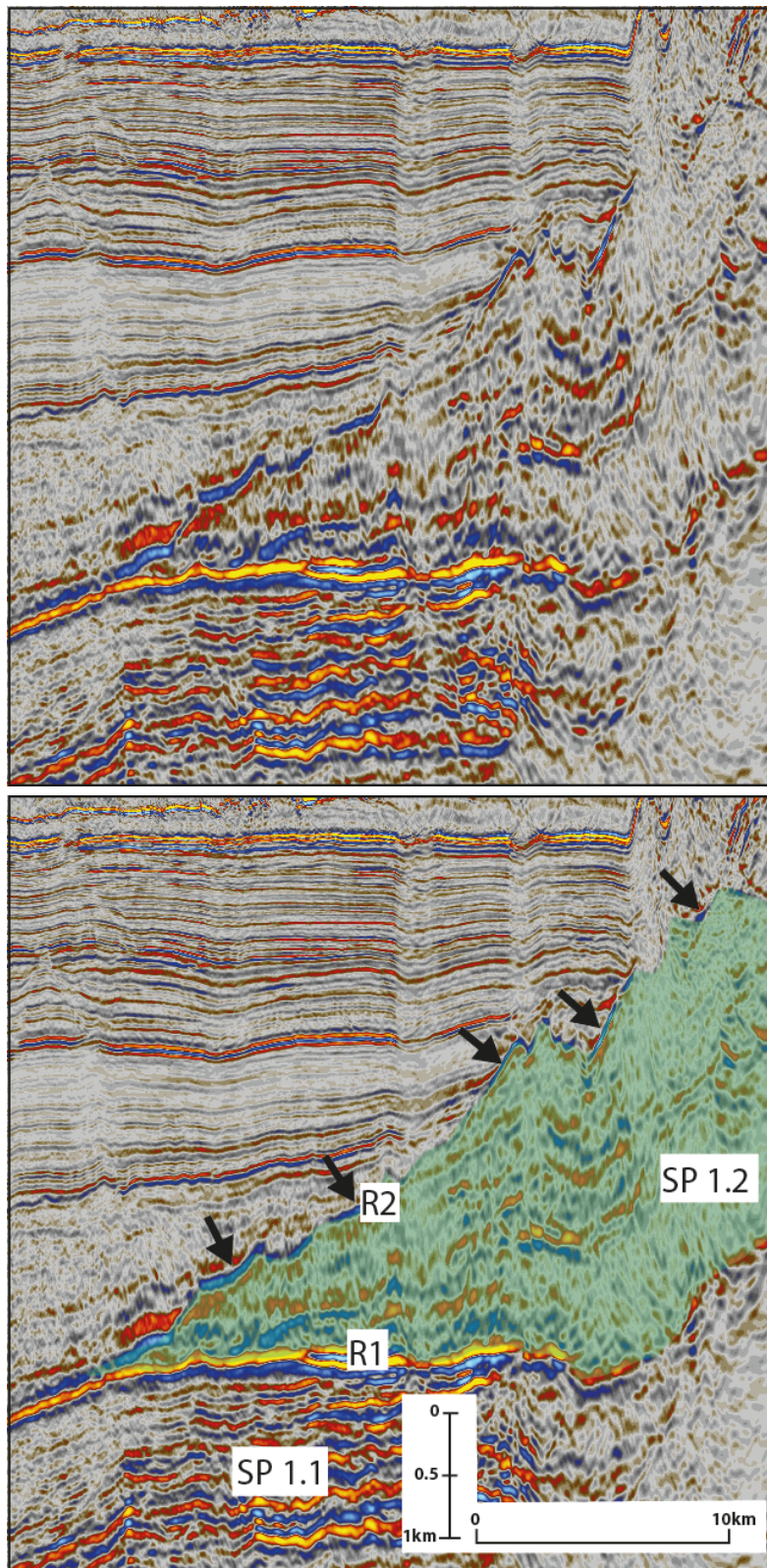


Figure 6.7: Close-up of SP 1.2 in section 3. **Upper figure:** Uninterpreted seismic package. **Lower figure:** Interpreted seismic package. Horizon R2 (marked by the arrows) is clearly marking the boundary around the carbonate build-up. The green area marks the SP 1.2, which is interpreted to be a carbonate platform.

Unit 2

Unit 2 represents a basin with sediment infill that is approximately 6 km thick at its thickest in these sections and consists of siliciclastic sediments. These sediments have accumulated most likely by massive subsidence of the basin. Unit 2 has been divided into three seismic packages.

SP 2.1

Horizon R1 is overlain by the Seismic Package (SP) 2.1. The SP appears chaotic, but some stratification in the lower part of the package in section 2 and 3 can be observed. The package seems to be onlapping the basin margin of Unit 1 updip from the basin, while it is thickening toward the basin. In section 3 the package appears to be pinching out on the carbonate margin of SP 1.2. SP 2.1 is interpreted to be of Late Cretaceous to Eocene age, with a mix of carbonates and siliciclastic sediments.

SP 2.2

SP 2.2 is bounded on the base by horizon R3 and on the top by horizon R4. There seems to be an almost uniform accumulation of the sediments in SP 2.2 in section 1. The lower part of the package is partly stratified and has higher amplitudes than the upper part of the package. The SP is cut by the fault zone in the eastern part of the basin and it is uncertain whether this package can be found on the other side of the fault zone or not.

The sediment accumulation in section 2 is also uniform. The package is stratified, with higher amplitudes at the base of the package. Some faulting in the upper part of the SP can be observed. The same stratification in SP 2.2 can also be seen in section 3. The package appears to be thickening towards the basin and it is onlapping the carbonate margin of SP 1.2 where the thickness is only a couple hundred meters. The sediments of SP 2.2 are interpreted to be of Oligocene age and are mainly dominated by siliciclastic sediments.

SP 2.3

The SP 2.3 is separated from SP 2.2 by horizon R4, and the sediments have been accumulated by subsidence. An increase in thickness towards the basin can be observed in section 1. The thickness changes from approximately 2 km by the fault in the middle of the section to 3 km in western side of section 1. Whether the SP is continuing on the other side of the fault zone and pinching out on the basin margin of Unit 1 is uncertain. The package is stratified, with higher amplitudes in the middle of the package. Faulting and folding of this package can be observed. The same characterization of SP 2.3 can be observed in section 3, only here the accumulation appears more uniform.

The most remarkable difference of this package between the sections can be observed

in section 2. The uniform accumulated, stratified layers have been severely faulted (figure 6.8). The faulting is continuous throughout SP 2.3 but dies out in SP 2.2 below and SP 3.1 above. The faulting must therefore have occurred during the beginning of deposition of the evaporites in SP 3.1. SP 2.3 has been interpreted to be of early Late Miocene age and is the last package of Unit 2.

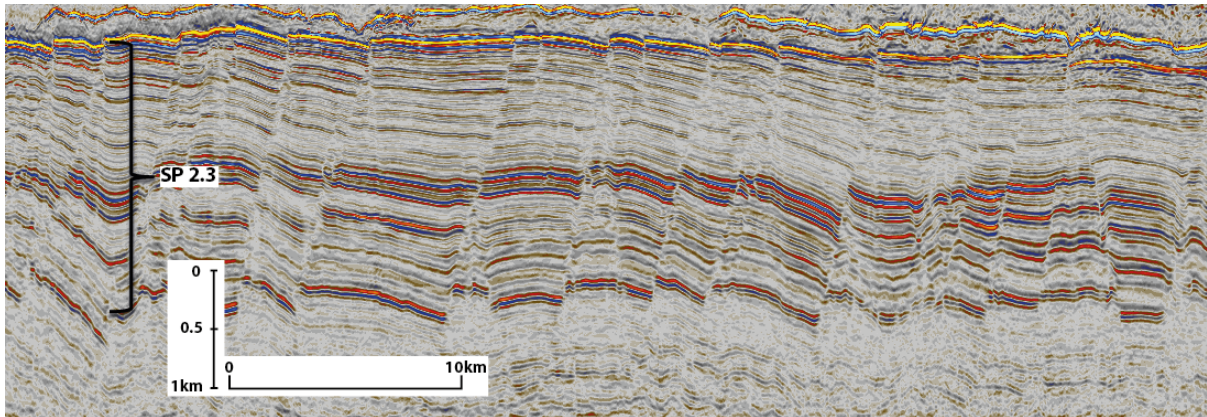


Figure 6.8: Severely faulting can be observed in SP 2.3 in section 2. The faulting dies out in the SP 2.2 below and in the SP 3.1 above.

Unit 3

Unit 3 is a part of the basin infill as Unit 2, but the base of Unit 3 is eroding the top of Unit 1 on the margin to the east. Unit 3 is approximately 2.2 km at its thickest in these sections, which is a lot thinner than Unit 1 and 2. Due to the thin seismic packages in the upper part of Unit 3 and the resolution of the pictures, the details of Unit 3 is hard to observe in section 1-3 (figure 6.2-figure 6.4).

SP 3.1

SP 3.1 is bounded at the base by R5 and at its top by R6. Horizon R5 is separating SP 2.3 in Unit 2 from SP 3.1 in Unit 3 in the basin, and separating Unit 1 from Unit 3 in the eastern margin. R5 is a regional unconformity surface that marks the beginning of the Messinian Salinity Crisis when a thick section of salt was deposited in the Mediterranean Sea (see chapter 3.2). R5 is a high-amplitude seismic reflection (peak, red/yellow color display) generated by the high negative acoustic impedance contrast between the underlying Oligocene clastics and the overlying Messinian evaporites. It is often referred to as Horizon N in literature. Horizon R5 is continuous and relatively undeformed. It is mainly conformable with the underlying Miocene reflections, but appears to be faulted in some areas. Some truncations can be observed in the marginal part of the area.

Horizon R6 marks the top of the Messinian evaporites and is an erosional surface. R6 is a high-amplitude seismic reflection (trough, blue color display) generated by an increase in acoustic impedance. In literature, this horizon is referred to as Horizon M. R6 has been faulted in larger degree than horizon R5, and is truncated by the upper intra-evaporitic horizons. The horizon is continuous and almost horizontal across the study area.

SP 3.1 is a thick evaporitic unit that internally is composed of an alternation of reflection-free facies and layered seismic facies. Three major high-amplitude reflection facies can be observed intercalating into the transparent facies (figure 6.9). The evaporite package is known as the Messinian evaporites and was deposited in the Late Miocene (Messinian) during the Messinian Salinity Crisis (MSC). Salt deformation can be observed in the evaporite package, where the middle and upper reflection levels are more deformed than the lower level, with both folding and faulting. Truncation of the upper level into horizon R6 can also be observed. The thickness of SP 3.1 varies from >1700 m in the basin to only a few meters where the salt wedge pinches out on the basin margin in east. Horizon R5 and R6 merge in this pinch-out point. A single seismic horizon is observed eastward of this convergence point (figure 6.15), characterized by a distinct erosional relief.

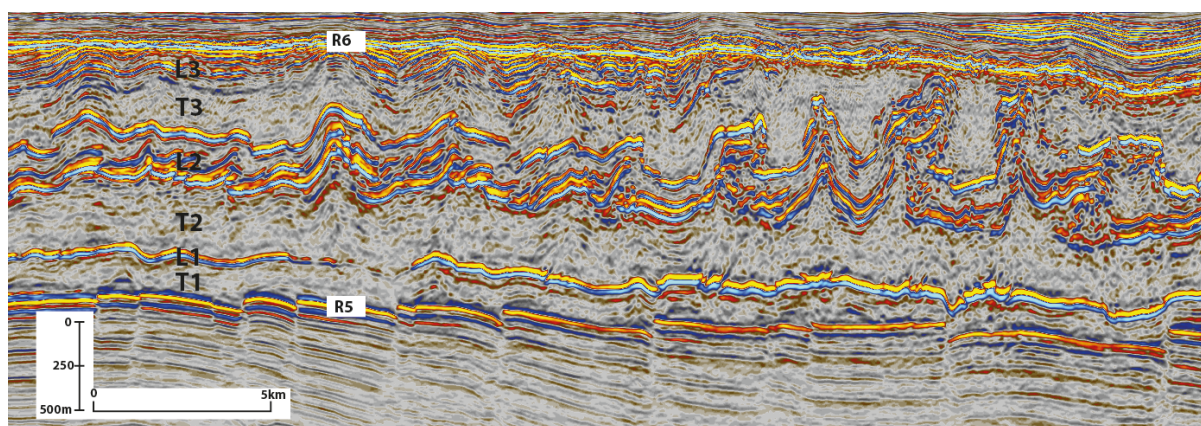


Figure 6.9: The figure shows a close-up of the Messinian salt (SP 3.1) in section 2. Two high-amplitude reflectors, R5 and R6, bound the salt. The evaporite package consists of intervals of transparent facies (T1-T3) and high-amplitude reflections (L1-L3). Faulting and folding of the reflective levels can be observed.

SP 3.2

SP 3.2 is bounded by the high-amplitude horizons R6 and R7, and represents a transition layer between the Messinian evaporites and the Pliocene marine sediments. The transition layer contains high-amplitude reflections within the layer, that are in some parts stratified and continuous, while in other parts appear discontinuous. A great thickness change of the layer can be observed, where the layer seems to be thinning towards the basin in west.

Several internal reflections can be observed where the layer is thicker, while in the areas where the layer is much thinner only one or two reflectors are present. The thickness of the layer changes from $\sim 150m$ at its thickest to only a few meters at its thinnest. SP 3.2 is absent in many of the areas where reflector R6 is faulted (figure 6.10). An important characteristics that can be observed is that this package tend to be abruptly cut many places, which may indicate that a channel have cut through the layer. Another important characteristic is that the layer breaks instead of being folded. This layer will be studied in more detail in chapter 7.

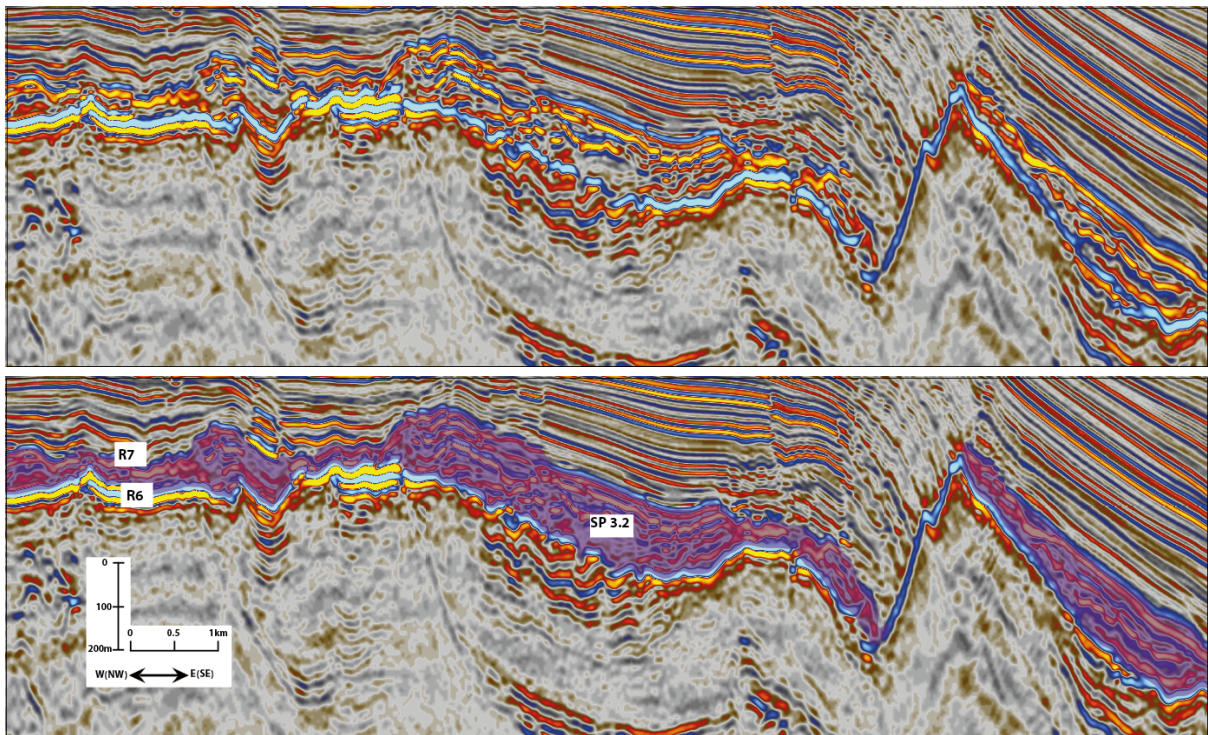


Figure 6.10: The transition layer (SP 3.2) between the Messinian evaporites and the Pliocene marine sediments contains high-amplitude reflections and thickness variations. The layer has been abruptly cut many places and faulted. This close-up is from seismic section 3.

SP 3.3

SP 3.3 (between R7 and R8) shows continuous and stratified layers with weaker amplitudes than SP 3.2. Higher amplitudes can be observed some places in the lower part of this package where SP 3.2 has been cut (figure 6.11). This could be channel fill that has been deposited where the transition layer (SP 3.2) has been cut. SP 3.3 consists of marine sediments from Pliocene age. These are the first sediments that were deposited after normal marine conditions were established, after the termination of the MSC.

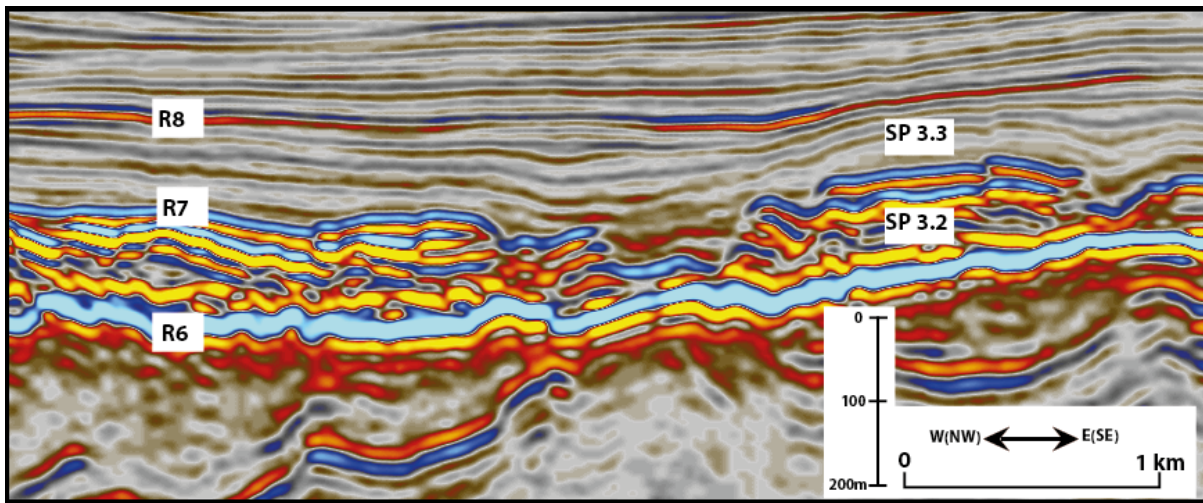


Figure 6.11: SP 3.3 in section 1 contains stratified and continuous layers with sediments of marine origin. The lower part of the package displays a different appearance than the rest of the package in the areas where SP 3.2 has been cut.

SP 3.4

SP 3.4 is the youngest package deposited and consists of marine sediments that are stratified and continuous. The appearance of SP 3.4 changes throughout the basin. Progradation of sediments towards the basin (west) can be observed in seismic section 1. This can be interpreted as a prograding seabed where the accommodation space was less than the sediment supply. figure 6.12 shows example of this prograding wedge of sediments.

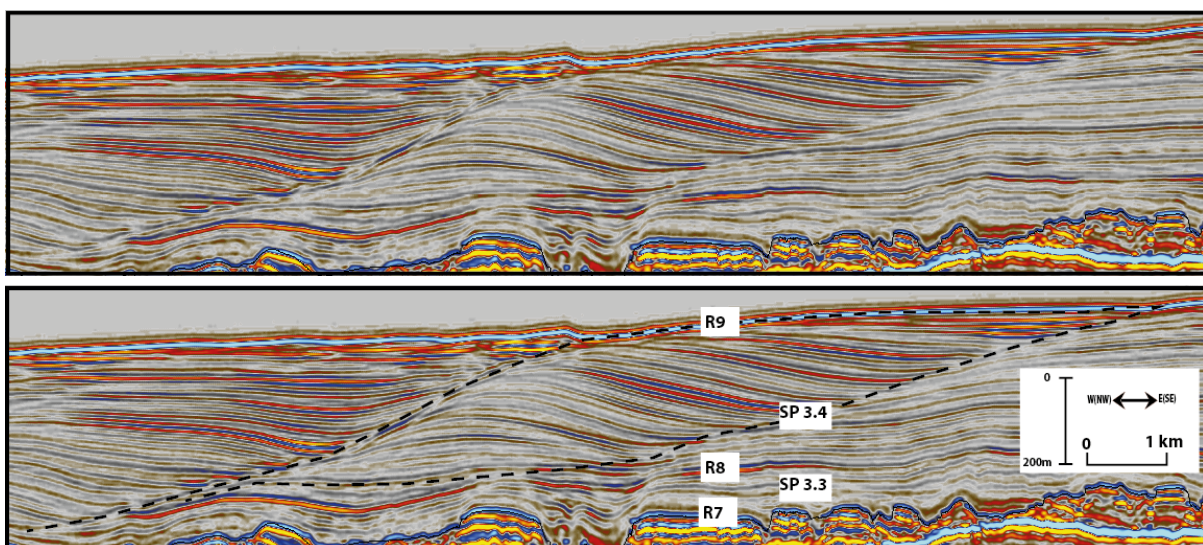


Figure 6.12: SP 3.4 consists of marine sediments that are stratified and continuous. Progradation of sediments towards west can be observed in section 1. This figure is a more detailed close-up of progradation from Inline 21660, which is oriented from W(NW)-E(SE).

Seismic section 3 reveals three different stress domains in the Pliocene-Pleistocene succession: a contractional domain with folding in the basin, an extensional domain with faulting in the slope areas and a translational domain between the other two (figure 6.13). In addition to the Plio-Pleistocene sediments, it can also be observed that the Messinian evaporites and the Transition layer have been partly folded in the contractional domain. The faulting in the extensional domain have also affected the top of the evaporites and the Transition layer. An approximate map of the structural domains based on the 3D seismic survey can be seen in figure 6.14.

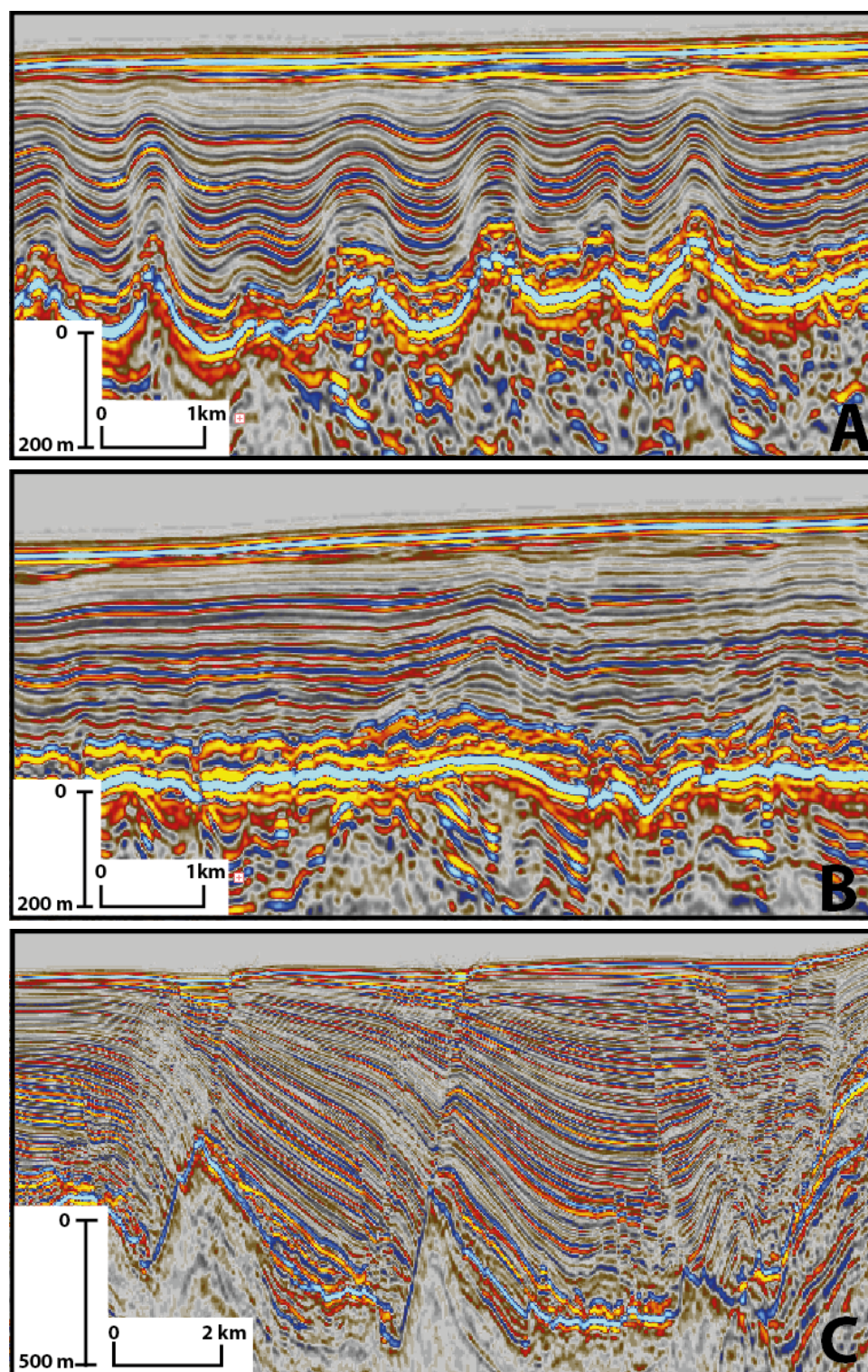


Figure 6.13: Three different stress domains in SP 3.4 can be observed in section 3. **(A):** Contractional domain in the basinal part of the area (west). It can be seen that the Plio-Pleistocene sediments and also partly the Messinian evaporites have been folded. **(B):** Translational domain in the middle of the area. The Plio-Pleistocene sediments are relatively undeformed. Only small extensional faults and contractional structures can be observed. **(C):** Extensional domain in the slope area (east), with large-scale faulting of the sediment succession.

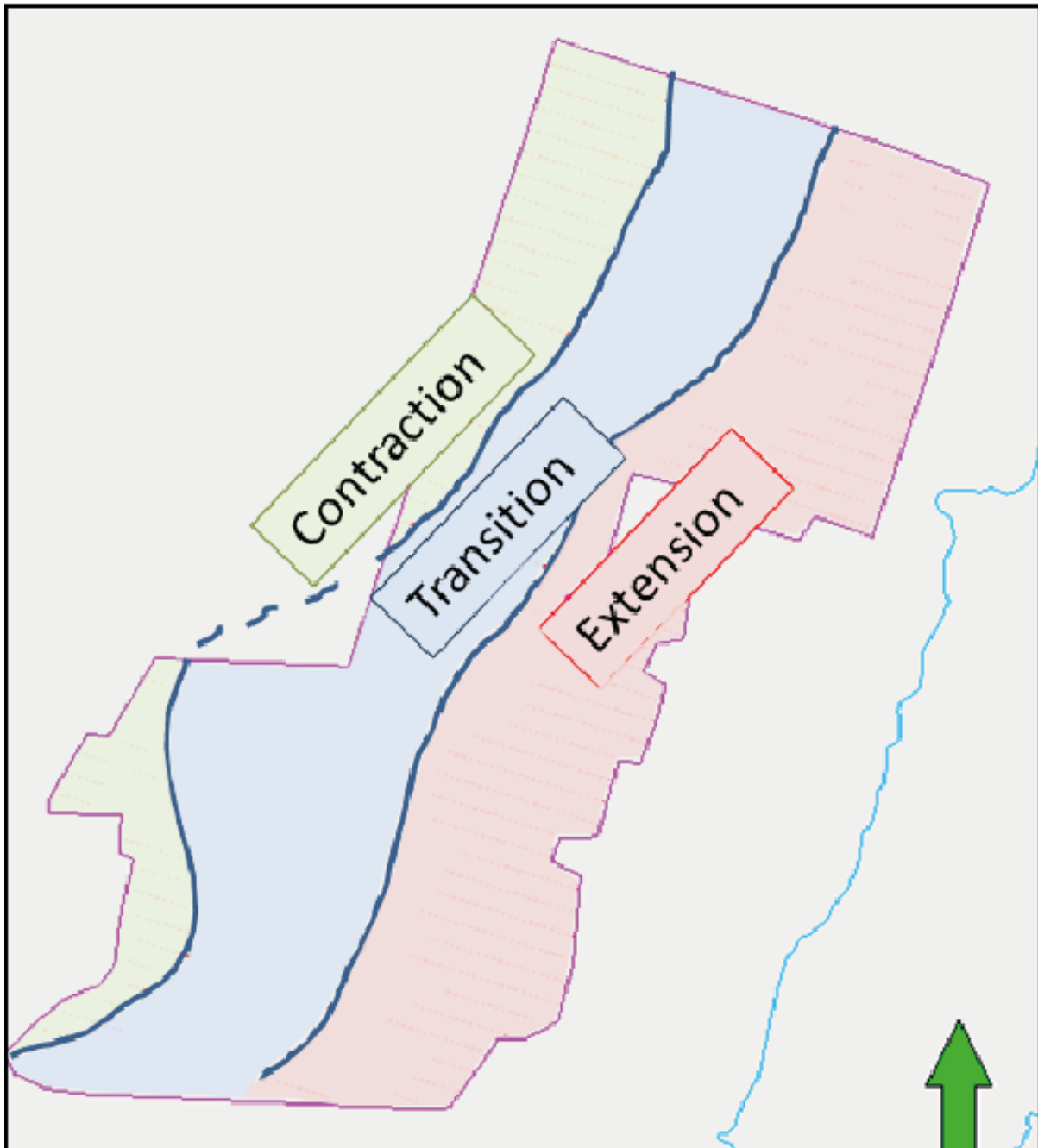


Figure 6.14: The map shows the approximate boundaries for the structural domains observed in the seismic survey. Three domains can be seen: An extension zone (pink) close to the margin, a transition zone (blue) in the middle, and a contraction zone (green) further out towards the basin. The dark blue lines mark the approximate boundaries. The light blue line is the coastline of Lebanon. The green arrow points the direction towards North.

6.3 Interpretation

Interpretation of the three seismic sections given in figure 6.2-figure 6.4 follows (figure 6.15 - figure 6.17).

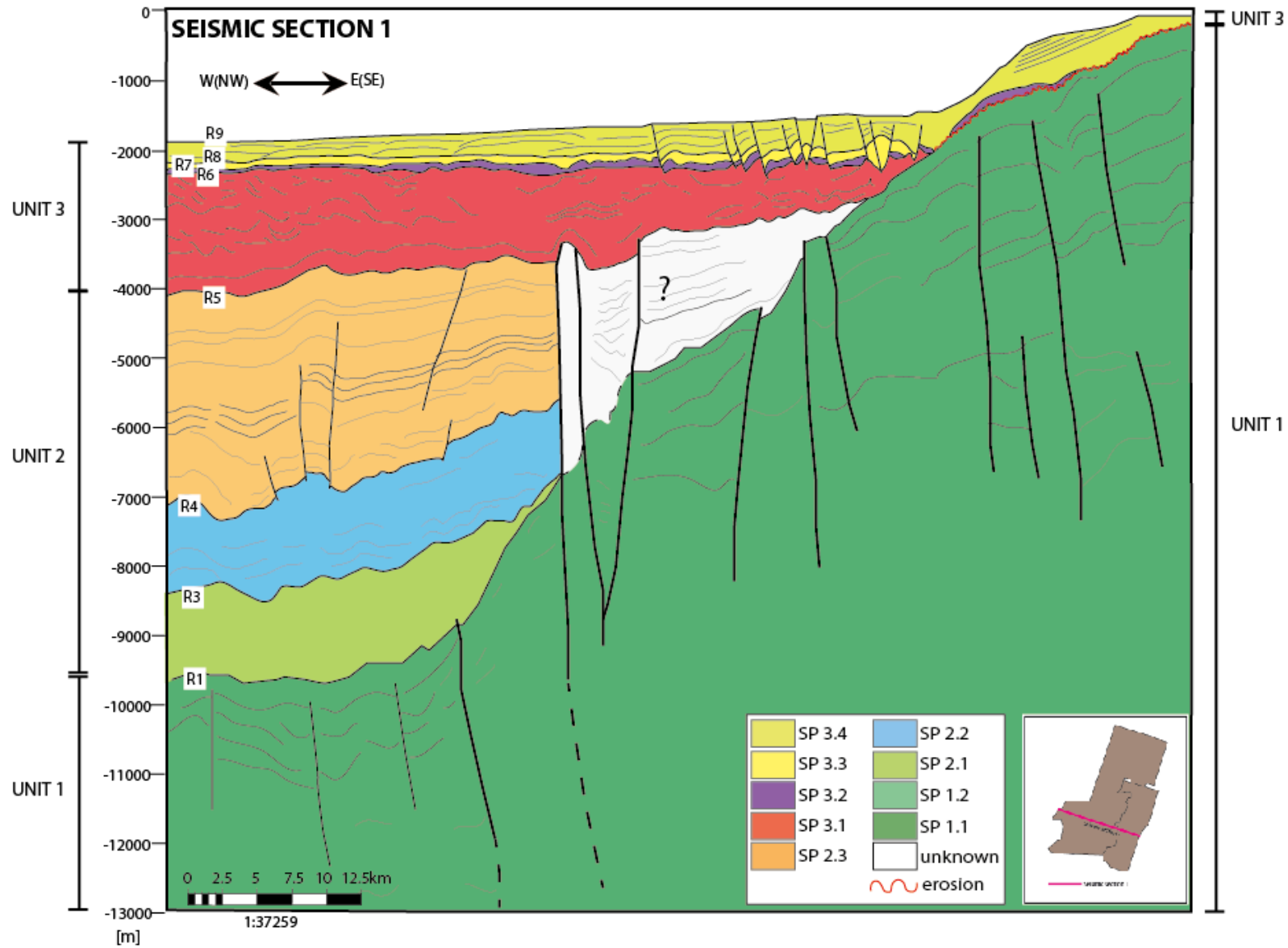


Figure 6.15: Geoseismic interpretation of seismic section 1 (figure 6.2). The figure shows the geological deposition in the Levant Basin. Location can also be seen in figure 6.1. As explained in the legend, each color represents a seismic package (SP 1.1 - SP 3.4). The white area means that it is unknown which seismic package it belongs to. This is because the major fault zone going through the area consists of many smaller strike-slip faults that have displaced the sediments. The units and reflectors are also marked in the interpretation.

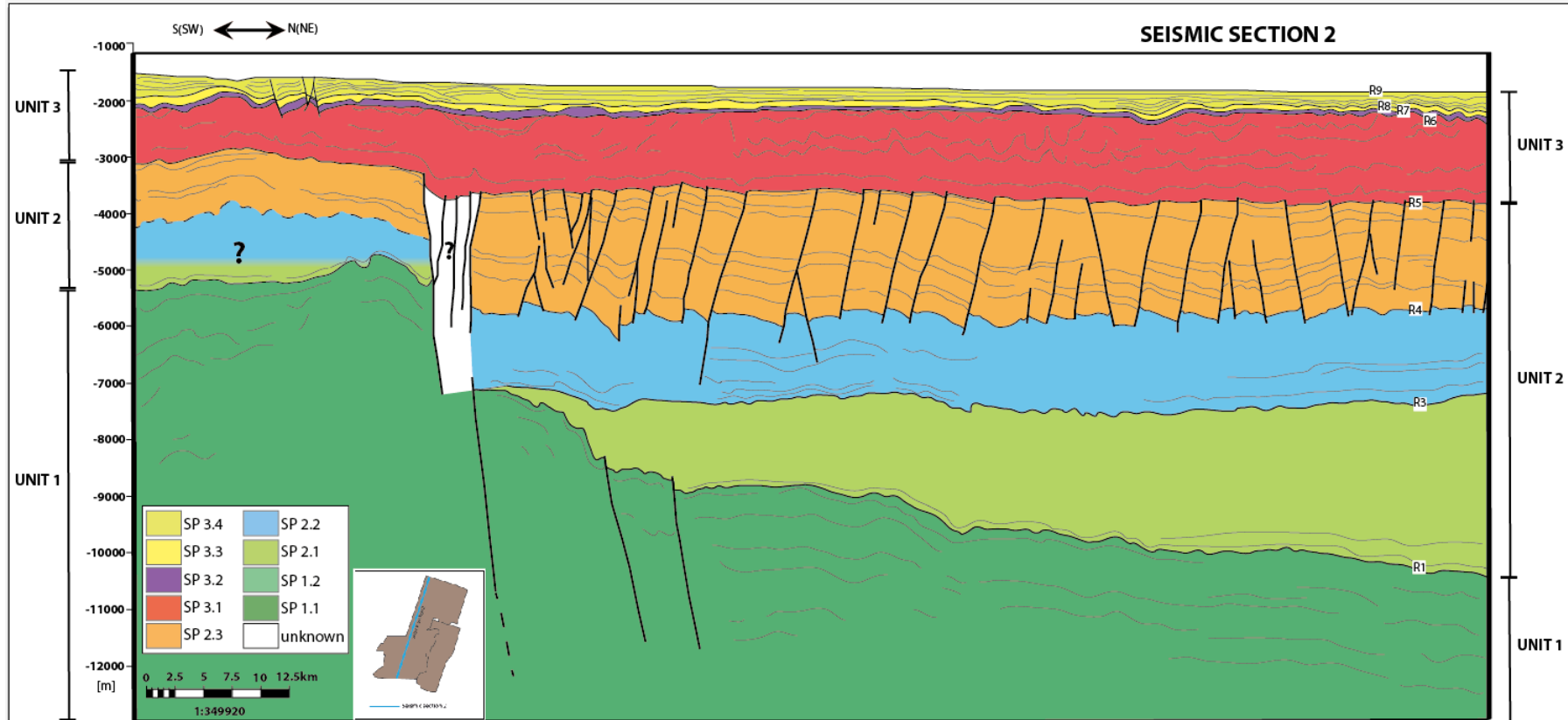


Figure 6.16: Geoseismic interpretation of seismic section 2 (figure 6.3). The figure shows the geological deposition in the Levant Basin. Location can also be seen in figure 6.1. As explained in the legend, each color represents a seismic package (SP 1.1 - SP 3.4). The white area means that it is unknown which seismic package it belongs to. This is because the major fault zone going through the area consists of many smaller strike-slip faults that have displaced the sediments. The units and reflectors are also marked in the interpretation.

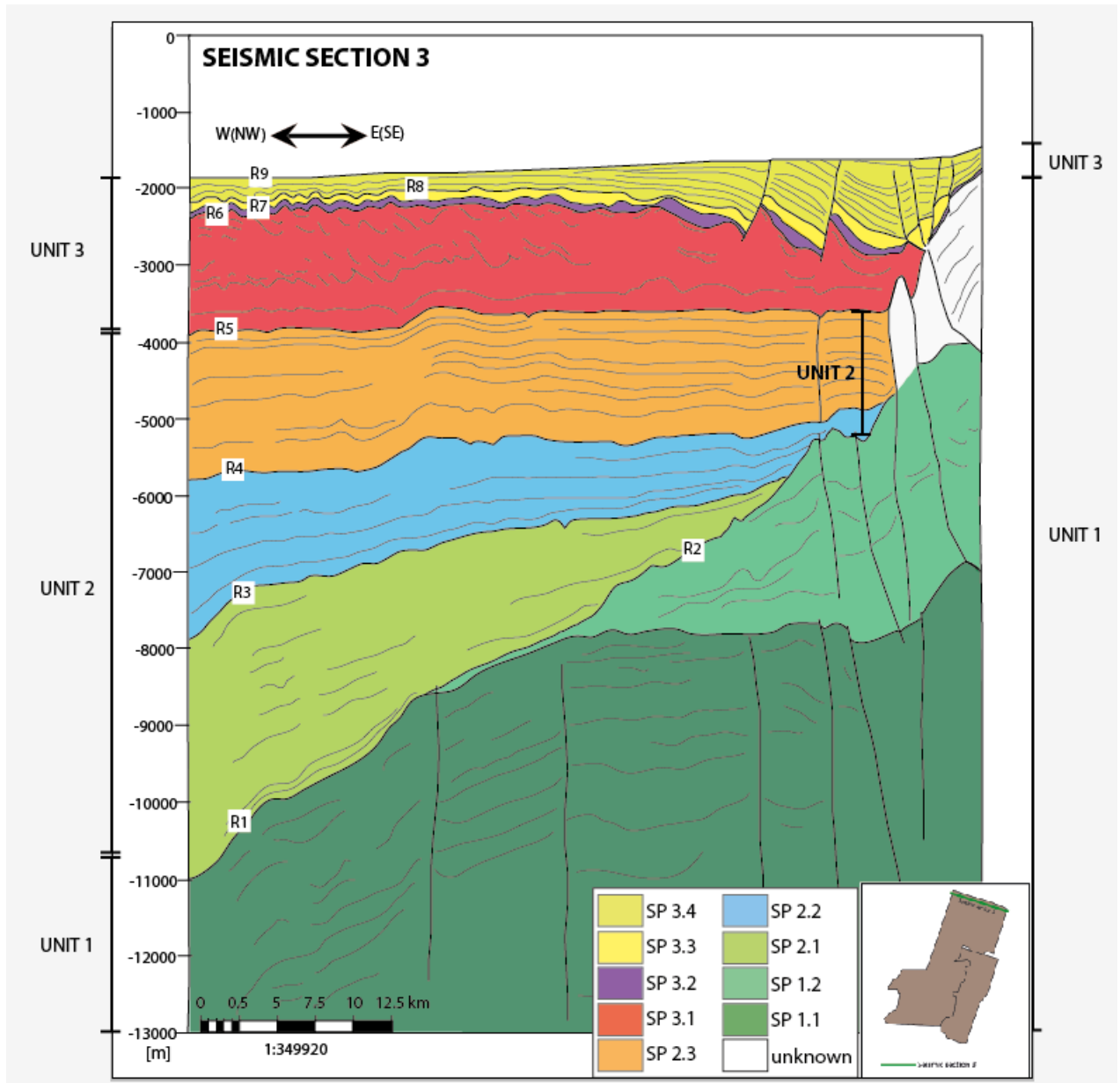


Figure 6.17: Geoseismic interpretation of seismic section 3 (figure 6.4). The figure shows the geological deposition in the Levant Basin. Location can also be seen in figure 6.1. As explained in the legend, each color represents a seismic package (SP 1.1 - SP 3.4). The white area means that it is unknown which seismic package it belongs to. This is because the major fault zone going through the area consists of many smaller strike-slip faults that have displaced the sediments. The units and reflectors are also marked in the interpretation.

Chapter 7

Detailed Seismic Interpretation

This chapter will, in more detail, explain the observations and interpretations that are made from the 3D seismic sections and attribute maps of the Messinian to Recent sediments. The order of deposition and deformation will be explained for the entire Messinian to Recent section, but the characteristics and observations of what is referred to as "the Transition layer" will be emphasized.

7.1 Evaporites

7.1.1 Deposition and deformation

The Messinian evaporites are deposited on top of a basal erosion surface that marks an important sea-level fall at the beginning of the Messinian Salinity Crisis. See chapter 2 for background information about the MSC. The evaporite package has a wedge-formed shape and the thickness in this area ranges from ~1800 m at its thickest in the basin to almost zero where it pinches out in the margin to the east. A thickness map of the salt has been generated, which can be seen in figure 7.1.

An increase in thickness from the margin in east towards the basin in west can be seen from the thickness map. However, some deviation from that trend can be observed in the map. A sinusoidal shaped belt, with mostly less thickness than what would be expected, can be found in the middle of the area stretching from SW to NE. The deviations in thickness seems to appear in the areas where base of the salt has been cut by a major fault zone that runs through the area (figure 6.2 - figure 6.4). The fault zone has roughly been interpreted in Petrel and mapped. The deviations in the thickness map of the salt

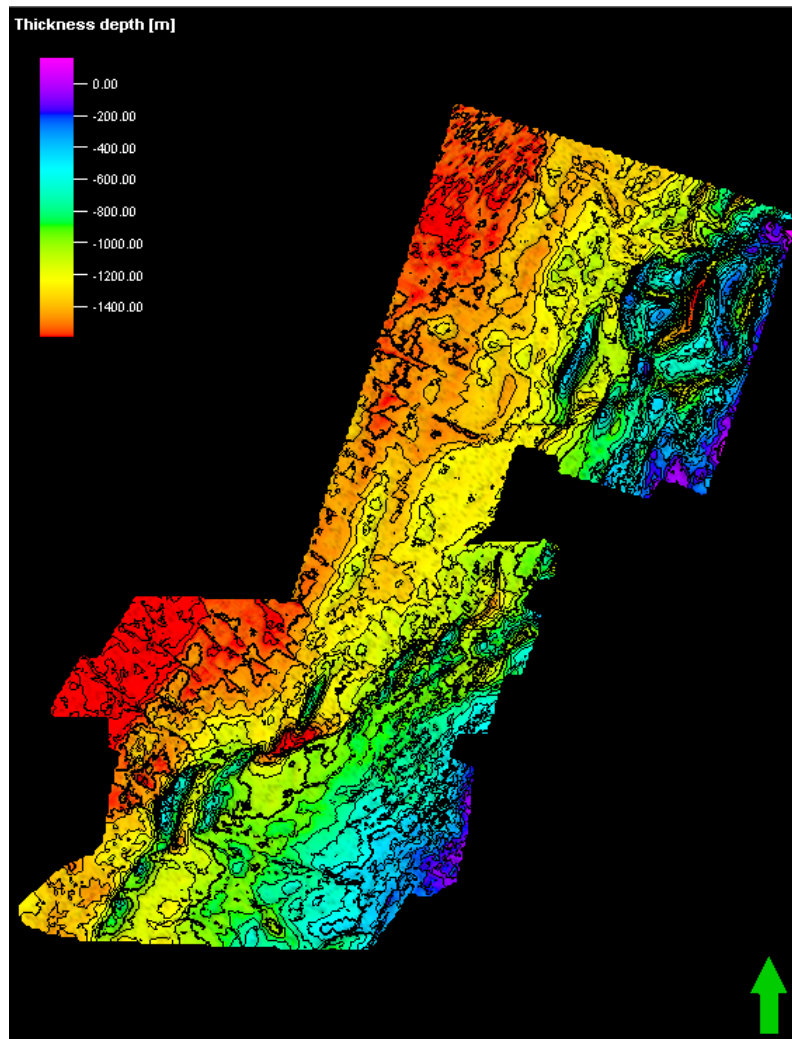


Figure 7.1: The figure shows a thickness map in meters of the evaporite package. This has been generated from the calculator in Petrel by subtracting surface top salt (R6) from base salt (R5). The color scale indicates that the thinnest areas are represented with purple, while the thickest areas are in red.

coincide with the mapped fault zone (figure 7.2). The fault zone is evident through Unit 2 and into Unit 1, but dies out in the salt package of Unit 3. The base of the salt (R5) has been uplifted by the fault zone, which makes the evaporites thinner in these areas.

The evaporite package is composed of three transparent levels and three intra-evaporite reflections with higher amplitudes that are bounded by horizon R5 and R6 (figure 6.9). Intra-evaporite reflection level 1 (L1) follows the topography of the base of the salt (R5) and appears quite continuous. Some faulting can be observed, but the reflections are very continuous and can be traced almost all the way to the easternmost areas. The middle and upper reflection layers (L2 and L3) are much thicker than L1 and have been folded and faulted with a dip towards NW. The degree of continuity is decreasing upward, where

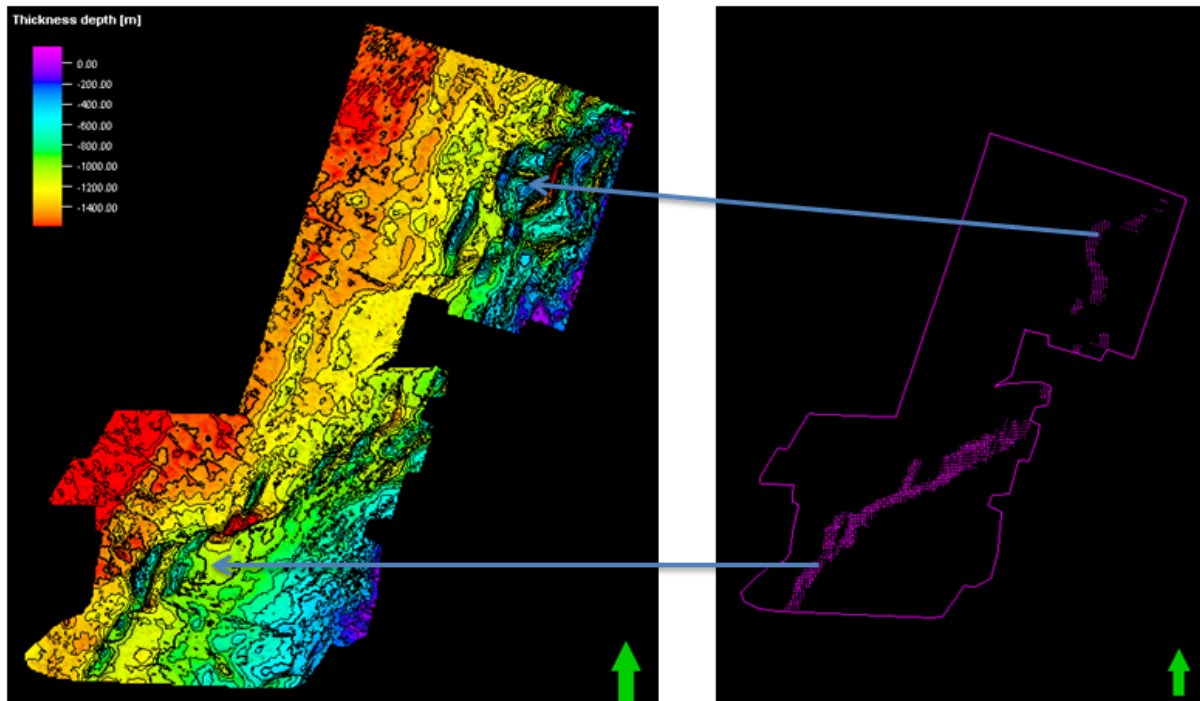


Figure 7.2: This figure shows how the fault zone is influencing the thickness of the salt body. This fault zone can be seen in the seismic sections where it is evident through Unit 2 and lifting up base of the salt. Because of this, the thickness of the evaporite package changes in this area. **Left:** Thickness map of the evaporites, where deviations in the thickness follow a sinusoidal shaped trend. For details, see figure 7.1. **Right:** The mapped fault zone has the same shape as the areas where the thickness changes in the thickness map is occurring.

L3 is only continuous in the the westernmost areas. It can be observed that L2 and L3 are more deformed than L1 (figure 6.9).

7.1.2 Top Evaporite Unconformity

An RMS amplitude map (figure 7.3) was generated for the upper 250 m of the salt package. A trend of high amplitudes can be found in the western part of the area, stretching from SW to NE. These high amplitudes correspond to the upper intra-evaporite reflections (L3) that is a ~300-400 m thick sequence of folded and faulted high-amplitude reflections.

A closer look at these reflections in the seismic sections reveals that the top of the sequence is truncating the continuous, almost flat horizon R6 that is the top of the salt (figure 7.4). The truncation of the upper intra-evaporite reflections with the high-amplitude surface that marks the top of the salt, indicates a regional unconformity. This is evident throughout the entire area and marks the end of evaporite deposition. Reflector R6 is more or less flat and continuous unless in the eastern areas where it has been faulted. The reflec-

tor can be traced throughout the entire study area and it is reasonable to believe that its unconformable character continue further out in the basin. Due to the large regional extent of this unconformity, it is interpreted to be a disconformity of aerial origin. The disconformity is either due to erosion or a period of non-deposition. This means that the water depth in the Levant Basin at this time must have been closer to 0 m and that the basin was completely desiccated at the end of the Messinian Salinity Crisis.

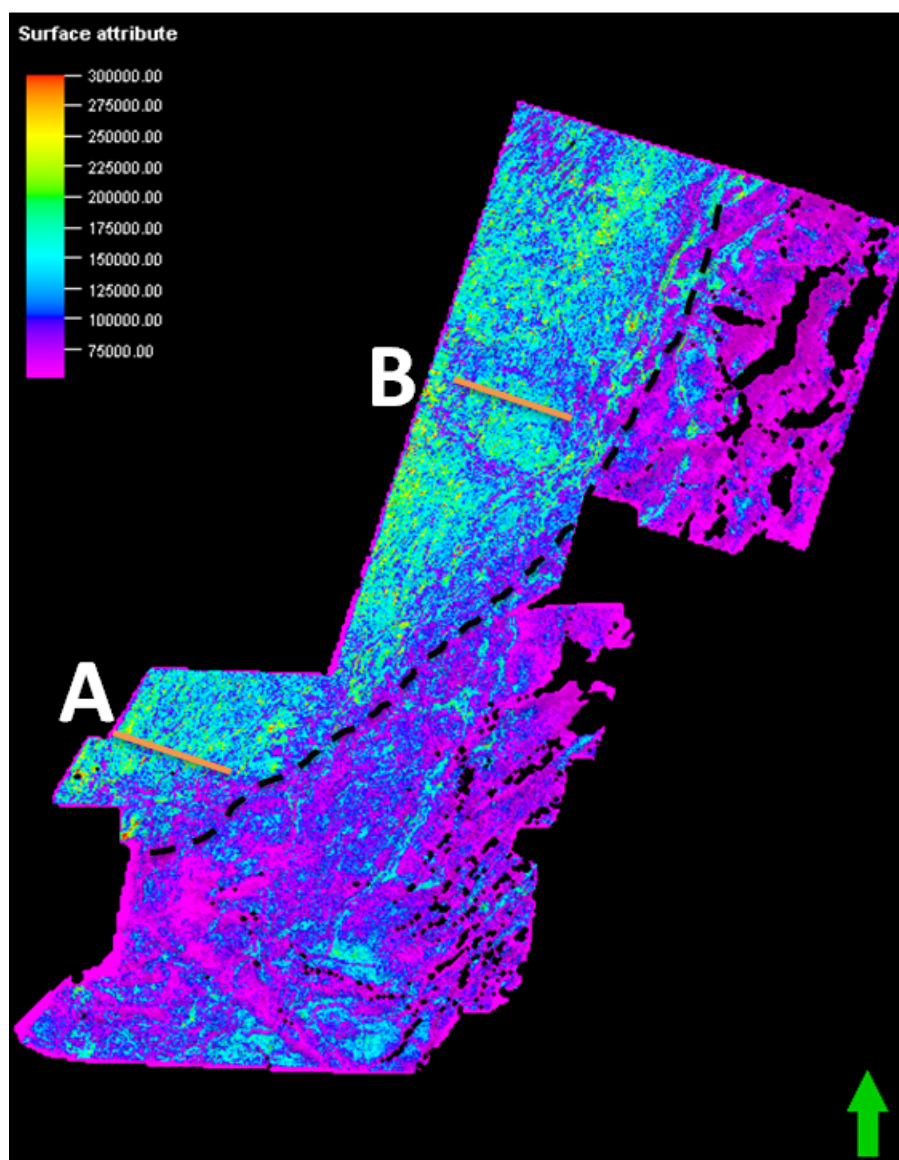


Figure 7.3: An RMS amplitude map is generated for the upper 250 m of the evaporite package. The map shows that the highest amplitudes (blue and green color) can be found in the western part of the study area. The trend is marked by a black, dashed line. The orange lines marked with A and B correspond to the two seismic close-ups seen in figure 7.4.

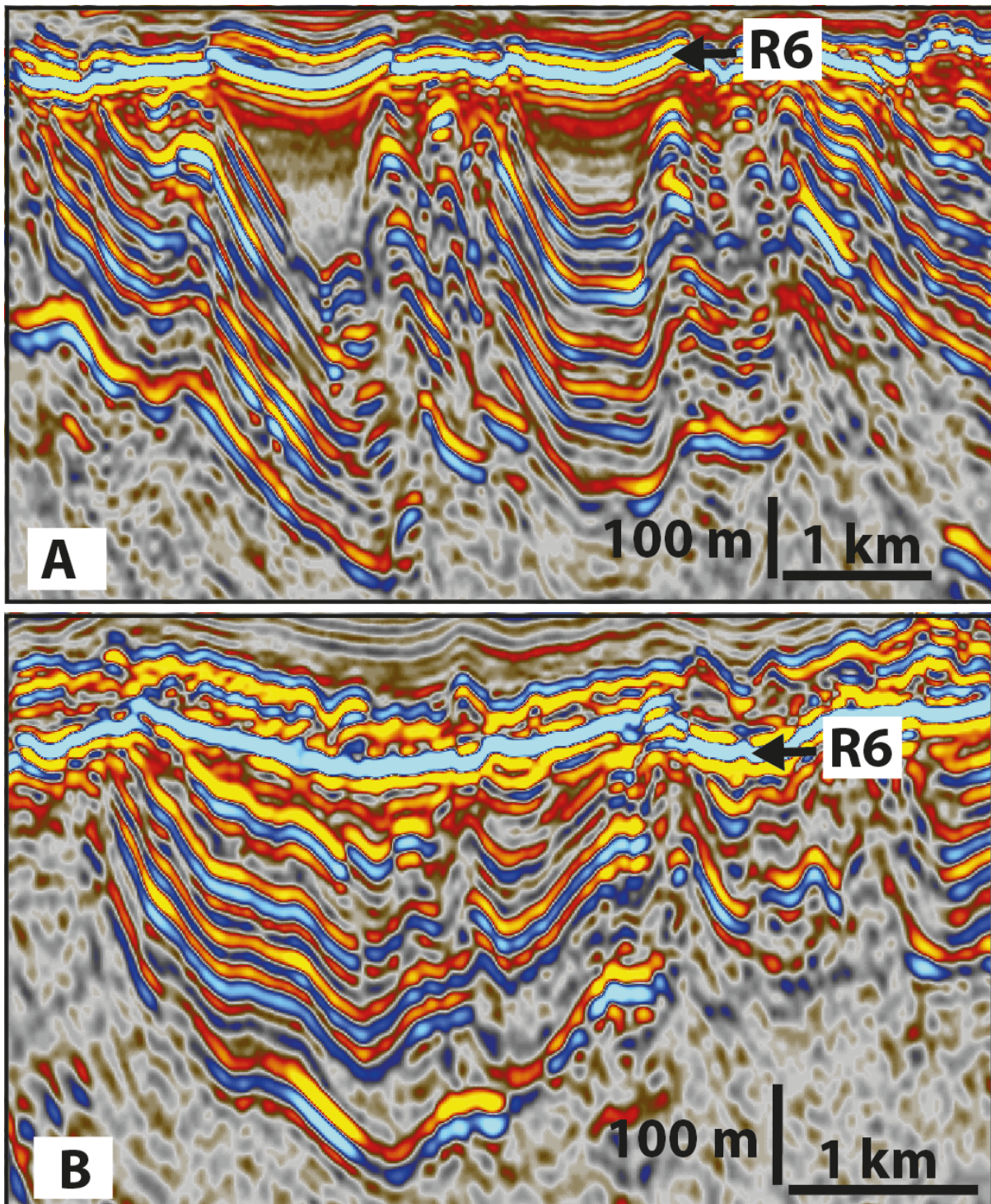


Figure 7.4: The seismic close-ups show examples of where the intra-reflectors of the upper part of the evaporite package are truncating the top of the salt (R6). The two figures are marked with A and B, and the location can be seen in figure 7.3.

7.2 Transition layer

A thin sedimentary package with high-amplitudes is deposited on top of the unconformable surface (top salt). This is a layer that has been deposited between the known Messinian evaporites and the Plio-Pleistocene marine sediments above. It will therefore be referred to as the Transition layer. The layer is more or less flat, but thickness changes within the layer can be observed.

The top of the layer is a high-amplitude, continuous surface that seems to have abruptly cut the layer. Some of the cuttings have the shape of a channel. This abrupt change in thickness indicates that the transition layer must have been exposed to some sort of erosion during and/or after deposition, either subaerial or submarine. The Transition layer is therefore bounded by two unconformities that appear different from each other.

7.2.1 Characteristics and observations from seismic

One of the biggest reasons why this layer stands out is because of the high amplitudes that the layer reflects compared to the marine sediments above. The layer is bounded by the high-amplitude, continuous reflector R6 (top salt) as the base and another high-amplitude reflector R7 at the top, where both R6 and R7 reflect change in depositional environment, shown as an unconformity. The reflectors within this package also reflect high amplitudes, which might indicate that there must be large variations within the layer. High amplitudes will generally be generated by large impedance (velocity x density) contrasts at geological boundaries.

The Transition layer is relatively thin compared to other packages and the thickness of the package is changing throughout the area. In the middle and eastern part of the seismic section the thickness of the transition layer is ranging between ~150-170 m at its thickest, while it is only 20-50 m in the western part of the area (figure 7.5). The thickness is close to zero in some places where the package seems to have been abruptly cut. An interesting observation is that in the western part of the study area where the transition layer is only ~20-30 m thick, top Transition layer (R7) is continuous and almost parallel to top of the salt (R6). The reflectors become much more discontinuous further east where the thickness of the transition layer increases.

Several continuous, high-amplitude reflections can be observed within the seismic package. It is, however, somewhat hard to trace these reflections due to the thickness change. The package appears to contain a mix of stratified and chaotic reflections.

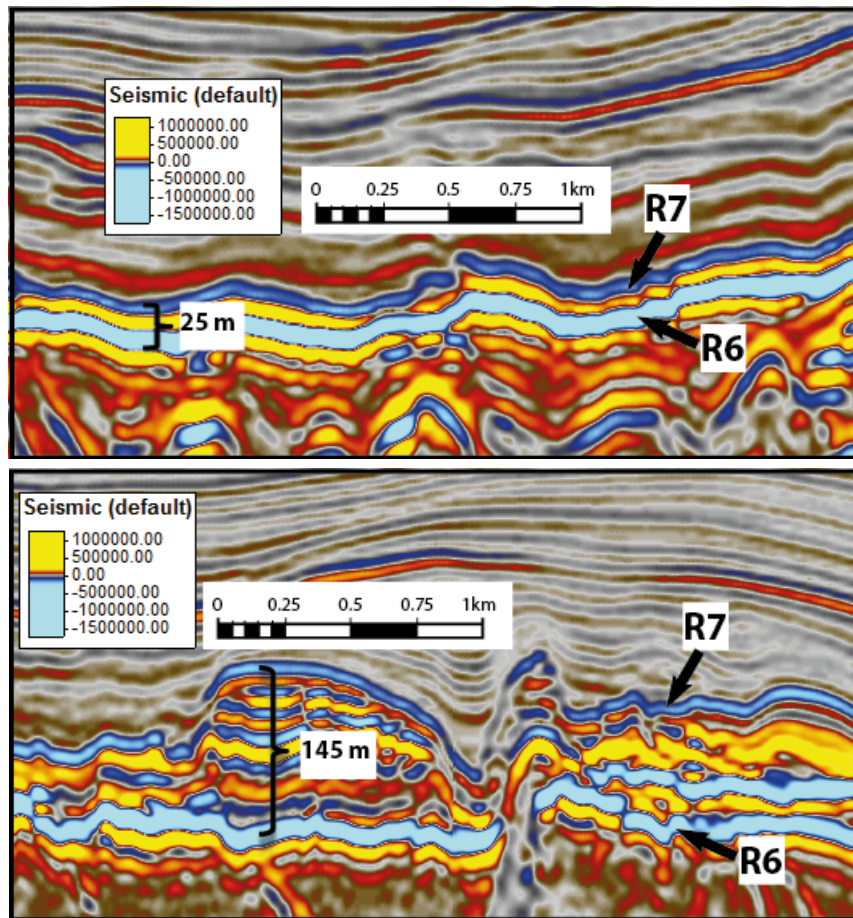


Figure 7.5: This figure shows the thickness variations that can be observed within the transition layer. **Upper picture:** In the distal areas the thickness of the Transition layer is ranging between only 20-50 m. The top of the layer (R7) appears to be semi-parallel to top salt (R6). **Lower picture:** In the more proximate areas of the basin, the thickness of the layer is significantly thicker and is ranging between ~ 150 -170 m at its thickest. Reflector R7 is changing elevation rapidly and appear to be cutting the thickest part of the layer.

The Transition layer seems to break instead of being folded and the layer follows the movement of the salt. It can be observed that the layer is faulted in the same areas as where horizon R6 (top salt) is faulted. In addition, smaller faults can be observed within the transition layer itself, without affecting base of the layer. Most of this faulting have not affected the marine sediments above, which means that the faulting must have occurred prior to deposition of SP 3.3 and SP 3.4.

The high amplitudes and parallel layering in the Transition layer do in parts of the area look very similar to the upper part of the salt (L3). figure 7.6 shows a close-up of a section where this occurs. From a detailed picture like this their appearance looks the same. However, the Transition layer is present on top of the salt in the entire study area, while the upper high-amplitude reflections within the salt is much more discontinuous

and have areas with transparent salt within it.

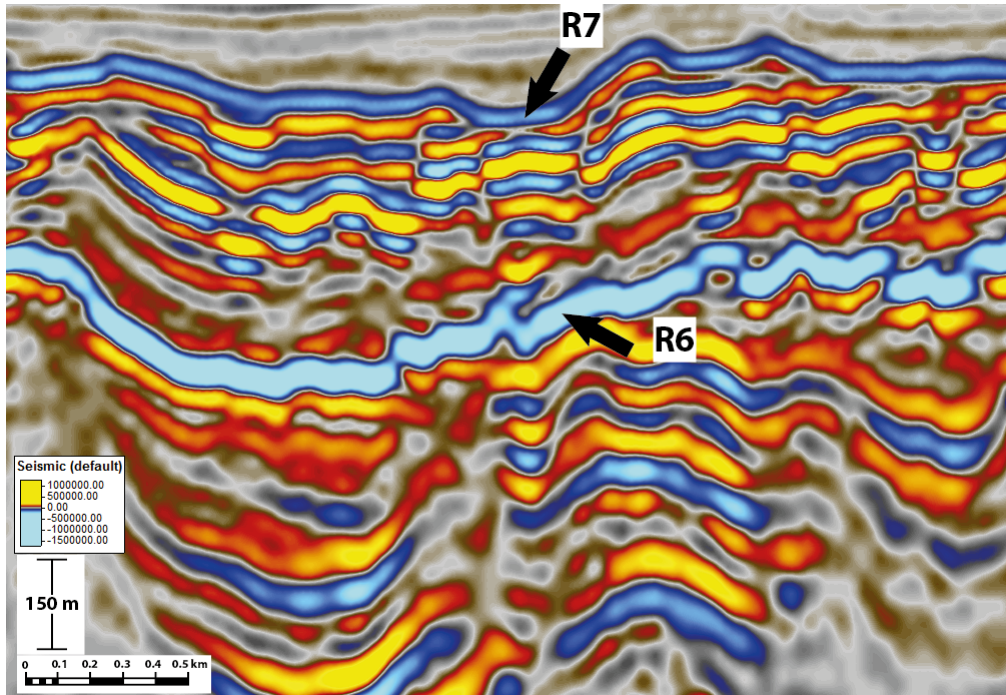


Figure 7.6: In some areas, the Transition layer seems to look very similar to the upper part of the evaporite deposits. The reflectors show the same high amplitudes, and except for the bright reflector R6, this could look like one layer. R7: top transition layer, R6: top salt.

7.2.2 Observations from attribute maps

A thickness map was created (figure 7.7) by subtracting horizon R6 (top salt) from horizon R7 (top transition layer), which gave the thickness of the Transition layer in meters. Several observations can be made from this map.

In figure 7.8.a the thickest areas of the thickness map have been enhanced. It can be seen that the thickest areas are in the middle of the survey, stretching from SW to NE. The thinnest areas have been enhanced in figure 7.8.b and features having the shape of channels can be observed here. By comparing the two maps it looks like the thinner features are cutting through the thicker areas. This can also be found in the seismic sections. By comparing the thickness map with the seismic, it can be seen that the thickest parts of the Transition layer have been abruptly cut in the areas where the channel-looking features appear. By comparing the thickness map with an RMS map that is generated from top salt to top Transition layer, it can be observed that the areas with less thickness reflect high amplitudes, while the thicker areas reflect lower amplitudes (figure 7.9).

In the north-western part of the thickness map some thicker features take shape (figure 7.10). They appear long, thin and continuous on the thickness map. In the seismic this looks like something that is pushing the already-existing reflections up. It is local geological features that also make the reflections above to bend. These push-ups must therefore have occurred after deposition of the sediments above. The amplitude responses inside these features are much lower than the rest of the layer.

An amplitude map for the minimum amplitude (figure 7.11) and the RMS amplitude (figure 7.12) was generated on horizon R7 (top transition layer). Both maps show that the highest (minimum and RMS) amplitudes can be found in the western part of the area. This corresponds to the same area as where the highest amplitudes were found in figure 7.3. However, the high amplitudes in this area might be due to the fact that horizon R7 is continuous in this area and it is easy to trace the correct reflector, compared to the eastern part where it is more faulted and harder to trace.

A maximum amplitude map (figure 7.13) with a window 50 m above horizon R7 gives the same result as figure 7.11 and figure 7.12. The results show that the highest amplitudes can be found in the western area. The southern part of the maximum amplitude map show in general much lower amplitudes than what can be observed in the western and northern part of the map. Within this low-amplitude area, some long and thin, high-amplitude features can be observed. These high-amplitude features appear in the same place as where the Transition layer has been deeply eroded. The map was generated with a window of 50 m above the top of the transition layer, meaning that the high amplitudes that are detected must come from the sediments deposited in the areas where the transition layer has been cut. It is therefore reason to interpret these features as channel fillings that has filled in the channels that were formed due to erosion of the transition layer.

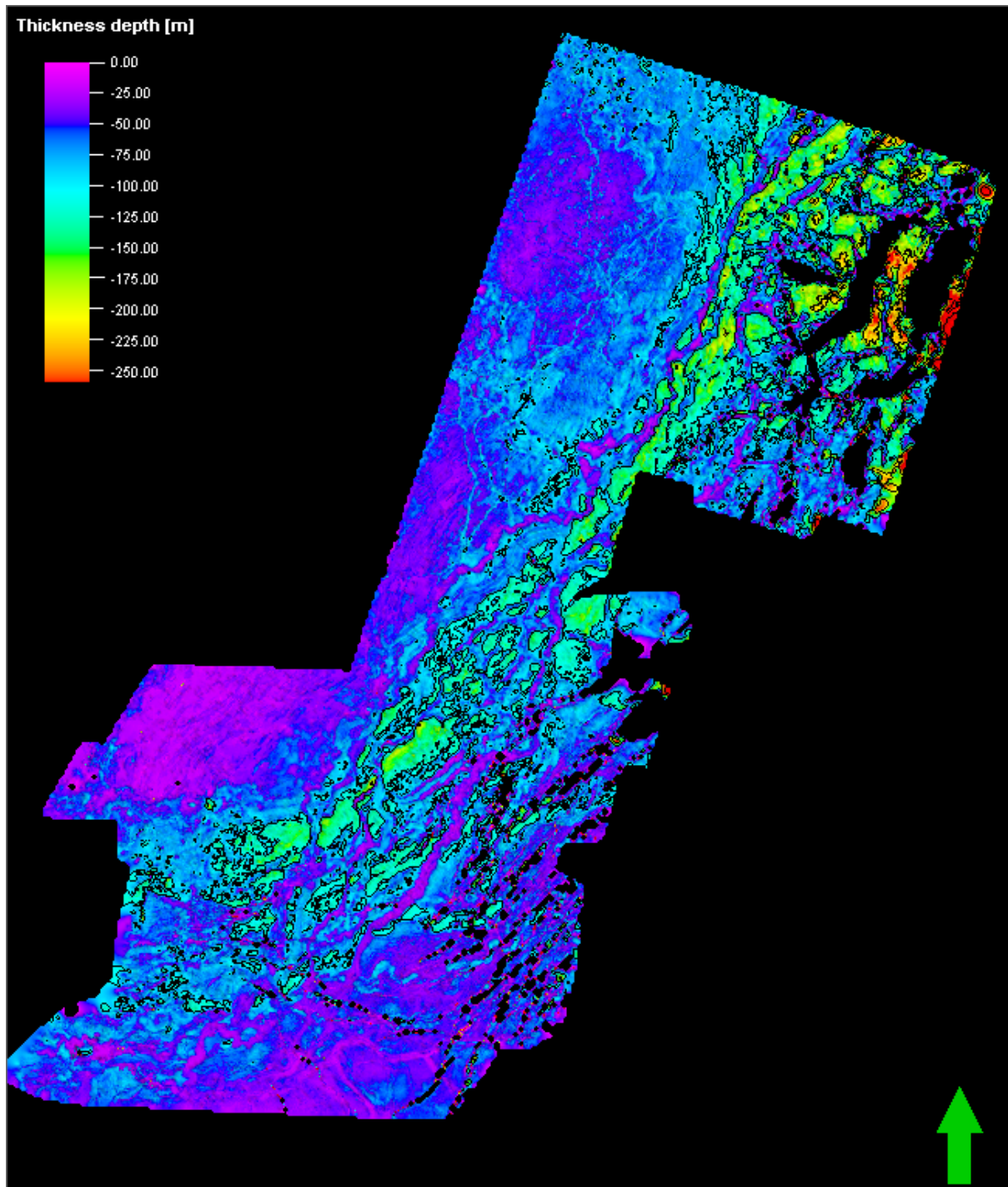


Figure 7.7: This is a thickness map in meters that is generated for the Transition layer, by subtracting surface top salt from surface top Transition layer. The thickest areas are assigned a green color and the thinnest areas have a purple color. The map shows that the thickest areas are in the middle of the map, stretching in SW-NE direction. The layer gets thinner further out in the basin. The thickness distribution is better shown in figure 7.8.

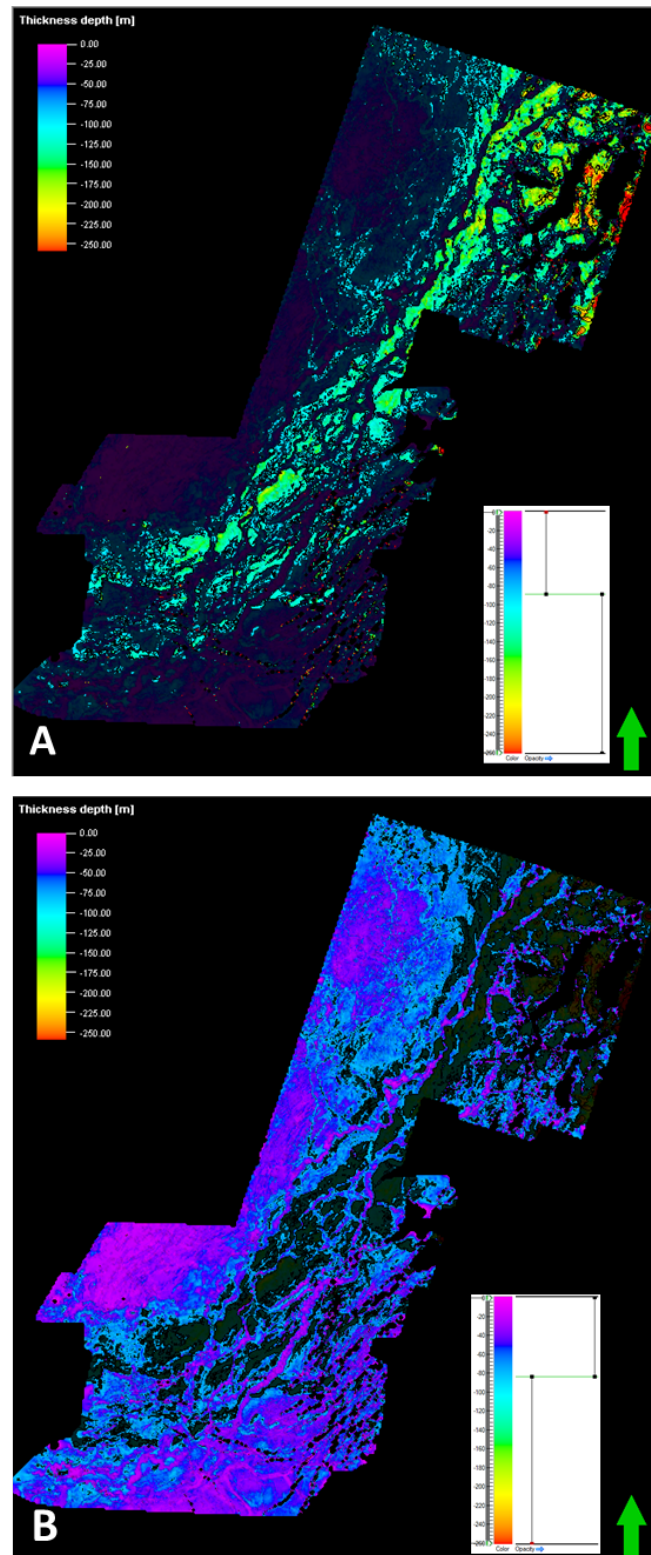


Figure 7.8: **A:** The opacity of the thickness map (figure 7.7) has been changed such that the thickest areas are enhanced. The thickest areas of the transition layer appear to be stretching from SW to NE. **B:** This map enhances the thinnest areas of the layer, which is mostly dominating the areas further out in the basin. It can be observed that thin features having the shape of channels are cutting through the thicker areas. The color scale in the lower right corner of the figures shows which thicknesses are included in the maps and which thicknesses that have been dimmed.

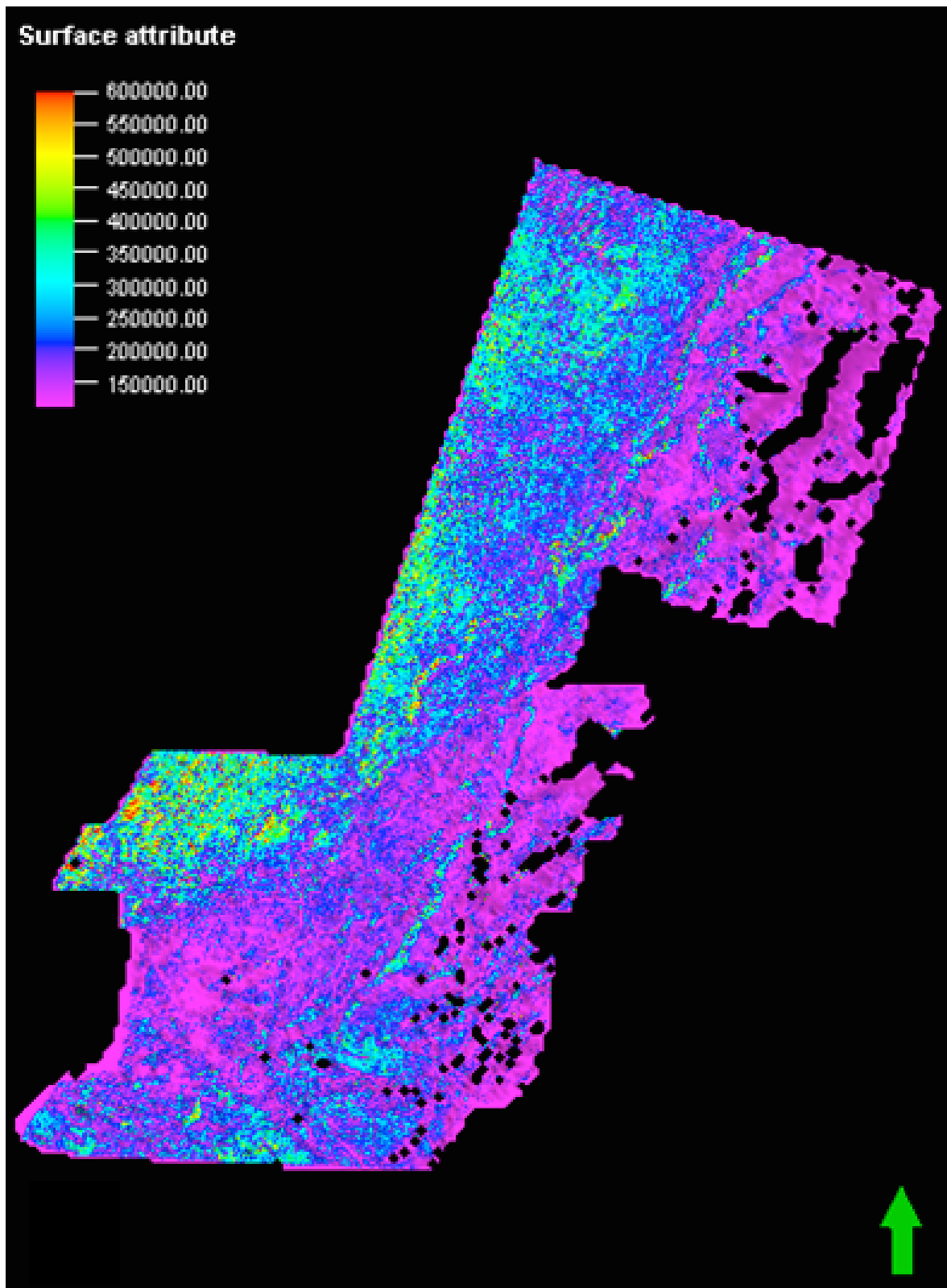


Figure 7.9: An RMS map is generated for the Transition layer (from top salt to top transition layer). By comparing this map to the thickness maps in figure 7.8, it can be seen that the areas with less thickness reflects high amplitudes, while the thicker areas reflects lower amplitudes.

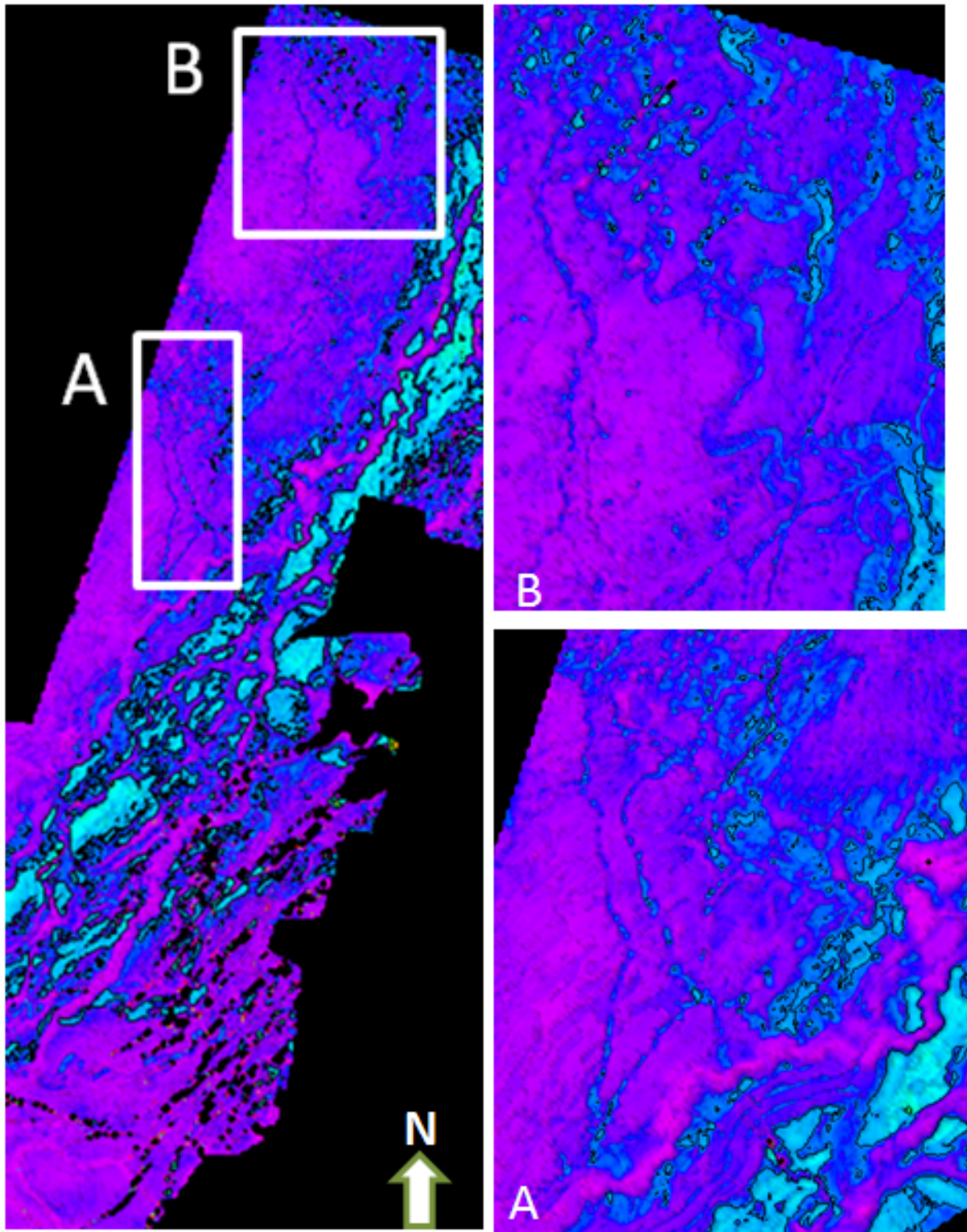


Figure 7.10: Thick features can be observed in the north-western part of the thickness map, where they appear long, thin, curvy and continuous. A and B are close-ups of these features.

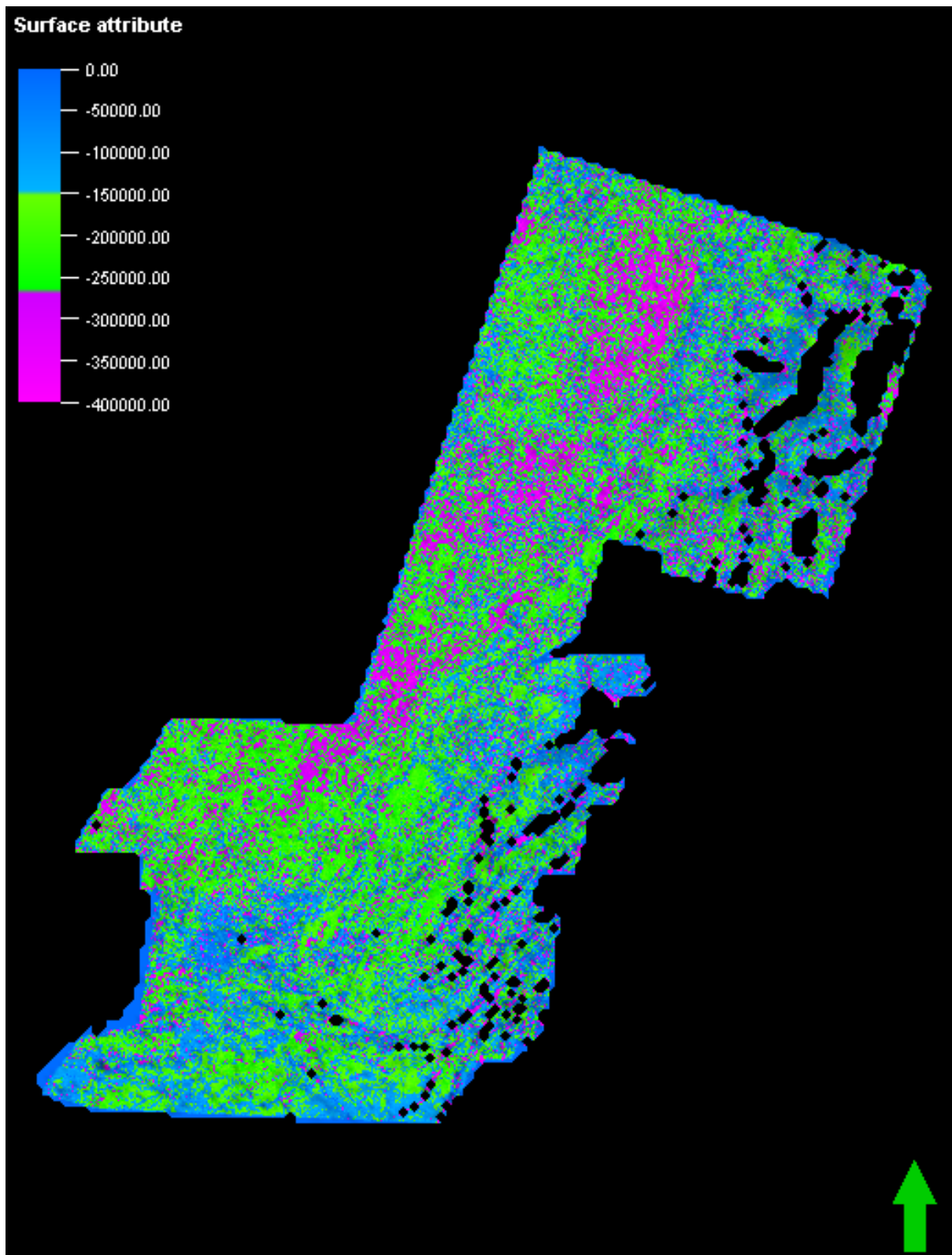


Figure 7.11: The map shows the minimum amplitude of the reflector R7 (top Transition layer, negative amplitude). The map shows that the highest minimum amplitudes can be found in the western part of the area. Pink color represents the highest minimum amplitudes and blue color represents the lowest minimum (closest to zero) amplitudes.

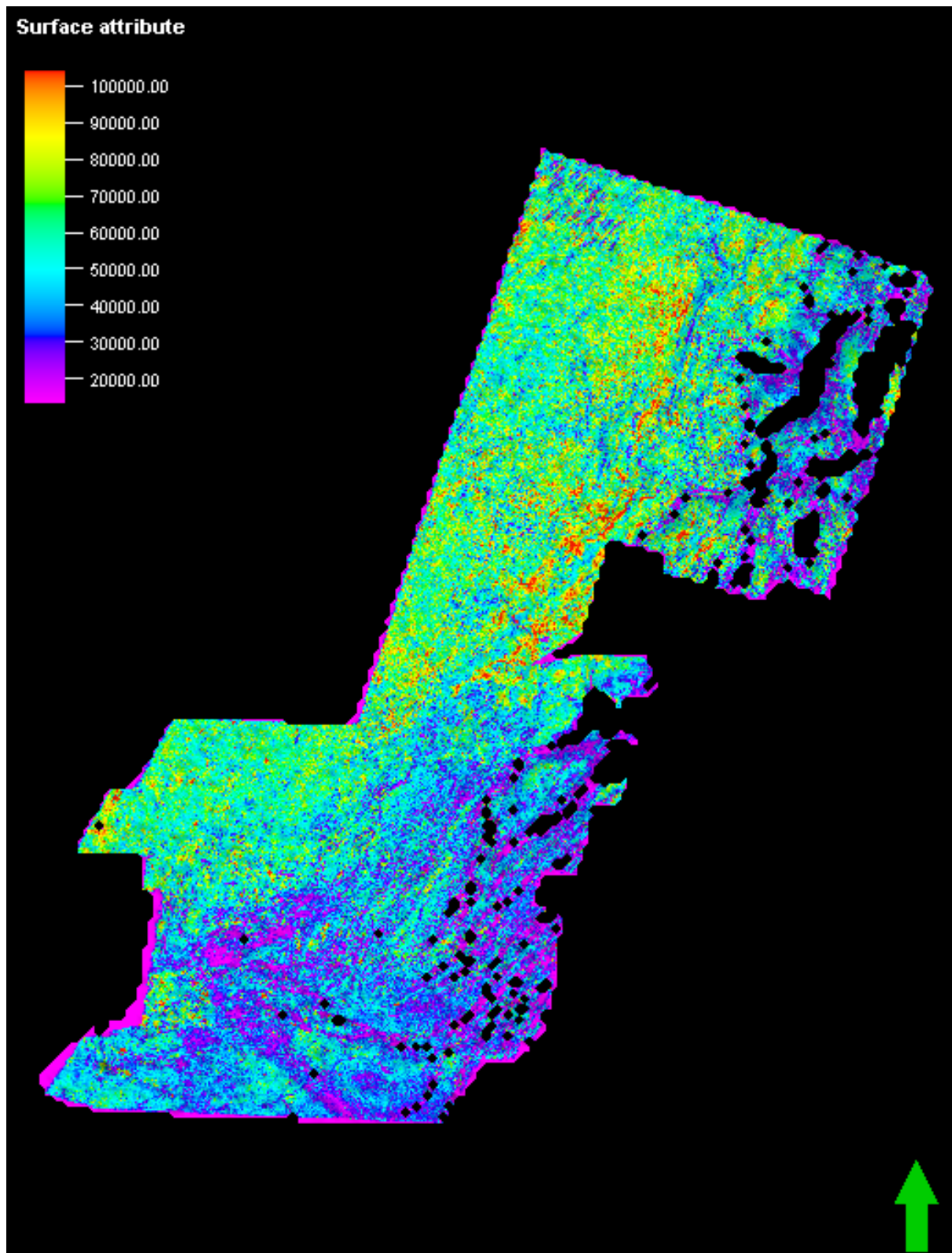


Figure 7.12: The map shows the RMS amplitude for reflector R7. The map shows that the highest RMS amplitudes can be found in the western part of the area. The highest RMS amplitudes are marked with red, yellow and green color (where red is highest). Purple and blue show the areas with lowest amplitudes.

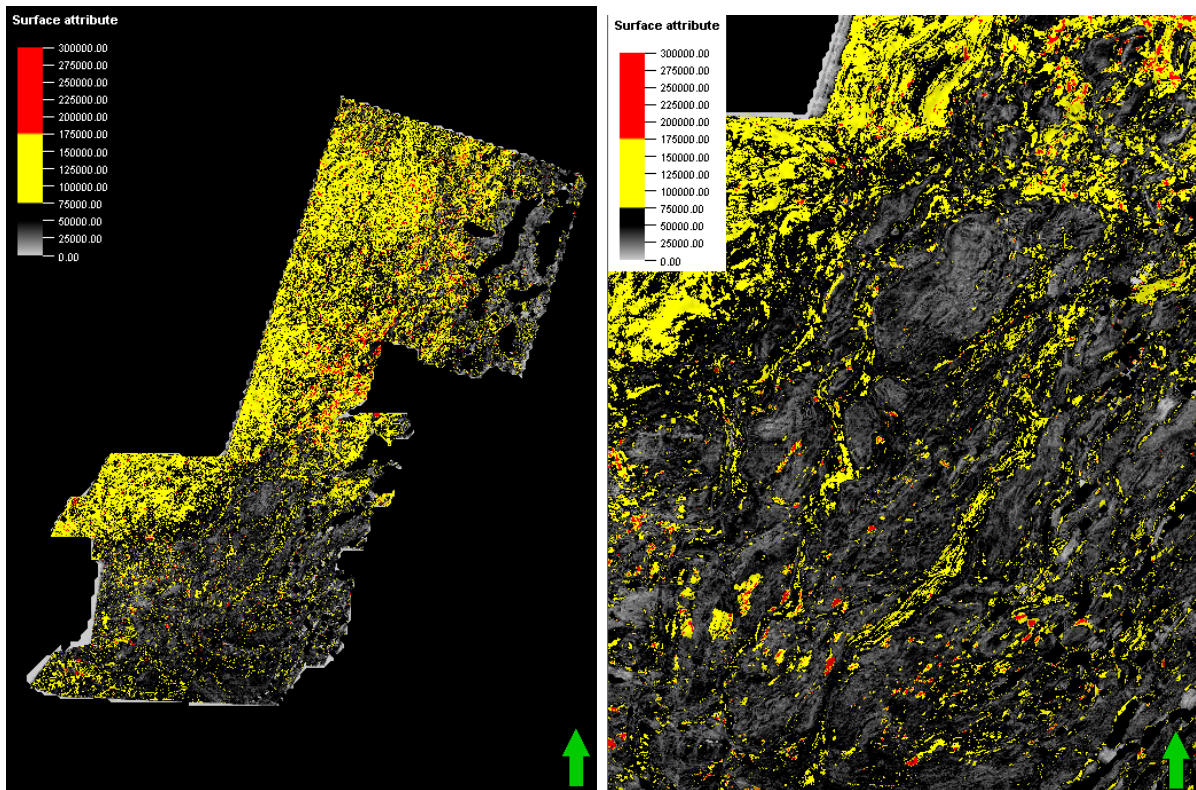


Figure 7.13: *Left:* A maximum amplitude map with a window of 50 m above horizon R7 (top transition layer) show that the highest amplitudes can be found in the north-western part of the area. This is the same result as what was found in figure 7.13. **Right:** A close-up of the low-amplitudes in the southern part of the area. The close-up reveals some thin, long features with high amplitudes. These features appear in the same areas as where the transition layer has been deeply eroded.

7.3 Marine deposits

Flat, parallel, continuous reflectors with lower amplitude than the Transition layer have been deposited on top reflector R7. These sediments are deep-marine sediments that were deposited as the Atlantic water flooded the Mediterranean after the MSC. The water depth today is ~ 1700 - 1800 m, and it is reasonable to believe that the water depth was about the same when these sediments were deposited. The first ~ 100 m of marine deposits appear more chaotic than the upper part, and can be separated from the upper part by a distinct, continuous reflector (R8). RMS amplitude maps for the marine sediments have been generated (figure 7.14), and resulting maps show a trend of higher amplitudes in the upper marine section (right figure) compared to the lower part (left figure). They appear to be fan-shaped depressions that have an E-W orientation (figure 7.15). These areas also show evidence of submarine erosion with deposition further out in the basin

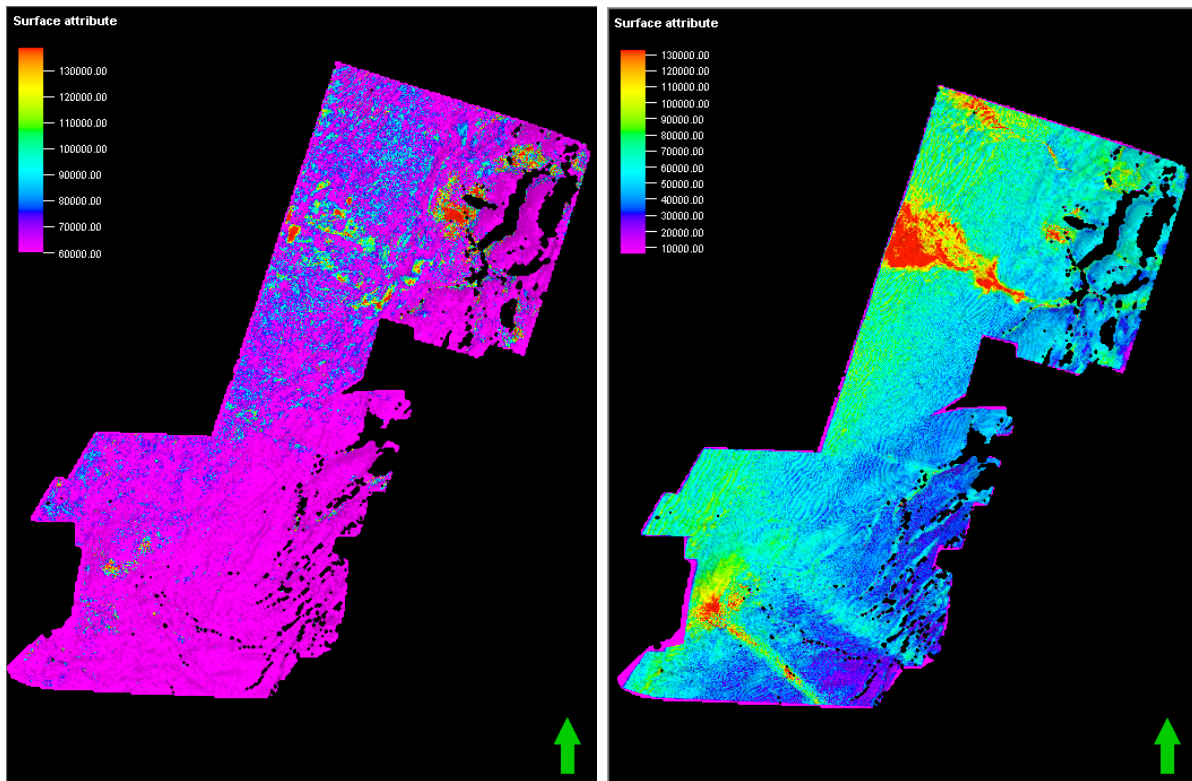


Figure 7.14: *left:* RMS amplitude map for the lower section of the Plio-Pleistocene sediments, between reflector R7 and R8. **Right:** RMS amplitude map for the upper section of the Plio-Pleistocene sediments, between reflector R8 and R9. Both maps show in general lower amplitudes than what was observed in figure 7.12, which is also what can be observed in the seismic. Some distinct high-amplitudes in the RMS map to the right can be observed. figure 7.15 shows an example of how these amplitude areas looks like in the seismic. Note: Reflector R8 has not been properly interpreted in the eastern area due to the faulting. The eastern area of both of these maps does therefore not show the exactly correct amplitudes, since both of the maps are generated by using reflector R8.

(figure 7.16).

As described in Chapter 6, there are observed three stress domains within this Plio-Pleistocene marine sediment package (SP 3.3 and SP 3.4). The contraction and extension that have affected these sediments (figure 6.13) have also affected the Transition layer and the upper evaporites. In the eastern part of the area, even the seabed has been faulted and subsided. Another episode of salt tectonics and deformation must therefore have occurred after deposition of the youngest sediments. In the extensional domain, detachment faults and growth structure are evident.

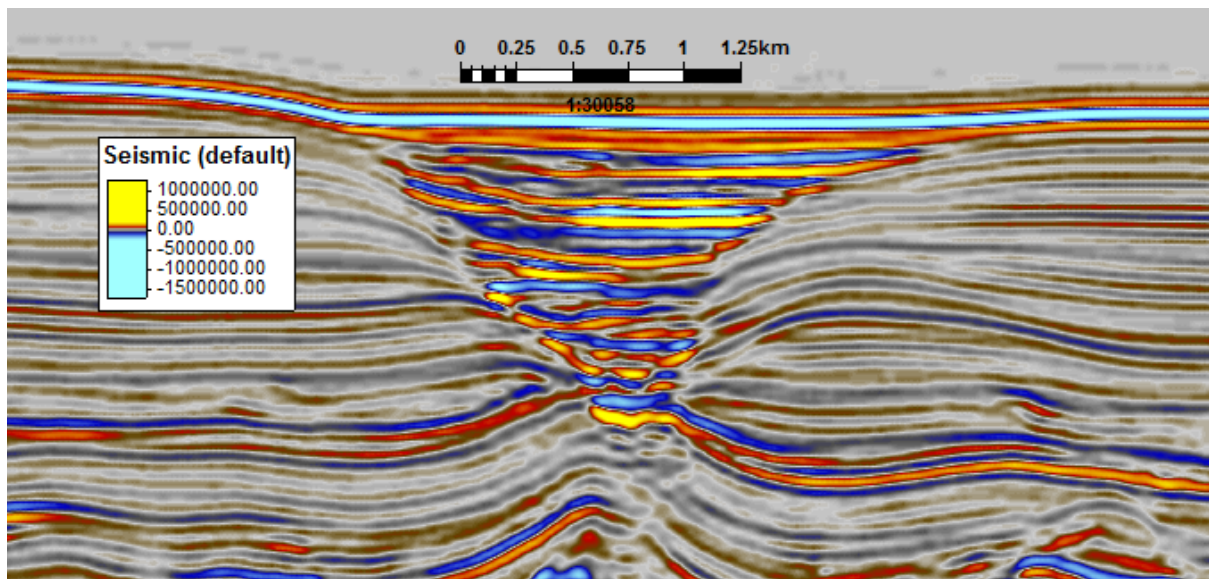


Figure 7.15: High-amplitude reflections in the upper marine layer are spotted on the RMS map (figure 7.14). This figure shows an example of how this looks in the seismic. The figure has an $W(NW)$ - $E(SE)$ orientation.

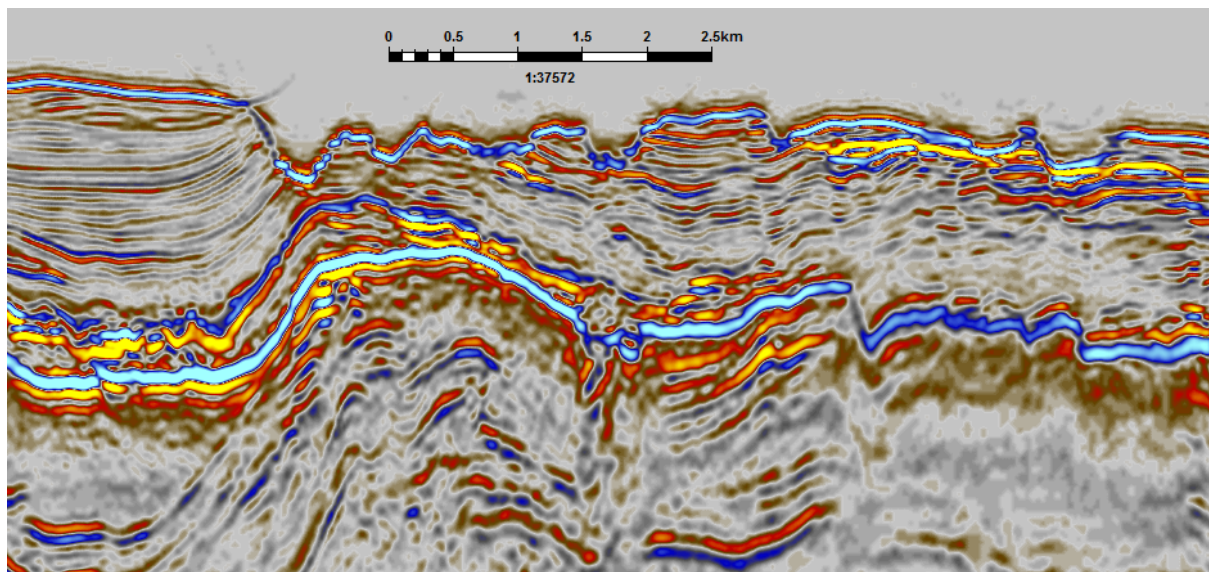


Figure 7.16: Submarine channels are spotted on the seafloor. This figure has an $S(SW)$ - $N(NE)$ orientation.

7.4 Scenarios

As already mentioned, two distinct reflectors that appear to be unconformable surfaces bound the Transition layer. The base unconformity (R6) is almost flat and continuous, while the top unconformity (R7) is more curvy and broken. Both reflectors have negative amplitude, but R6 has higher negative amplitudes than R7 (figure 7.17). Both reflectors have been faulted in the marginal areas of the basin (east). The unconformity of R6 seems to be regional, and erosion or non-deposition has occurred all over the study area. The Transition layer seems to have been eroded in the areas where it is thickest, and the erosion is more channelized compared to what observed on R6.

Due to the characteristics of the unconformity, the origin of top salt is believed to be of subaerial origin. The origin of the Transition layer is, however, not as easily determined.

There are several possible scenarios for the deposition of the Transition layer:

1. Early Pliocene marine sediments
2. The Yafo Sand Member
3. Lago Mare deposits
4. Upper evaporite deposits
5. Fluvial deposits

These scenarios will be further discussed in the next chapter.

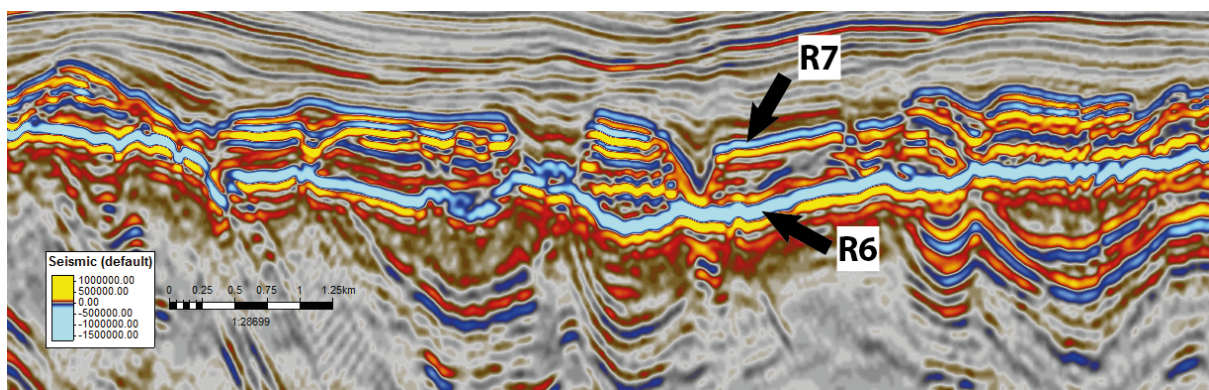


Figure 7.17: Two erosion surfaces R6 and R7 are bounding the Transition layer. R6 appear to be a regional unconformity with very high negative amplitude. R7 has negative amplitude that is lower than R6, and the erosion seems to be channelized.

Chapter 8

Discussion

The deposition and evolution of sediments in the Levant Basin has been described in the previous two chapters. The main focus of this thesis has been the Transition layer that was deposited on top of the Messinian evaporites. Three topics that are highly relevant for the origin of the Transition layer will be discussed in this chapter. The first topic will include the different phases of salt tectonics that have affected the evaporites it self and the younger sediments above the evaporites. The second topic deals with the unconformity that separates the Messinian evaporites from the Transition layer, and the third topic will present different scenarios for the origin of the Transition layer.

8.1 Salt tectonics

The knowledge about the early stages of gravitational spreading, in particular initial flow regime of salt and localization of detachments, is limited. This is because of the extreme strains that occur within the salt layers (Cartwright *et al.* , 2012). Internal continuous seismic reflections act as markers for deformation within the salt. These are rare to image on the seismic, due to the reflectivity of salt. The internal reflections of the Messinian salt, however, are very well imaged on the seismic. This means that the Messinian evaporites are excellent to study in order to understand the initial flow regime of the salt.

Deformation and movement of salt is evident in the seismic sections. At least two major episodes of deformation due to salt tectonics must have occurred in this area. There have most likely been several smaller episodes of deformation in addition to the bigger ones, but the following are the two major phases.

The first episode of deformation can be seen within the evaporites itself, where the intra-evaporite reflections are folded and faulted (figure 6.9). Detailed study shows an individual deformation pattern for each of the intra-evaporite sequences. The deformation within the salt shows a northward direction of movement (figure 8.1). The upper intra-evaporite reflections are truncating the top salt horizon (figure 8.3), which is continuous and not folded as the reflectors below. This indicates that the salt must have been deformed after and possibly during deposition of the evaporites, but prior to the unconformity that marks the end of the MSC (marked by R6). This claim is supported by Bertoni & Cartwright (2007b) who argue that this phase of deformation occurred during the Messinian. According to Bertoni & Cartwright (2011), this first phase of salt tectonics can be explained by subsidence driven steepening of the basin margin due to deposition of the basinal evaporites.

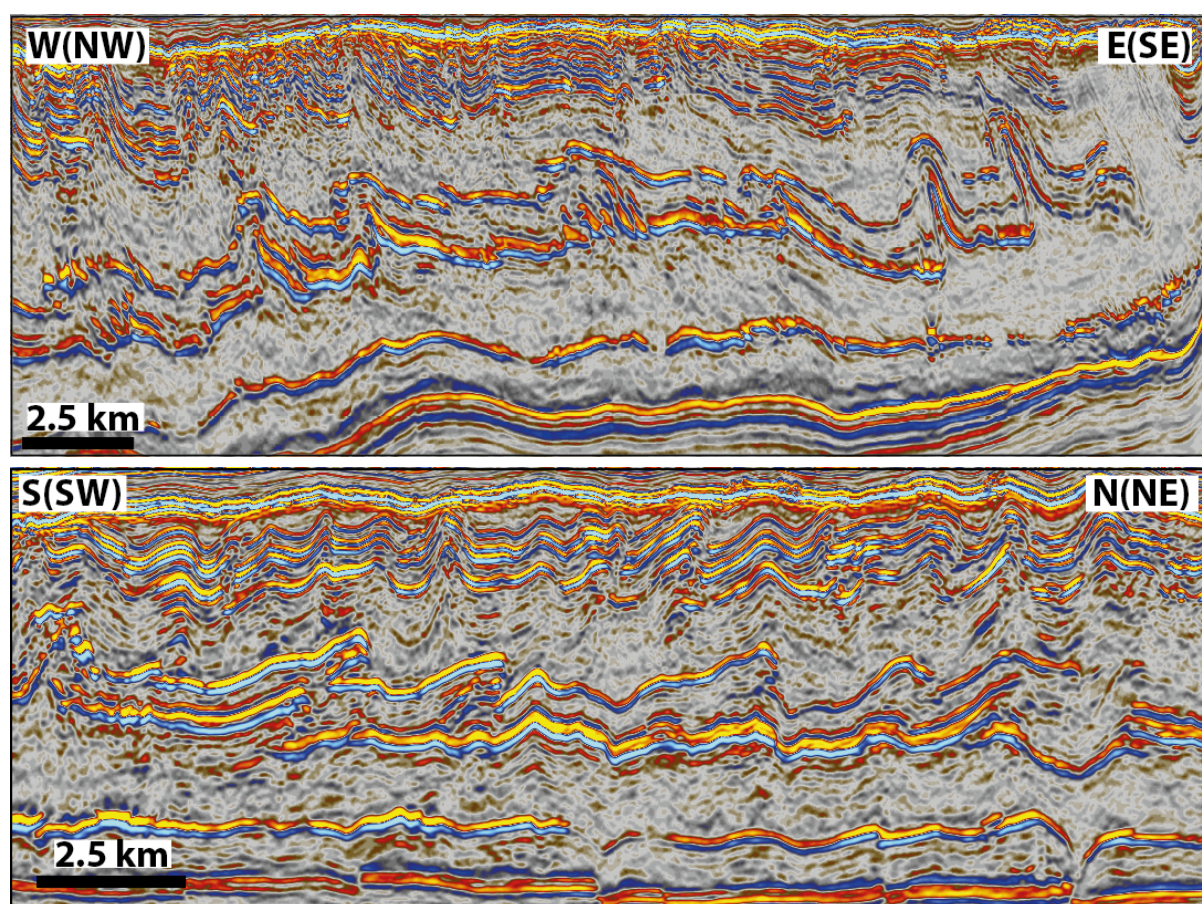


Figure 8.1: The intra-evaporite reflectors are folded and faulted, and show the first phase of salt deformation. The middle and upper part of the intra-evaporite reflectors show more deformation than the lower reflectors. The **upper** picture shows a W-E section. The internal deformation show that the salt movement is in the W(NW) direction. The **lower** picture shows a S-N section. The internal deformation show a salt movement going in the N(NE) direction. This means that the salt has moved in a northern direction during deformation.

The second major episode of salt tectonics is both affecting the Plio-Pleistocene cover and the evaporites. Salt-related structures such as extensional growth faults at the lower slopes of the margins and folding in the more distal areas, in addition to salt diapirs and salt rollers can be observed (figure 6.13). Based on the tectonic structures, the area can be divided into three main stress domains, with an extensional domain in the eastern margin and slope, a translational domain at the base of the slope and in the proximal areas of the basin, and a contractional domain in the distal basin (figure 6.14). The active faults in the extensional domain even penetrate the seafloor. This episode of salt tectonics must therefore have occurred recently, after deposition of the Quaternary sediments. This second phase of salt tectonics is well documented in literature. Bertoni & Cartwright (2007b) argue strongly for gravity-driven, thin-skinned deformation of the Plio-Pleistocene sediments that is post-dating the evaporites. According to Cartwright *et al.* (2012), the inferred flow velocity of the Messinian evaporites is higher at the top of the package than at the base, but the highest velocity is just below the top of the Messinian evaporites. Based on this, an asymmetrical Poiseuille flow profile was suggested (figure 8.2). This flow profile indicates that the top of the evaporites moved faster than its base, which is as expected in a thin-skinned system of gravity spreading. According to the authors, the greatest shear-strain gradient is in the uppermost Messinian, indicating that this is the main detachment.

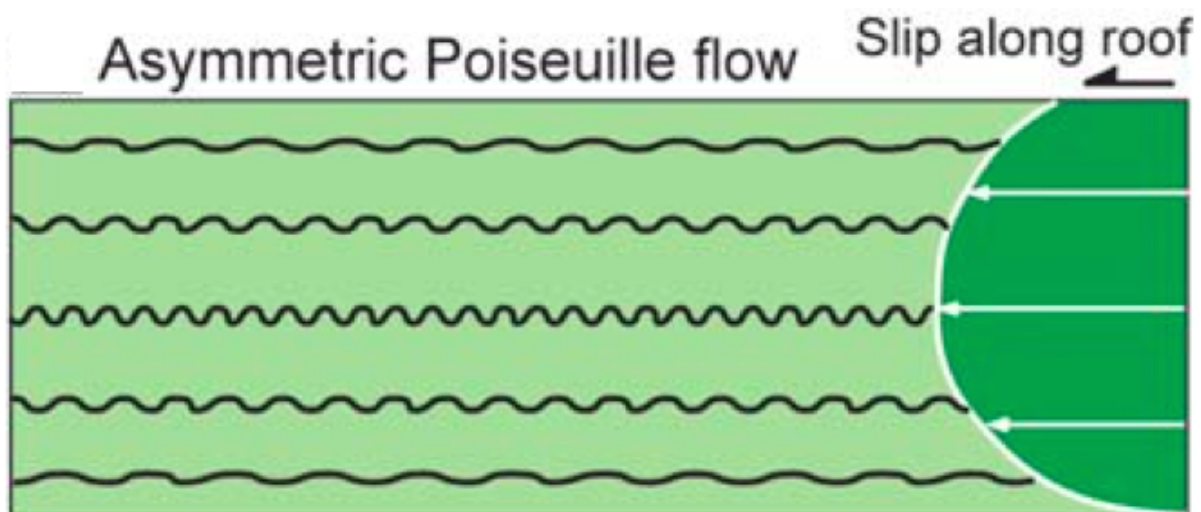


Figure 8.2: Cartwright *et al.* (2012) argue for an asymmetrical Poiseuille flow profile for the Messinian evaporites. They argue that the flow velocity of the Messinian evaporites is higher at the top of the package than at the base, but the highest velocity is just below the top of the Messinian evaporites. This flow profile fits what is expected in a system of thin-skinned gravity tectonics. Buckle folds symbolize shortening in competent units. Source: Cartwright *et al.* (2012).

8.2 Top salt unconformable surface

In the project that was carried out prior to this thesis (Solem, 2013), I studied the literature in order to get an overview of the present state of knowledge and to highlight the disagreements that revolves around the salinity crisis (see chapter 2). One of the main topics that were discussed was whether there was constant inflow of Atlantic water into the Mediterranean Sea or if the water came in sporadically. In this study, internal amplitude reflections can be observed within the evaporite package (figure 6.9 and figure 8.1). These high-reflective layers may represent different depositional sequences due to cyclic infill of marine water.

The high-amplitude reflections within the salt appear to be highly deformed and the upper intra-units are truncated by a high-amplitude reflection that marks the top of the salt (figure 8.3). This unconformity has a regional extent and is therefore expected to be of subaerial origin rather than submarine. This disconformity represents either a period of non-deposition or erosion. According to Hsü (1974), stromatolites, nodular anhydrite and diatoms are all found at the end of the evaporite sequences and are evidence very shallow-water conditions and desiccation. This supports the hypothesis that the unconformity on top of the evaporites is a disconformity generated by subaerial exposure.

Salt behaves very different from other sediments, as it moves like a plastic. In periods of desiccation, water-streams may dissolve the upper part of the salt and redistribute it. Because of this, the top of the salt will always be flat. As the salt moves, the internal layers will deform, but the top of the salt will maintain flat. The truncation of the upper internal reflections to the top salt (R6) can therefore represent a period of non-deposition where the upper deformed layers of the salt have been dissolved and redistributed. A second explanation might be that after the first phase of deformation, the upper part of the evaporite sequence was exposed and eroded. According to Bertoni & Cartwright (2007b), this unconformity is a widespread areal erosion with a truncation that is typical for a regression surface. The top of the salt will therefore represent the peak in relative sea-level fall during the Messinian desiccation event.

Ben-Gai *et al.* (2005) have studied the southeastern Levant, and states that the area was subaerially exposed and had a well-developed drainage system after the deposition of the evaporites. This formed a well-defined erosive unconformity in the slope area that gradually transformed into a correlative conformity in the deep basin. This forms a type 1 sequence boundary, meaning that there was a relative sealevel fall below the position of the present shoreline.

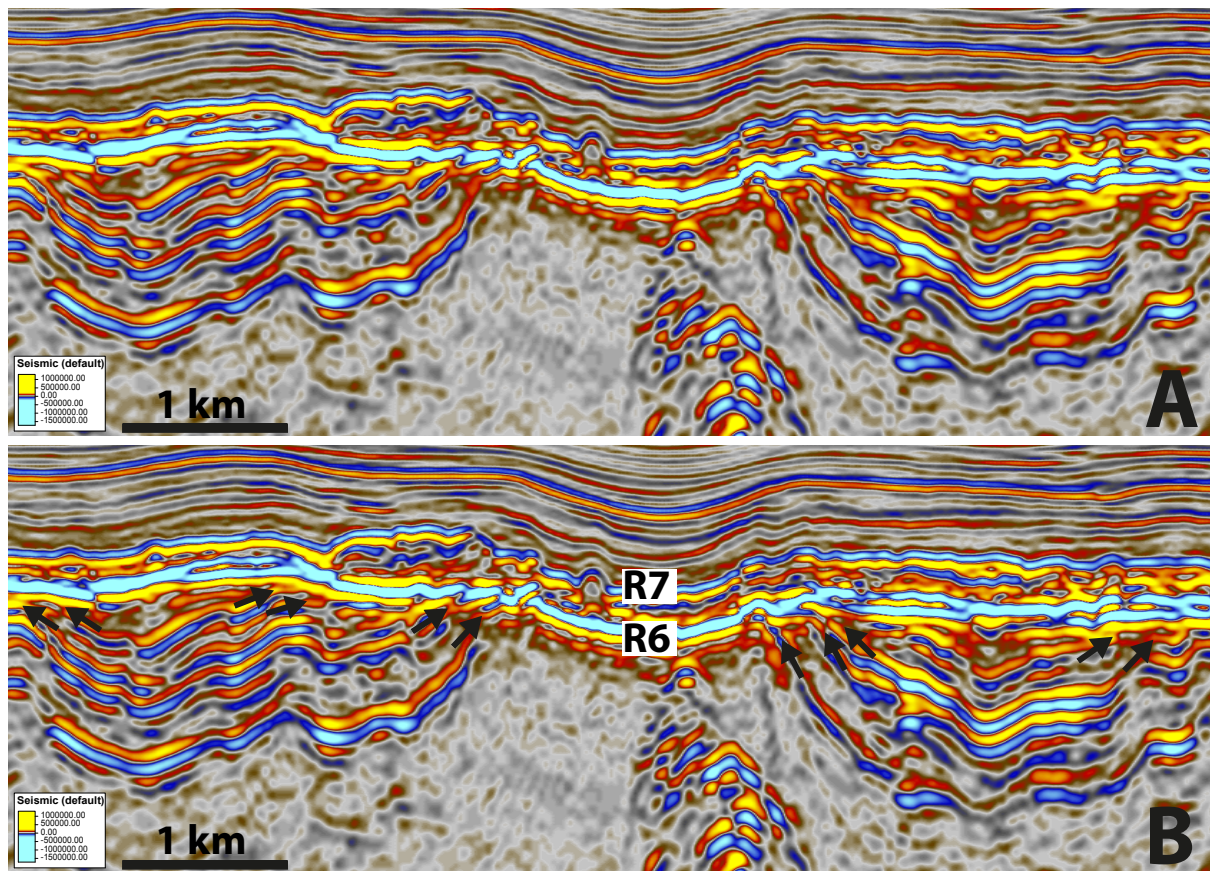


Figure 8.3: The figures show how the upper intra-evaporite reflectors are truncating the top salt unconformity. This means that the upper part of the evaporite package have most likely been eroded at the end of the salinity crisis. It could, however, also indicate a period of non-deposition where the upper part of the salt has been dissolved and redistributed flat. This truncation can be observed throughout the entire study area where the upper intra reflectors are present. The seismic section is oriented W-E. **A:** Plain seismic section, **B:** Arrows pointing out truncation.

8.3 Deposition of Transition layer

The origin of the Transition layer has not been exactly determined, even with a detailed seismic interpretation. In the following section, different scenarios for the deposition of the Transition layer will be suggested and discussed. Firstly, the Transition layer will be compared to different deposits that are known to exist on top of the evaporites in the Mediterranean area, in order to see if this could be the explanation of its origin. Secondly, a new proposal for the origin of this layer will be made, where modern analogues will be used to support the arguments.

8.3.1 Marine deposition

According to literature (see chapter 2) the MSC was terminated when the marine gateways between the Atlantic Ocean and the Mediterranean Sea opened and normal marine conditions were restored. There are two general opinions of how this happened. According to Hsü (1974) the western gate were irreparably crushed at the beginning of the Pliocene and Atlantic water flooded the partly desiccated Mediterranean basins. A second opinion is that the Mediterranean Sea was gradually refilled as the gateways opened (Riding *et al.*, 1998). Both of them argue for an abrupt change in deposition, going from evaporites to marine sediments. In the first scenario it would be reasonable to expect to find deep-marine deposits on top of the evaporites as the flooding of the Mediterranean happened rather fast. In the latter scenario, however, it would be more fair to expect a transition from shallow-marine to deep-marine deposits on top of the evaporites. In either case, marine sediments are deposited on top of the evaporites. According to Hsü (1974), the earliest Pliocene sediments directly overlying the evaporites contain deep-water faunas (benthonic ostracod and foraminiferal), which was found after examinations of the cores from the Deep Sea Drilling Project (DSDP). It is not mentioned whether the faunas were found in all cores or not.

Therefore, based on literature and drill cores (where most of them are from the western Mediterranean), the Transition layer would represent the first marine deposits after the Mediterranean Sea was flooded. It is, however, clear that the Transition layer do not look the same as the marine sediments above (figure 7.17). If the Mediterranean Sea was gradually refilled, the Transition layer could represent a transition from shallow marine to deep marine, giving it a different appearance than the deep marine deposits above. Still, the unconformity on top of the Transition layer will need an explanation. If the Mediterranean was gradually refilled, the unconformity could mark an episode of non-

deposition where the top of the layer was exposed to submarine erosion. This would explain the abruptly cutting of the layer, where the erosion was more channelized. The top of the Transition layer is clearly different from the base, which can be explained by a subaerial erosion at the base and a submarine erosion on the top. Since the literature claims that the evaporite deposits are directly overlain by marine Pliocene sediments, this would be a reasonable explanation. The only thing that opposes this is the fact that the sediments in the Transition layer do not slide on detachment faults as the marine sediments above do. It simply does not behave in the way one would expect a marine layer filled with water would do under deformation.

8.3.2 Yafo Sand Member

A package of high-amplitude, continuous, subparallel, and high-frequency seismic reflections have been observed offshore Israel in the eastern Mediterranean (southern part of the Levant Basin). This package has an approximately constant thickness of 70 m and has been penetrated by six exploration wells (unpublished well reports from BG-Group). It consists of marls interbedded with siltstones and sandstones and is termed the Yafo Sand Member of Early Pliocene age. The Yafo Sand Member is bounded at its base by a strong amplitude, continuous and flat-lying seismic reflection, and at its top by a surface of stratal discontinuity. Overlying the sands is a unit named the Yafo Mudstone Member. It was deposited during a major transgression and consists of moderate- to low-amplitude, subparallel continuous and medium-frequency aggradational seismic reflections (Frey-Martinez *et al.* , 2007).

The characteristics of the Yafo Sand Member with the overlying Yafo Mudstone Member are very similar to the Transition layer with the overlying marine deposits that have been observed offshore Lebanon. According to Gardosh (n.d.), the Yafo Sands were transported into the basin from the southeast and were deposited in submarine fans and lobes. These sands act as reservoir rocks for gas of bacterial origin, and the reservoirs are either found as horizontal and beds or dome-shaped sand mounds. An interpreted, time-migrated seismic profile (figure 8.4.a) shows the Yafo Sand and four gas field of the Yafo petroleum system. The upper boundary of the Yafo Sand Member in this section looks very similar to what can be observed in the Transition layer (figure 8.4.b).

There are, however, reasons to claim that the Transition layer cannot be the same as the Yafo Sand Member. First, Frey-Martinez *et al.* (2007) mapped the regional extent of the sand, which shows that the Yafo sands are geographically restricted to the offshore extension of the Afiq and el-Arish submarine canyons, offshore Israel (figure 8.5). They were transported in to the basin from the southeast as a part of a prograding and aggrading slope wedge, and locally deposited on the slopes where the Messinian evaporites are pinching out. The Transition layer can be found on top of the evaporites in the entire northern part of the Levant basin, from the margin to the deep basin, and is not locally restricted as the Yafo Sands. Second, the mounds and domes that appear in the Yafo Sand Member has a rather chaotic core with flat, parallel layers on the side (figure 8.6). This does not fit the observed characteristics of the Transition layer, where the thickest areas also have flat, semi-parallel layering.

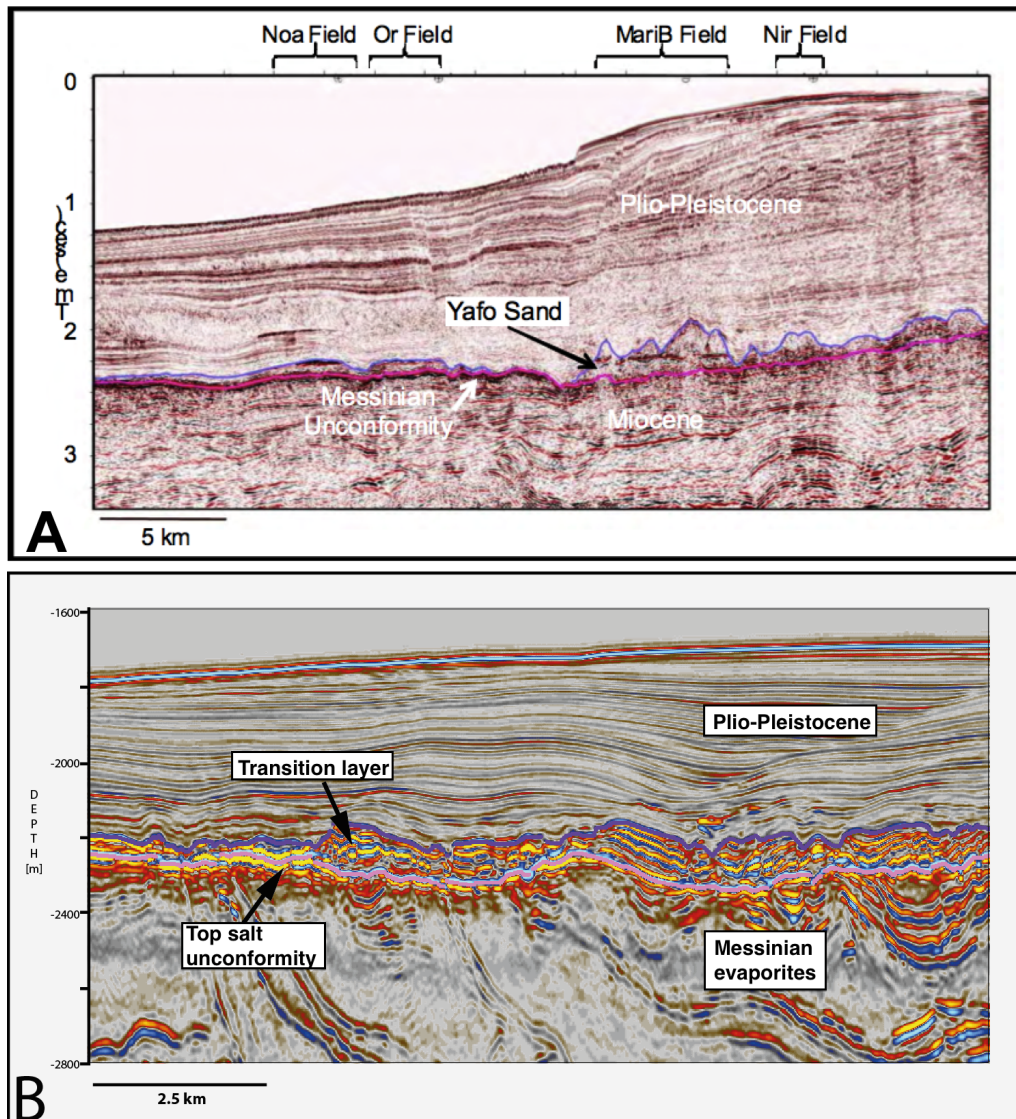


Figure 8.4: This figure shows a comparison of the Transition layer observed in the northern part of the Levant Basin (offshore Lebanon) with the Yafo Sand Member observed in the southern Levant Basin (offshore Israel). **A:** An interpreted, time-migrated seismic profile showing the Yafo Sand Member and four gas fields of the Yafo petroleum system. The lower Pliocene Yafo Sand Member is the reservoir rock. Source: Gardosh (n.d.). **B:** An interpreted, depth-migrated seismic profile showing the Transition layer. Notice the similarities in the upper boundary of the Yafo Sand Member and the Transition layer. It can also be observed that in figure **A** the Messinian evaporites have pinched out and the Yafo Sands are deposited on top of the unconformity in the slope. While in **B** the Transition layer is overlaying the evaporites.

Figure 8.5: Map showing the regional extent and distribution of the Yafo Sand Member offshore Israel. It can be seen that the Yafo sands are geographically restricted to the offshore extension of the Afiq and el-Arish submarine canyons, offshore Israel. The study area of this thesis is further north in the Levant Basin (offshore Lebanon). Since these sands are locally deposited in the slope-area offshore Israel, it is not reasonable to correlate this deposit to the Transition layer. Source: Frey-Martinez et al. (2007).

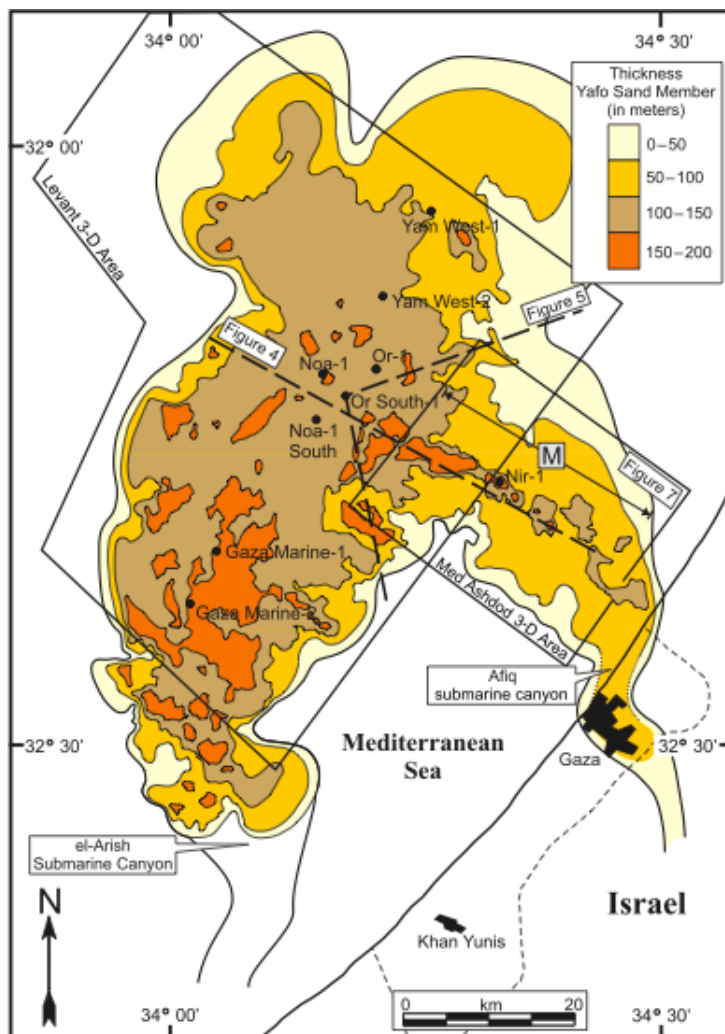
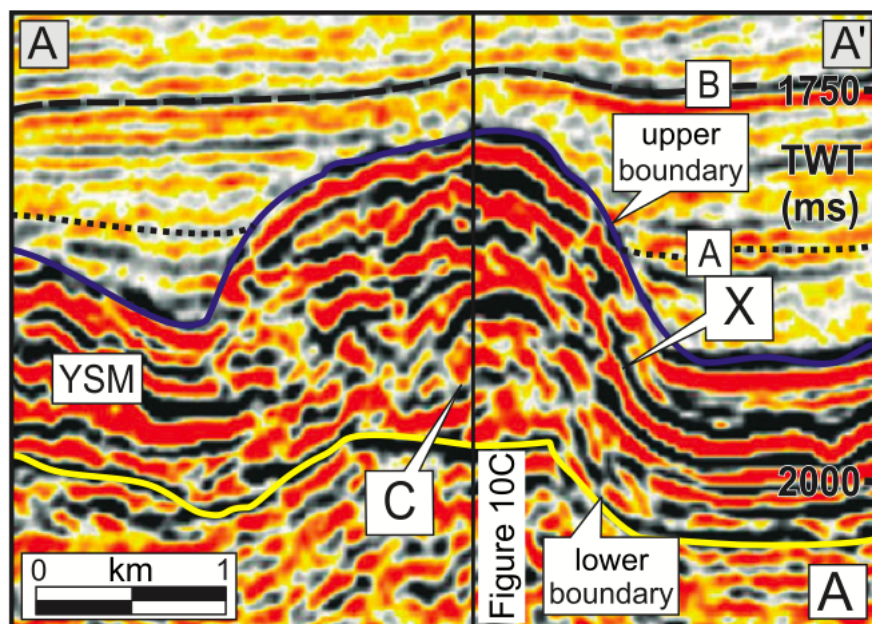


Figure 8.6: Dome-shaped features with chaotic cores are typical in the Yafo Sand Member. The shape of the features may appeal to the thicker areas of the Transition layer. However, the thickest areas of the Transition layer have flat, semi-parallel layering, not a chaotic core as the domes have. Source: Frey-Martinez et al. (2007).



8.3.3 Upper Evaporite Unit

Looking back at the project previously conducted (Chapter 2, Solem (2013)), the Messinian evaporites are usually divided into two parts; a lower unit that contains the lower evaporites and the main salt, and an upper unit that contains the upper evaporites. The lower and upper unit is separated by an unconformity that generally is thought to be an erosional surface. In Bertoni & Cartwright (2011), the Upper Unit is identified by a group of parallel and relatively continuous reflectors of relatively high amplitude. It is deposited above the main salt (called the mobile unit) and below the Plio-Pleistocene sediments. According to the author, the Upper Unit is only evident in the western Mediterranean Sea, not in the eastern part. There is, however, observed a bedded reflective unit at the top of the main salt in the Nile deep sea fan and in the Antalya basin (eastern Mediterranean Basin). This unit resembles the upper evaporite unit found in the Western Basin, but may also be of Pliocene age.

The characteristics of this layer and the fact that it is separated from the main salt by an erosional surface, gives it many similarities to the Transition layer. Also, since a similar layer has been observed locally other places in the Eastern Basin, there is reason to believe it could be found locally in the Levant Basin too. Rouchy & Caruso (2006) states that there is a huge sedimentary and hydrological change going from the Lower unit to the Upper unit. The Upper Evaporites are dominated by non-evaporitic deposits, interbedded with evaporite layers with a clear cyclic pattern. This may explain the bright amplitudes within the Transition layer.

8.3.4 Brackish Lago Mare deposit

According to Krijgsman *et al.* (1999) and Krijgsman & Meijer (2008), the upper evaporites were deposited at the same time as the Lago-Mare. This is fresh to brackish water deposits of lacustrine origin, which is considered to have preceded the marine reflooding and is related to the drainage of the Paratethys. Hsü *et al.* (1977) states that faunas give reason to believe that at the end of the Messinian, the western part of the Mediterranean was spilled by marine waters before the eastern basins were. Therefore, marine facies from the uppermost Messinian in the western basins can be equivalent in part to the late Messinian Lago-Mare in the eastern basins. There is a close connection between the Upper evaporites and the Lago Mare deposits, and several authors refer to them as one (Krijgsman *et al.* (1999), Bowman (2012)). This is because the Upper evaporites were deposited in a non-marine, deep Mediterranean basin forming a large Lago Mare

(Krijgsman *et al.*, 1999). The Lago Mare deposits conformably overlie the halite unit in deep basinal areas and onlap the Messinian erosional surface (top salt) in shelfal areas and marginal basins (Bowman, 2012). The Lago-Mare facies are recognizable on seismic data due to their interbedded nature. A cyclic alternation of sandstones, conglomerates, marls and gypsum gives alternations of high and low amplitude reflectors. This alternating sequence is repeated several times within the Lago Mare facies. The upper part of the Lago Mare facies has records of fluvio-deltaic systems, and channels of subaerial origin have been reported. According to Bowman (2012), each precessional cycle within the Lago Mare facies consists of a repeated sequence of subaerial exposure and channel incision; inflow and flooding of fresh-water that leads to the establishment of brackish/lacustrine conditions; deposition of channel sands and lacustrine silts and mud; marine flooding; evaporation and drop in base level; and deposition of evaporites, gypsum/anhydrite, before the entire sequence is repeated again.

Couto *et al.* (2014) divide the Lago-Mare facies into three events that occurred at different times during the Messinian: Lago Mare 1, Lago Mare 2 and Lago Mare 3. For the case of the Transition layer, Lago Mare 2 would be of interest. Lago Mare 2 represents an intermediate Lago Mare episode that is directly overlying the evaporites in the Mediterranean central basins. It is usually related to a freshwater input ending the evaporitic phase, but this is still unsatisfactorily documented. Locations of interest for the Lago Mare 2 are at site 60 and 61 (DSDP and ODP holes), which is south of Cyprus and west of the Levant Basin.

Due to the fact that the Lago Mare facies are reported at all drill sites in the eastern Mediterranean Sea, the chances are high to find the deposits in the northern part of the Levant Basin too. There is also reason to believe that the degree of freshwater compared to marine water will change depending on the location in the Mediterranean. This is supported by the drilling reports where it is, as an example, showed that the sedimentary development in the different basins was not the same within the Lago Mare. The flat, high-amplitude reflection of the Transition layer can be explained by the cyclic alternation of the evaporites, gypsum, anhydrites and clastics that has been documented in the Lago Mare facies. The abrupt change in thickness and the top of the Transition layer may, as already mentioned, reflect an episode of erosion where channels have been cut. This fits well with the channels of subaerial origin that can be observed within the upper part of the Lago Mare.

A seismic section from offshore Sirt Basin, Libya, where the Lago Mare deposits are overlying the Messinian evaporites have been published by Bowman (2012) (figure 8.7). The cyclical and channelized nature of the Lago Mare facies can be observed clearly in this

section. According to the authors, the channels were later filled by seismically transparent clastic sediments. This transparent infill cannot be observed within the Transition layer.

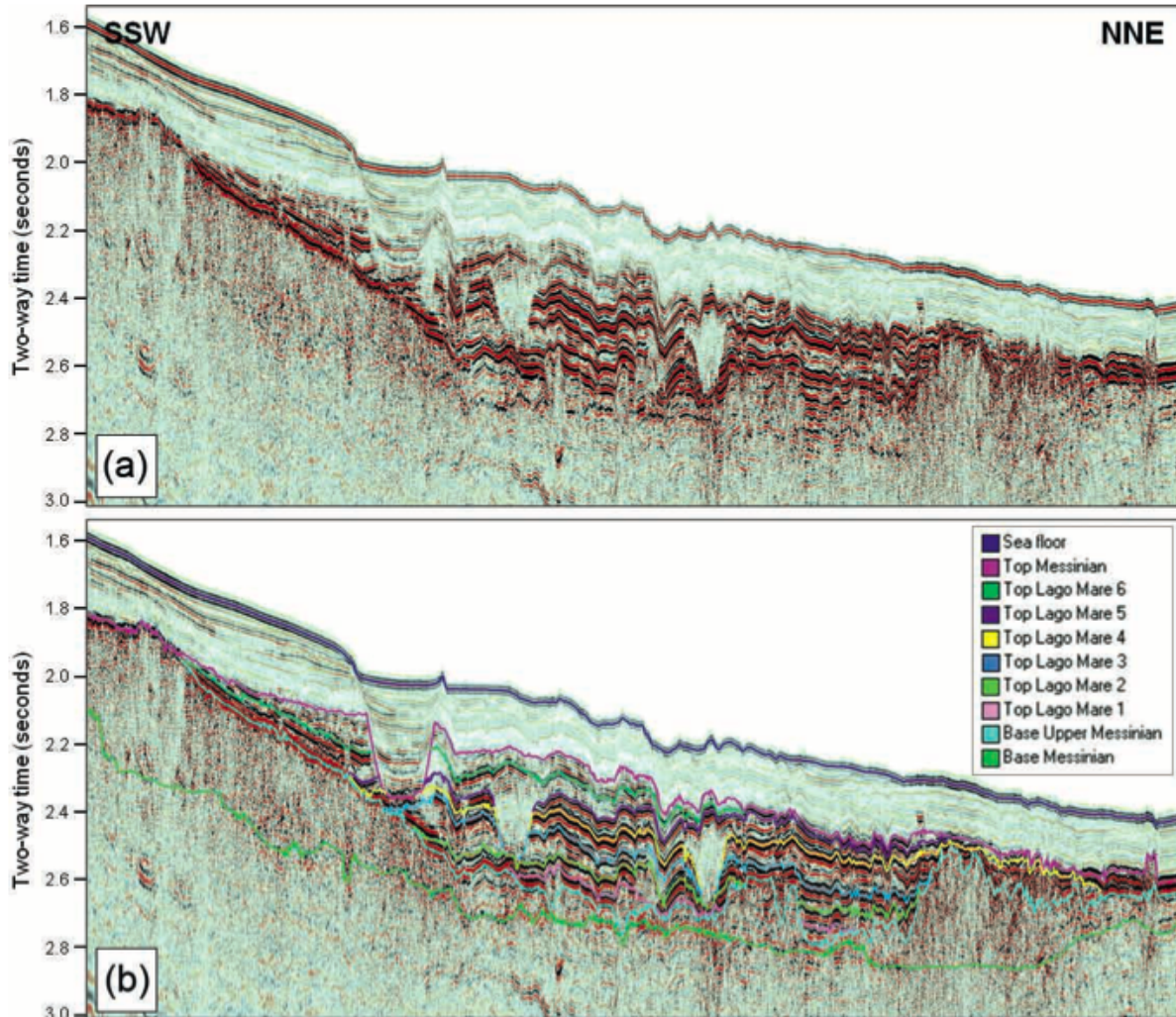


Figure 8.7: Seismic section showing the Lago Mare facies in the offshore Sirt Basin. Two versions of the same line are displayed: (A) uninterpreted; (B) interpreted. The cyclical and channelized nature of the Lago Mare facies can be observed clearly, with seven individual units identified. The alternating high and low amplitudes and the channels within the Lago Mare have a many similarities to the Transition layer. The channels within the Lago Mare deposits are filled with sediments that appear transparent on the seismic. This is not the case for the Transition layer. Source: Bowman (2012).

8.3.5 Fluvial deposit

Even though the suggested scenarios fit the description of the Transition layer, there are still some questions that need to be answered. If the Transition layer is of marine origin, why doesn't the layer look similar to the marine sediments above? And why is the upper boundary of the Transition layer so highly reflective if it doesn't indicate a change in lithology or deposition? A scenario based on the appearance of the Transition layer and modern analogues will now be proposed.

It can be observed that the Transition layer is significantly different from the marine Pliocene sediments above. The deep-marine package above consists of fine grain sediments that appear very uniform and reflects relatively low amplitude. They are filled with water and will therefore deform easily. Detachment faults and growth faults can be observed, as the package has deformed due to salt tectonics. The Transition layer on the other hand has not deformed in the same way and no detachment faults can be observed here. They appear to consist of hard, consolidated sediments that have been deposited flat and have been well lithified. They do, in other words, not behave the way that is expected if they were marine deposits.

One observation that can be taken from the amplitude maps is that the channels are not as visible as what would be expected, at least if they are submarine. Submarine channels are usually visible on amplitude maps, as they tend to be filled with high-amplitude reflecting sands. This new scenario favors a fluvial deposition of the Transition layer where the key is not to look at the amplitude maps, but instead to look at the topography itself. The thickness map reveals how channels are cutting through the thickest deposition that are deposited flat (figure 8.8). This is a key observation that is an important characteristic for this layer.

Gradient is required in order to develop submarine channels. An example of this is figure 8.9 that shows a submarine channel system in the Pacific Ocean. The surface map of the seabed (figure 1, Appendix) shows this gradual deepening, even though channels are not visible on this map. The Transition layer is relatively flat, and no big gradient existed when the layer was deposited. The only gradient that can be observed today is due to salt tectonics.

A proposed scenario for this layer is therefore that after deposition of the Messinian evaporites there was a period of desiccation (marked by the flat disconformity on top of the evaporites). During this period, rainwater would make streams, and together with rivers of water coming from the Nile, channels would develop. Evaporites are relatively

impermeable and water will not soak into them. Water will therefore flow long distances and will not require gradient. As the channels find a preferable path, clastic sediments and reworked evaporites will be deposited on the channel sides.

Modern Analogue 1 - Mono Lake

There are modern examples where this sort of deposition occurs, and where channels and canyons are cut even though the base is flat. The first example is from the *Mono Lake, California, USA*. The lake exists on top of evaporites. A lake like this will be created when there is enough runoff from rain. It exists because the evaporites are impermeable and water will not soak into the ground. The lake will therefore exist until all the water has evaporated. figure 8.10 shows a picture taken of Mono Lake. The area is flat with an existing lake and deposits of evaporites and clastic sediments on the sides of the lake. This analogy can be transferred to the Transition layer where a thick section of sediments stretching from SW to NE have been deposited (figure 8.11). It is possible that the layer was eroded during deposition and then the sediments were re-deposited further west where a small lake with shallow water, like the Mono Lake, existed. This can explain why the Transition layer is much thinner further west compared to the middle and eastern side (figure 7.5).

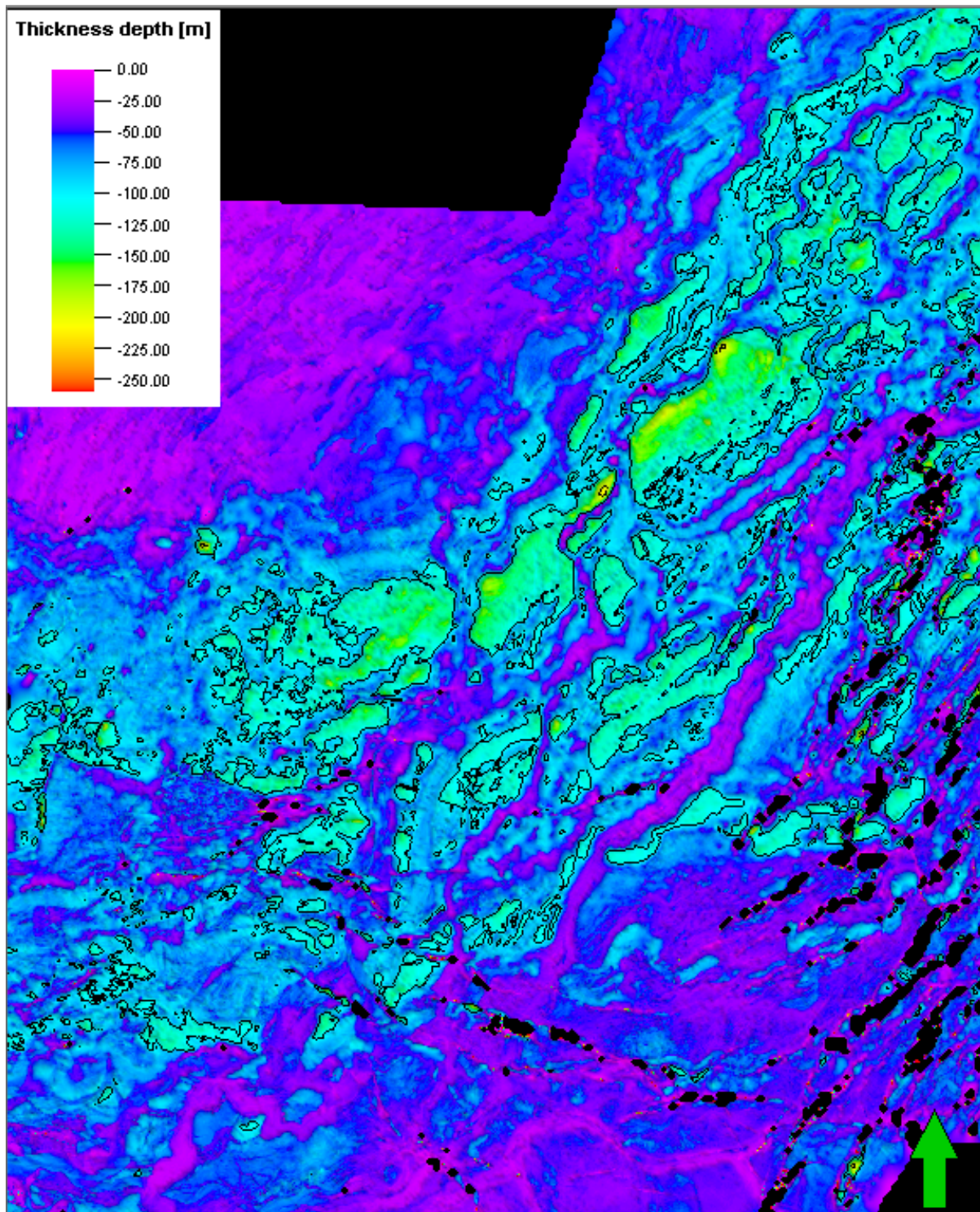


Figure 8.8: Thickness map of the Transition layer with a close-up of the southern part of the study area. See (figure 7.7) for thickness map of the entire study area. This map shows how the thickest deposits of the layer are cut by channels without any gradient. This is essential information for the characterization of this layer. Purple color marks the thinnest areas, while green/yellow marks the thickest areas. The thickest areas are stretching from SW to NE, and the channels are cutting straight across this.

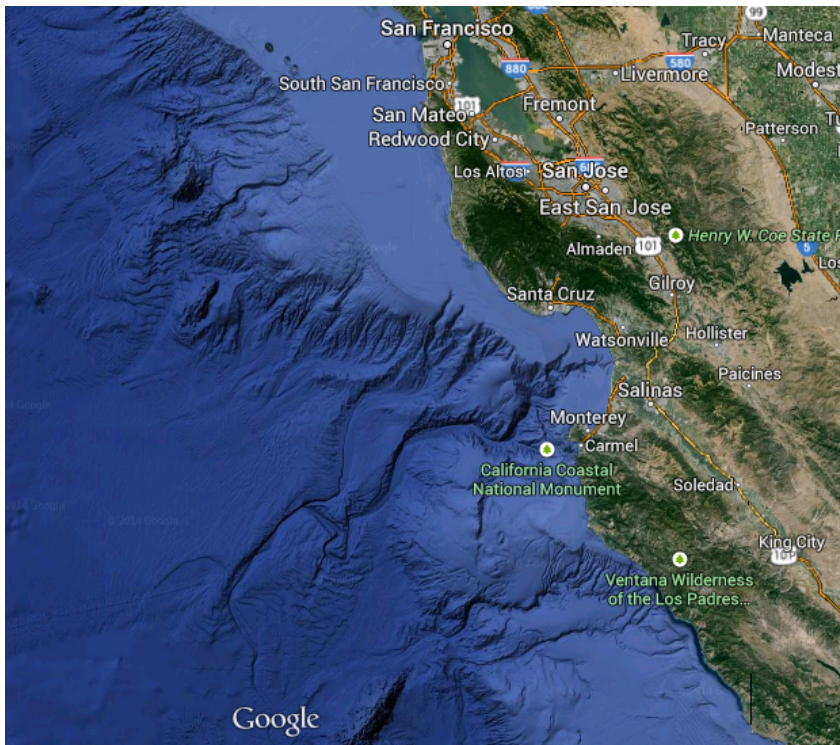


Figure 8.9: The figure shows an example of a submarine channel system in the Pacific Ocean where a steep gradient is present. This is not the case for the channel development in the Transition layer, where the layer has been deposited flat. The picture is a screen-shot from google maps.



Figure 8.10: Picture of Mono Lake in California, USA. The picture shows an example of flat evaporite layer where sediments are deposited on the sides. A small lake like this will exist until it evaporates, since the evaporite deposits under the lake are impermeable. Private photo: John Comstock.

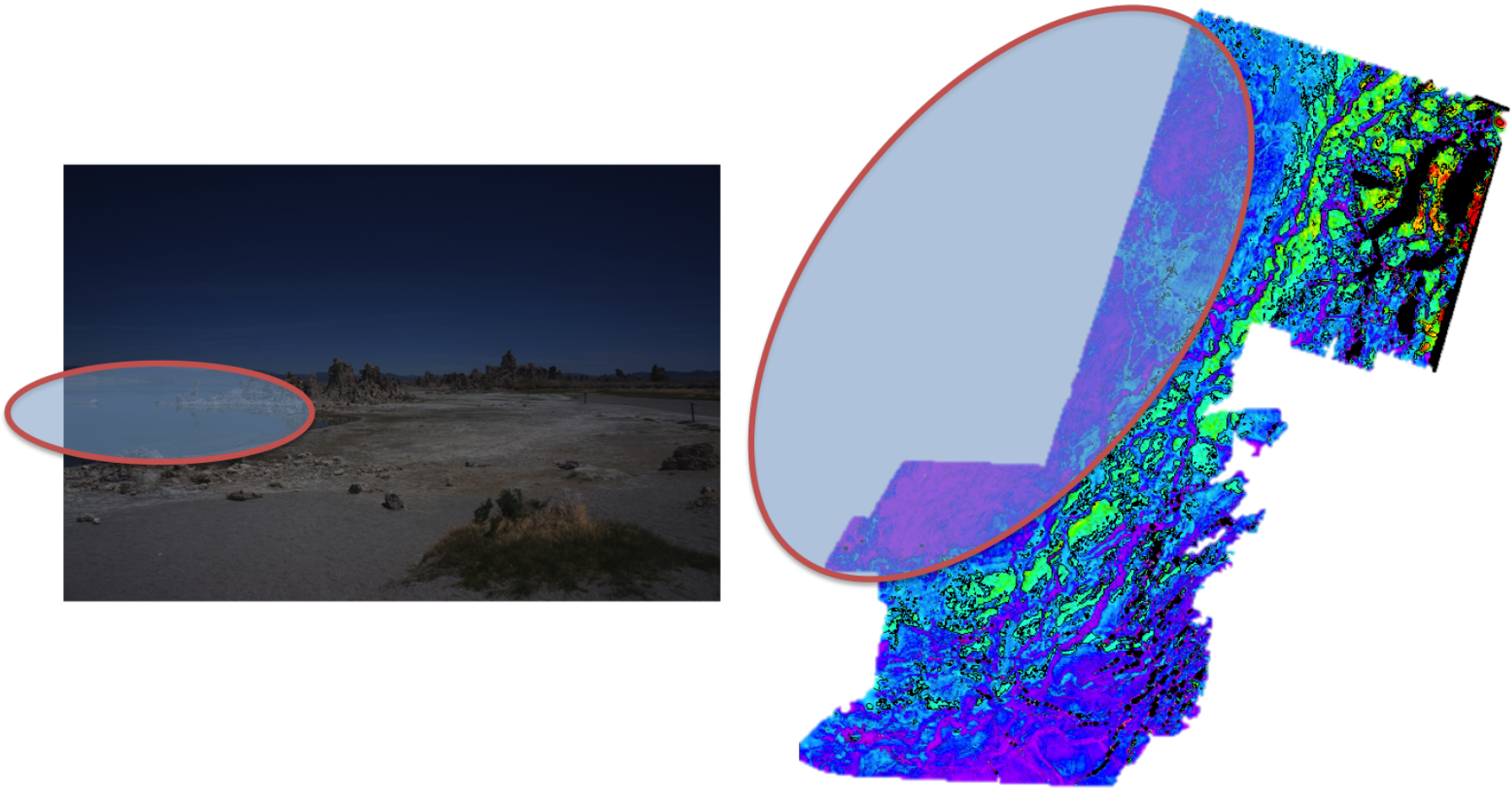


Figure 8.11: The figure shows how Mono Lake and the evaporite deposits can be an analogue to the Transition layer. The thickest areas of the Transition layer may have deposited first. The layer can then have been eroded by channels that re-deposited the sediments further out where a small lake such as Mono Lake existed. This can explain the thickness differences that are observed between the western and middle/eastern areas of the Transition layer (figure 7.5). **Left:** Mono Lake, California. Red circle marks the lake. **Right:** Thickness map of the Transition layer. Red circle marks the suggested location for where a small lake like the Mono Lake could have existed.

Modern Analogue 2 - Death Valley

A second analogue that favors this scenario is the *Death Valley (USA)*. The Death Valley is a desert valley with flat areas covered by evaporites. The flat areas of the Death Valley show very clearly how it is possible to have channels in a areas with no gradient (figure 8.12). It can be observed that as the water travels in channels on the evaporites, it will dissolve some of the upper evaporites and deposit a mixture of clastic sediments and reworked evaporites on the sides (figure 8.13). As deposition of sediments continues, water will continue to travel in the same path. This is because it is easier to dissolve evaporites compared to clastic sediments. The deposits on the sides will then slowly build up, while the channel will travel in the almost same path all the time (figure 8.14). This looks exactly the same as what can be observed in the seismic sections of the Transition layer. If comparing this to the Transition layer, it will mean that the observed channels haven't necessarily been cut by erosion at the end of deposition. The channels may have started on a flat desiccated surface, where the side banks have built up next to the channels. Most reasonably, a combination of both erosion after deposition and prior/at the same time as deposition have occurred. figure 8.15 and figure 8.16 show a good example of a flat evaporite ground with channels traveling without any gradient and depositing sediments on the side.



Figure 8.12: The pictures show a salt lake in Death Valley where the ground is flat, but channels do still exist. The water can travel on top of the evaporites for a long distance, and dissolve and re-distribute sediments. A channel like this can be better seen in the lower picture. The area seen in these pictures are more than 40 km long and 15 km wide. Private photo: John Comstock.



Figure 8.13: *The picture shows the sediment distribution. The evaporites are in front of the picture. This is where the water will prefer to travel, due to impermeability and the ability of dissolving evaporites. A mixture of clastic sediments and reworked evaporites can be seen behind the evaporites, having a darker color than the white evaporites. Private photo: John comstock.*



Figure 8.14: This picture shows an example that look very similar to what can be observed in the seismic sections of the Transition layer. This is an analogue to the abrupt cutting of the thicker parts of the Transition layer. This small canyon can either have been made by sediments building up on the sides of a channel, or by a channel eroded the already existing sediment package. A combination of this may have happened during deposition of the Transition layer. Privat photo: John Comstock.



Figure 8.15: *This picture is from Badwater in the Death Valley. It shows the channel existing on the evaporites without any gradient. When it is water here, the channels created will slightly dissolve some of the upper evaporites and redistribute the sediments further out. Because of this, the top of the evaporites will continue to stay flat. A mixture of reworked evaporite and clastic sediments are deposited on the sides of the channel. Private photo: John Comstock.*



Figure 8.16: The picture shows a close up of figure 8.15. Water prefers to travel on top of the evaporites (white color in the middle of the picture) and will deposit a mixture of reworked evaporites and clastic sediments on the sides. Private photo: John Comstock.

8.4 Difficulties

The good quality of data and the complex tectonic history makes the northern Levant Basin a very interesting, but difficult area to work with. The biggest issue in this study has been that no well data was available for me from the study area (northern Levant Basin). The interpretation of the seismic data has been very demanding due to this, but also because of the large amounts of data and the tectonic history. The interpreted seismic horizons and packages could therefore not be properly determined as it is only based on appearance and information from literature. The proposed ages for the different packages are therefore not necessarily correct. One of the goals for this thesis has been to gain an understanding of the origin of the Transition layer. Different scenarios have been proposed, where more than one of them seems possible. Due to lack of necessary data it has not been possible to make a correct correlation between the Transition layer and other deposits in the eastern and western Mediterranean Sea. It is therefore no basis for drawing a conclusion for the origin of the Transition layer.

8.5 Geological Reconstruction

From the data interpreted in this thesis it has been attempted to reconstruct the geological history of the Levant Basin from the Messinian time to now. Figures were drawn in order to visualize the development (figure 8.17 - figure 8.23). It must be noted that these are purely schematic and not to scale. See chapter 7 for the fully described interpretation.

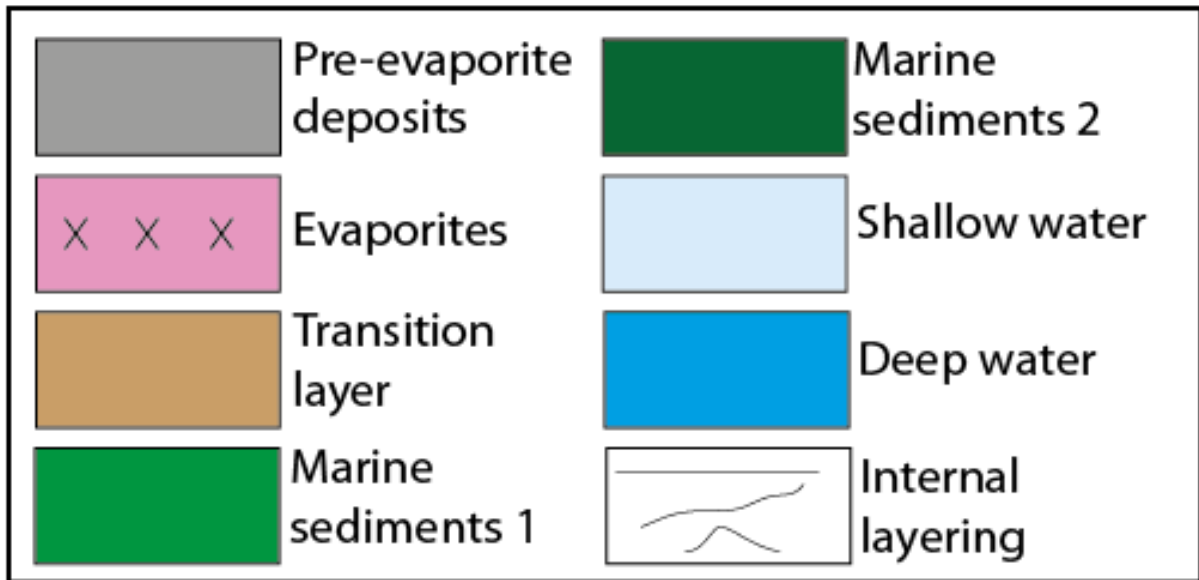


Figure 8.17: This is the legend describing what can be seen in the following four figures (Stage 1 to 7).

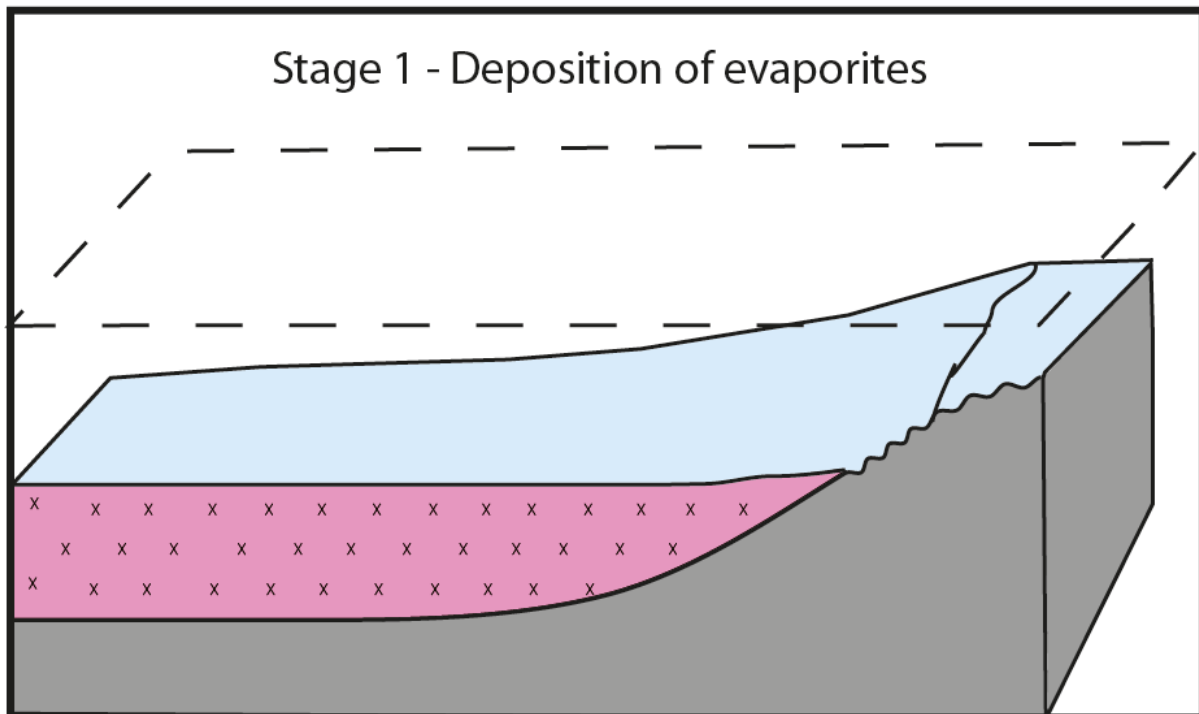


Figure 8.18: Stage 1: Deposition of Messinian evaporites by cyclic infill of marine water from the Atlantic Ocean. The evaporites have a thickness of maximum 1800 m in the basin, and is wedging out towards the margin.

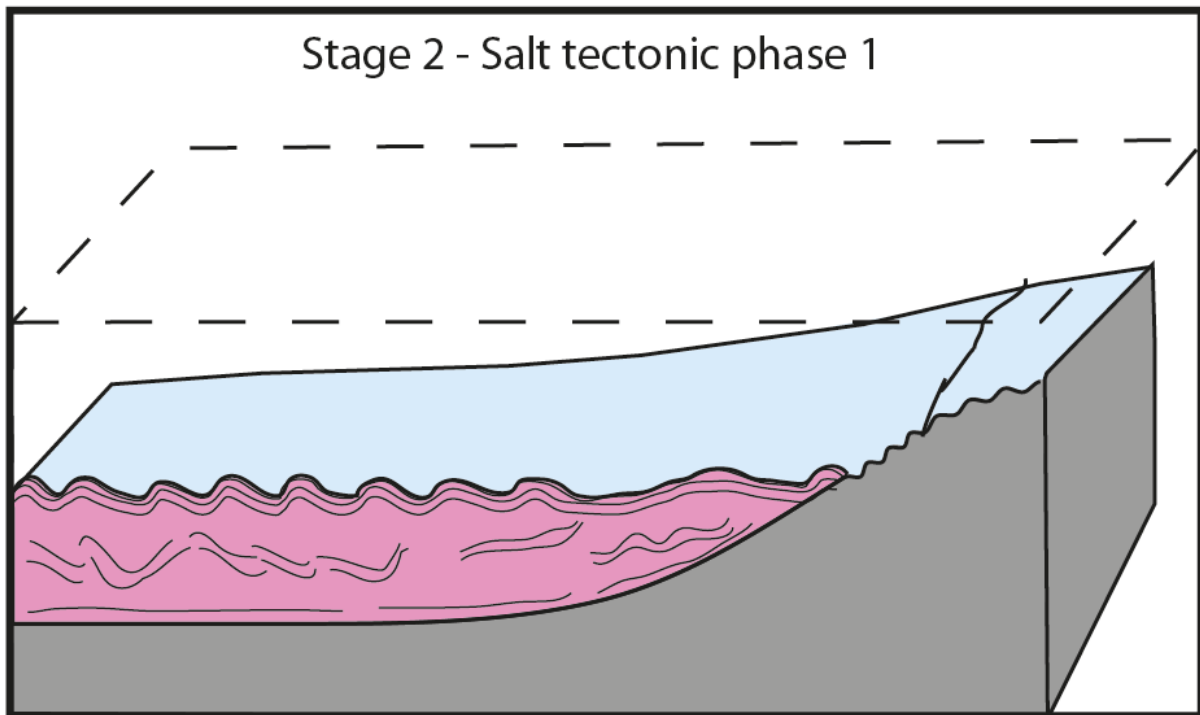


Figure 8.19: Stage 2: The first phase of salt tectonics occurred at the end of evaporite deposition. Evidence of this can be seen by deformation of the intra-evaporite reflectors. The upper part of the evaporites has deformed and moved more than the lower part.

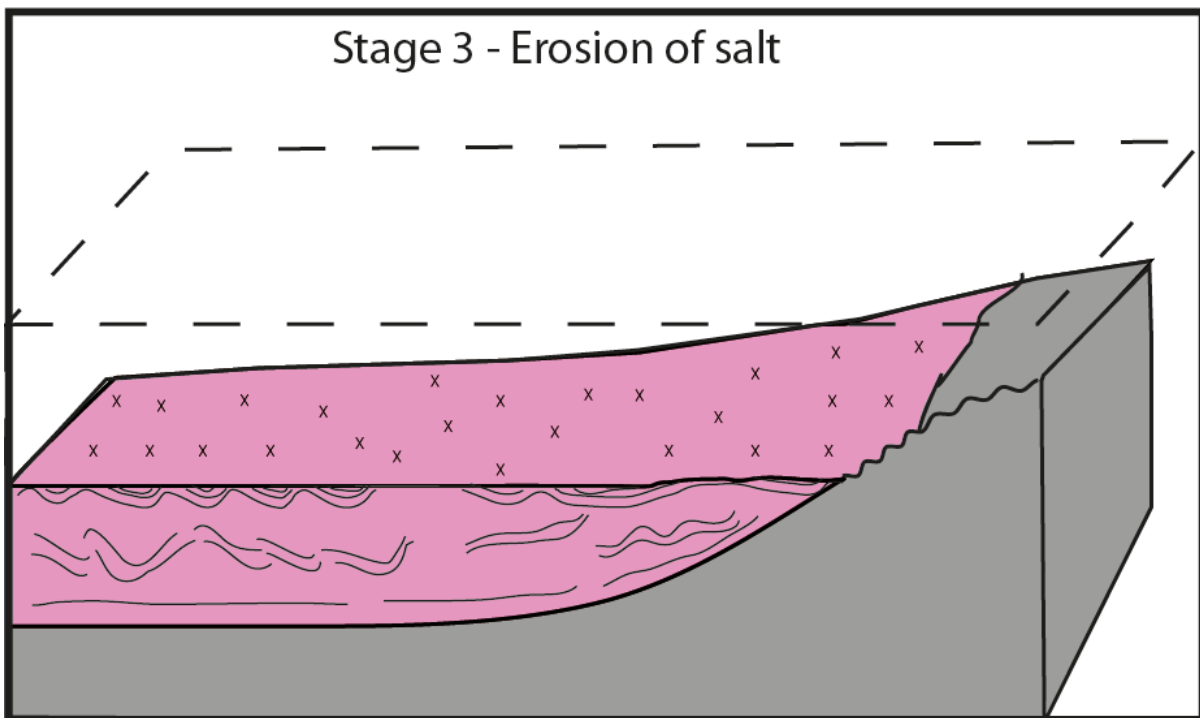


Figure 8.20: Stage 3: After deposition and deformation, the upper part of the evaporites was aerially exposed and eroded. This marks an episode of desiccation at the end of the Messinian Salinity Crisis. This erosion is marked by a continuous, high-amplitude reflector on top of the salt. The upper intra-reflectors are truncating this erosion surface.

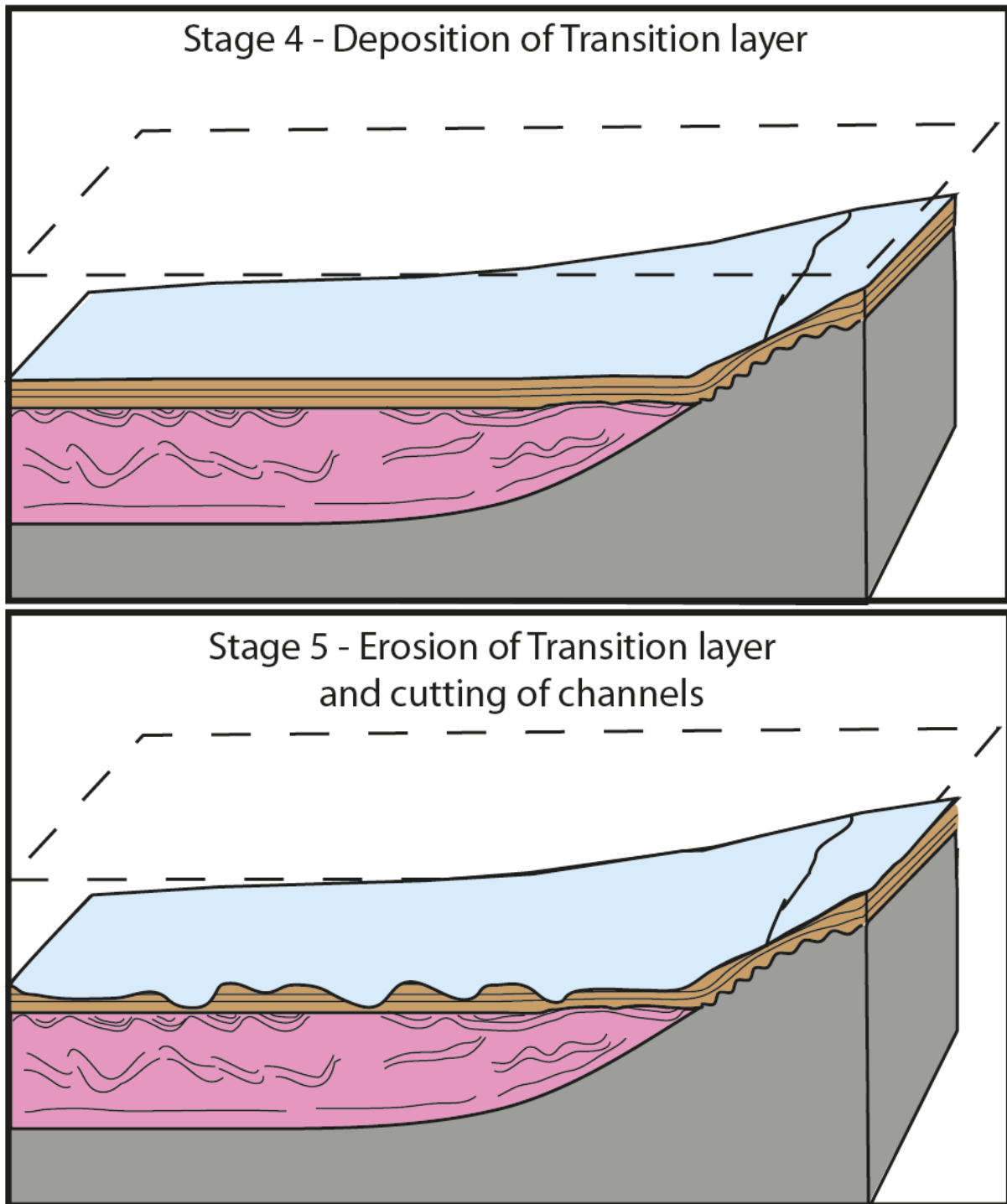


Figure 8.21: Stage 4 and Stage 5: The Transition layer deposited on top of the erosional surface (top salt). This layer is recognized by its continuous, high-amplitude reflectors. Stage 5 may either follow Stage 4 or occur at the same time as Stage 4. The Transition layer can either be deposited flat, then exposed to erosion (subaerial or submarine) where channels were developed. Or, the channels can develop at the same time as the layers are deposited. Meaning that the channels stay more or less in the same place and sediments are depositing and building up on the sides of the channel. This depends on which scenario for the origin of the Transition layer is chosen. The correct scenario cannot be decided before well data for the layer is available. According to the colors in the figure, the Transition layer was deposited in shallow water (light blue color). This would be the case for all scenarios except if the layer is of deep marine origin.

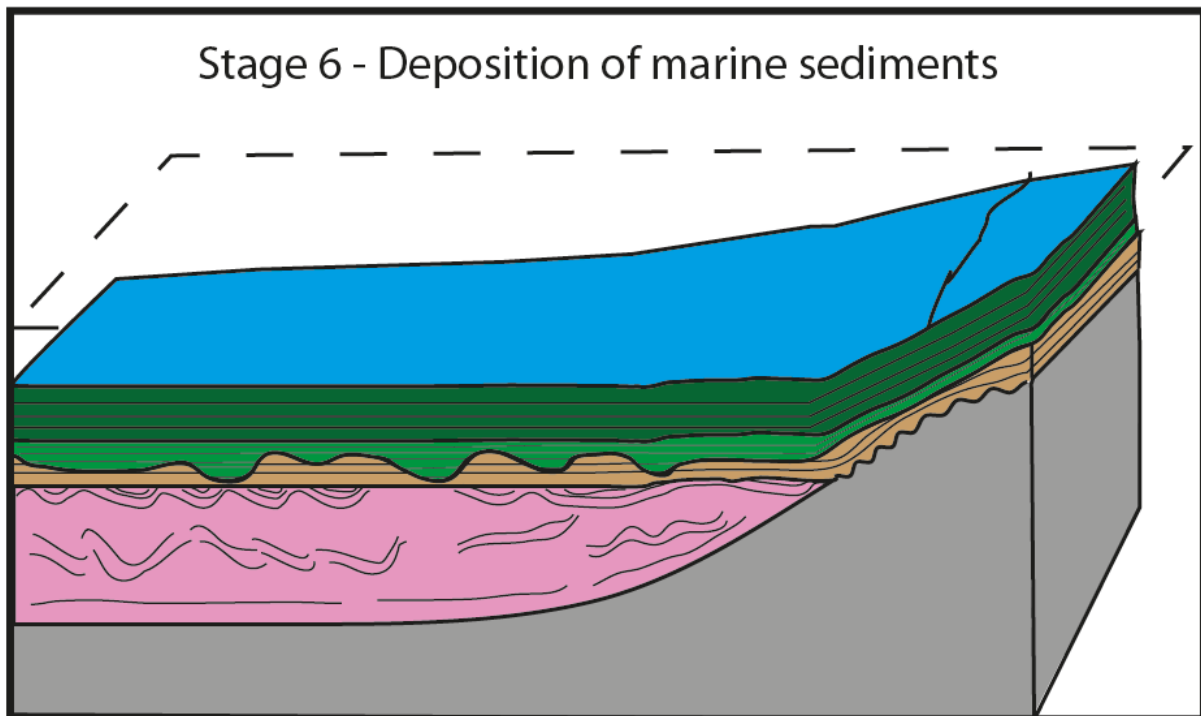


Figure 8.22: Stage 6: Deep-marine sediments of Pliocene-Pleistocene age have deposited on the top of the Transition layer. These were deposited when the gateways between the Atlantic Ocean and the Mediterranean Sea were crushed and normal marine conditions were re-established. In this figure there have been used two different colors for the marine deposits (light and dark green), in the legend named Marine sediments 1 and Marine sediments 2. The reason for this division is that in chapter 7 and chapter 6 a reflector (R8) has been interpreted, dividing the marine succession in two.

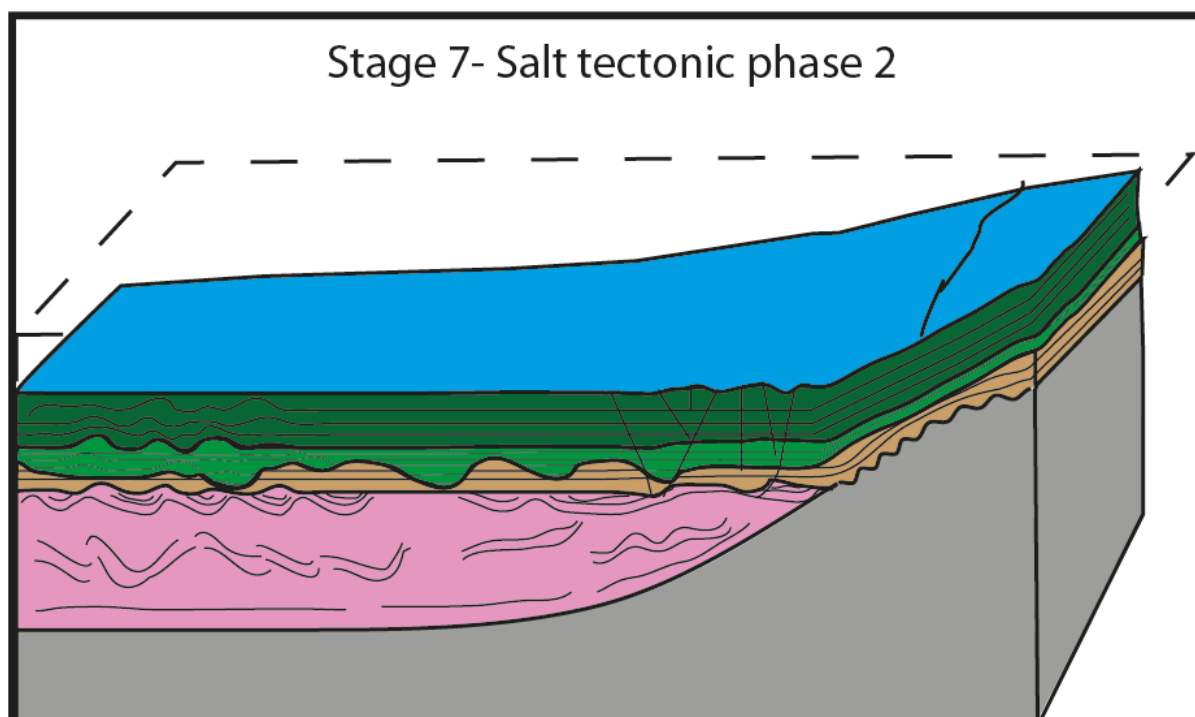


Figure 8.23: Stage 7: The second phase of salt tectonics is post-dating the evaporite deposition. The deformation has influenced the entire Pliocene-Pleistocene section, the Transition layer and the top of the evaporites. Deformation in the seabed can also be observed, meaning that the deformation must have taken place relatively recently. Three stress domains can be observed: extension close to the margin (right), contraction in the deep-basin (left) and a transition zone in the middle. This tectonic phase is well documented in the literature, where it is linked to gravity-driven, thin-skinned deformation.

Chapter 9

Conclusion

The evolution of the northeastern Levant Basin, offshore Lebanon, was interpreted on the basis of observations derived from seismic sections exclusively. The results of this study are summarized below:

- The regional geological history of the Levant Basin has been interpreted. The Levant Basin is a rift-basin with a passive margin to the east. The basin can be divided into three units. Unit 1 consists of Late Cretaceous and older sediments that are making up the foundation of the deep rift-basin and the passive margin to the east. Unit 2 consists of sediments of Late Cretaceous to Late Miocene age that have been accumulated by subsidence of the basin. A thick sequence of Messinian (Late Miocene) evaporites marks the start of Unit 3. The evaporite sequence is between 1 and 2 km thick in the deep basin, and is pinching out towards the margin. The "Transition layer" has been deposited on top of the Messinian evaporites and appear to be a high-amplitude, continuous sedimentary layer. The upper part of Unit 3 consists of Pliocene-Pleistocene deep-marine sediments that were deposited when normal marine conditions were re-established.
- The evaporite sequence consists of alternation of transparent facies and intra-evaporite reflectors with higher amplitudes. This might be an indication of cyclic infill of marine water during the Messinian Salinity Crisis, giving several depositional sequences. The evaporites are bounded by two unconformities, where the base is an erosion surface that marks an important sea-level fall at the beginning of the MSC. The top is an unconformity of subaerial origin. Regional truncation of upper intra-evaporite reflectors gives reason to interpret this as a subaerial erosion surface. This gives reason to believe that the Levant Basin, and maybe the entire

eastern Mediterranean, was desiccated at the end of the Messinian Salinity Crisis.

- Observations from the seismic sections give evidence of two major phases of salt tectonics. The first phase took place at the end of evaporite deposition in the Late Messinian. This can be seen by deformation of the internal reflectors within the evaporite sequence, where the upper reflectors are truncating the erosional surface on top of the salt. Deformation must therefore have occurred during or after deposition of the last evaporites, but prior to the final erosion that marks the end of the MSC. The second phase of salt tectonics post-dates evaporite deposition, and has affected the entire Plio-Pleistocene succession, including the evaporites and the seabed. This can be seen as extensional growth faults at the lower slopes of the margins and folding in the more distal areas. This phase is well documented in literature where it is linked to gravity-driven, thin-skinned deformation.
- Several scenarios have been proposed for the origin of the Transition layer. These are: marine deposition, Yafo Sand Member, Lago Mare deposit, Upper evaporite deposit and fluvial deposit. Based on seismic observations of the Transition layer and described characteristics of other coeval deposits in the Mediterranean area, it is most likely that the Transition layer is either a fluvial deposit, a Lago Mare deposit, or a part of the Upper evaporites. The latter two are often considered to be coeval. No well data from the study area was available for this thesis. The origin of the Transition layer can therefore not be correctly determined.

Chapter 10

Further Work

A lot of work can be done in this area. With available well data a correct correlation between the different parts of the Mediterranean Sea would be possible. Cores through the Transition layer could then be studied and the origin of the layer could be determined with more accuracy. The Levant area is an attracted hydrocarbon province. The southern part of the Levant Basin, offshore the Nile Delta, hosts a world-class hydrocarbon province. Recent discoveries indicate that the central part of the basin, offshore Israel, also have a significant hydrocarbon potential, with biogenic gas and various oil shows (Gardosh *et al.* , 2006). As of today, no wells have been drilled in the northern part of the basin, offshore Lebanon, which has been the study area of this thesis. An interesting topic for further work would therefore be to explore the petroleum potential in this area. For that, exploration wells and cores would be necessary. The Levant Basin holds an estimated 3.5 Tcm (123.6 Tcf) of gas and 1.7 Bbbl of oil. Of this, 846 Bcm (30 Tcf) of natural gas and 660 Mmbbl of oil is estimated to be the potential reserves offshore Lebanon. However, these estimates cannot be validated since not a single well has been drilled here (Newman, 2013). Several potential reservoir rocks are found in the Levant Basin, from Cenozoic, Cretaceous and Jurassic. This includes both sandstones and limestones. Impermeable seals are found in the Messinian Salt, shales and marls of the Paleogene, Neogene, Cretaceous and Jurassic, and Triassic evaporites. The most common source rock in the region occurs in rocks of Mesozoic age. Oil-prone source rocks are found in the Upper Cretaceous, while Triassic-Jurassic source rocks are often gas-prone (Roberts & Peace, 2007).

References

- Ben-Gai, Y., Ben-Avraham, Z., Buchbinder, B., & Kendall, C.G.St.C. 2005. Post-Messinian evolution of the Southeastern Levant Basin based on two-dimensional stratigraphic simulation. *Marine Geology*, **221**, 359–379.
- Bertoni, C., & Cartwright, J.A. 2005. 3D seismic analysis of circular evaporite dissolution structures, Eastern Mediterranean. *Geological Society*, **162**, 909–926.
- Bertoni, C., & Cartwright, J.A. 2006. Controls on the basinwide architecture of late Miocene (Messinian) evaporites on the Levant margin (Eastern Mediterranean). *Sedimentary Geology*, **188-189**, 93–114.
- Bertoni, C., & Cartwright, J.A. 2007a. Clastic depositional systems at the base of the late Miocene evaporites of the Levant region, Eastern Mediterranean. *Geological Society, London, Special Publications*, **285**, 37–52.
- Bertoni, C., & Cartwright, J.A. 2007b. Major erosion at the end of the Messinian Salinity Crisis: evidence from the Levant Basin, Eastern Mediterranean. *Basin Research*, **19**, 1–18.
- Bertoni, C., & Cartwright, J.A. 2011. *Seismic Atlas of The Messinian Salinity Crisis markers in the Mediterranean and Black Seas*. Commission for the geological map of the world, Society geologique de France. Chap. 10.
- Bowman, S.A. 2012. A Comprehensive review of the MSC facies and their origins in the offshore Sirt Basin, Libya. *Petroleum Geoscience*, **18**, 457–469.
- Buchbinder, B., & Zilberman, E. 1997. Sequence stratigraphy of the Miocene-Pliocene carbonate-siliciclastic shelf deposits in the eastern Mediterranean margin (Israel): effects of eustasy and tectonics. *Sedimentary Geology*, **112**, 7–32.
- Butler, R.W.H., McClelland, E., & Jones, R.E. 1999. Calibrating the duration and timing of the Messinian salinity crisis in the Mediterranean: linked tectonoclimatic signals in thrust-top basins of Sicily. *Journal of the Geological Society*, **156**, 827–835.

- Cartwright, J., Jackson, M., Dooley, T., & Higgins, S. 2012. Strain partitioning in gravity-driven shortening of a thick, multilayered evaporite sequence. *Geological Society, London, Special Publications*, **363**, 449–470.
- Clauzon, G., Suc, J.P., Gautier, F., Berger, A., & Loutre, M.F. 1996. Alternate interpretation of the Messinian salinity crisis: Controversy resolved? *Geology*, **24**(4), 263–366.
- Couto, D.D., Popescu, S.M., Suc, J.P., Melinte-Dobrinescu, M.C., Barhoun, N., Gorini, C., Jolivet, L., Poort, J., Jouannic, G., & Auxietre, J.L. 2014. Lago Mare and the Messinian Salinity Crisis: Evidence from the Alboran Sea (S. Spain). *Marine and Petroleum Geology*, **52**, 57–76.
- Druckman, Y., Buchbinder, B., Martinotti, G.M., Tov, R. Siman, & Aharon, P. 1995. The buried Afiq Canyon (eastern Mediterranean, Israel): a case study of a Tertiary submarine canyon exposed in Late Messinian times. *Marine Geology*, **123**, 167–185.
- Frey-Martinez, J., Cartwright, J., Hall, B., & Huuse, M. 2007. Clastic Intrusion at the Base of Deep-water Sands: A Trap-forming Mechanism in the Eastern Mediterranean. *Pages 49–63 of: Hurst, A., & Cartwright, J. (eds), Sand Injectites: Implications for Hydrocarbon Exploration and Production, AAPG Memoir*, vol. 87.
- Gardosh, M. n.d.. Review of Petroleum Systems and Hydrocarbon Plays of the Levant Margin, Offshore Israel. 573–597.
- Gardosh, M., Druckman, Y., Buchbinder, B., & Rybakov, M. 2006 (December). *The Levant Basin Offshore Israel: Stratigraphy, Structure, Tectonic Evolution and Implications for Hydrocarbon Exploration*. Prepared for the Petroleum Commissioner, Ministry of Infrastructure. Geological Survey of Israel and The Geophysical Institute of Israel.
- Gardosh, M., Druckman, Y., Buchbinder, B., & Calvo, R. 2008. *The Oligo-Miocene deepwater system of the Levant Basin*. Prepared for the Petroleum Commissioner, The Ministry of National Infrastructure. The Geophysical Institute of Israel, The Geological Survey of Israel.
- GeoconservationUK. *South Elmsall Quarry, West Yorkshire*.
- Hawie, N., Gorini, C., Deschamps, R., Nader, F.H., Montadert, L., Granjeon, D., & Baudin, F. 2013. Tectono-stratigraphic evolution of the northern Levant Basin (offshore Lebanon). *Marine and Petroleum Geology*, **48**, 392–410.

- Hsü, K.J. 1974. The Miocene Desiccation of the Mediterranean and its Climatological and Zoogeographical Implications. *Naturwissenschaften*, **61**, 137–142.
- Hsü, K.J., Cita, M.B., & Ryan, W.B.F. 1973. *The Origin of the Mediterranean Evaporite*. Vol. 13. Deep Sea Drilling Project. Chap. 43, pages 1203–1231.
- Hsü, K.J., Montadert, L., Bernoulli, D., Cita, M.B., Erickson, A., Garrison, R.E., Kidd, R.B., Mèlierès, F., Müller, C., & Wright, R. 1977. History of the Mediterranean salinity crisis. *Nature*, **267**(June), 399–403.
- Hudec, M.R., & Jackson, M.P.A. 2007. Terra infirma: Understanding salt tectonics. *Earth-Science Reviews*, **82**, 1–28.
- Kendall, A. C. 1988. *Evaporites and Hydrocarbons*. Columbia University Press. Chap. Aspects of Evaporite Basin Stratigraphy.
- Krijgsman, W., & Meijer, P.Th. 2008. Depositional environments of the Mediterranean "Lower Evaporites" of the Messinian salinity crisis: Constraints from quantitative analyses. *Marine Geology*, **253**, 73–81.
- Krijgsman, W., Hilgen, F.J., Raffi, I., Sierro, F.J., & Wilson, D.S. 1999. Chronology, causes and progression of the Messinian salinity crisis. *Nature*, **400**(August), 652–655.
- Lie, Ø., Skiple, C., & Lowrey, C. 2011. New Insight into the Levantine Basin. **8**(1), 24–27.
- Newman, Nicholas. 2013. *Levant Basin Holds Massive Energy Potential*.
- Riding, R., Braga, J.C., Martin, J.M., & Sánchez-Almazo, I.M. 1998. Mediterranean Messinian Salinity Crisis: constraints from a coeval marginal basin, Sorbas, southeastern Spain. *Marine Geology*, **146**, 1–20.
- Roberts, G., & Peace, D. 2007. Hydrocarbon plays and prospectivity of the Levantine Basin, offshore Lebanon and Syria from modern seismic data. *GeoArabia*, **12**(3), 99–124.
- Rouchy, J.M., & Caruso, A. 2006. The Messinian salinity crisis in the Mediterranean basin: A reassessment of the data and an integrated scenario. *Sedimentary Geology*, **188-189**, 35–67.
- Schwab, F.L. *Sedimentary rock - Evaporites*.
- Solem, H. B. 2013 (December). *The Messinian Salinity Crisis - Highlighting the controversies*. Unpublished.

Appendix

The Appendix contains the surface maps that are produced for horizons R4-R9. Note that the color scale is different for each map.

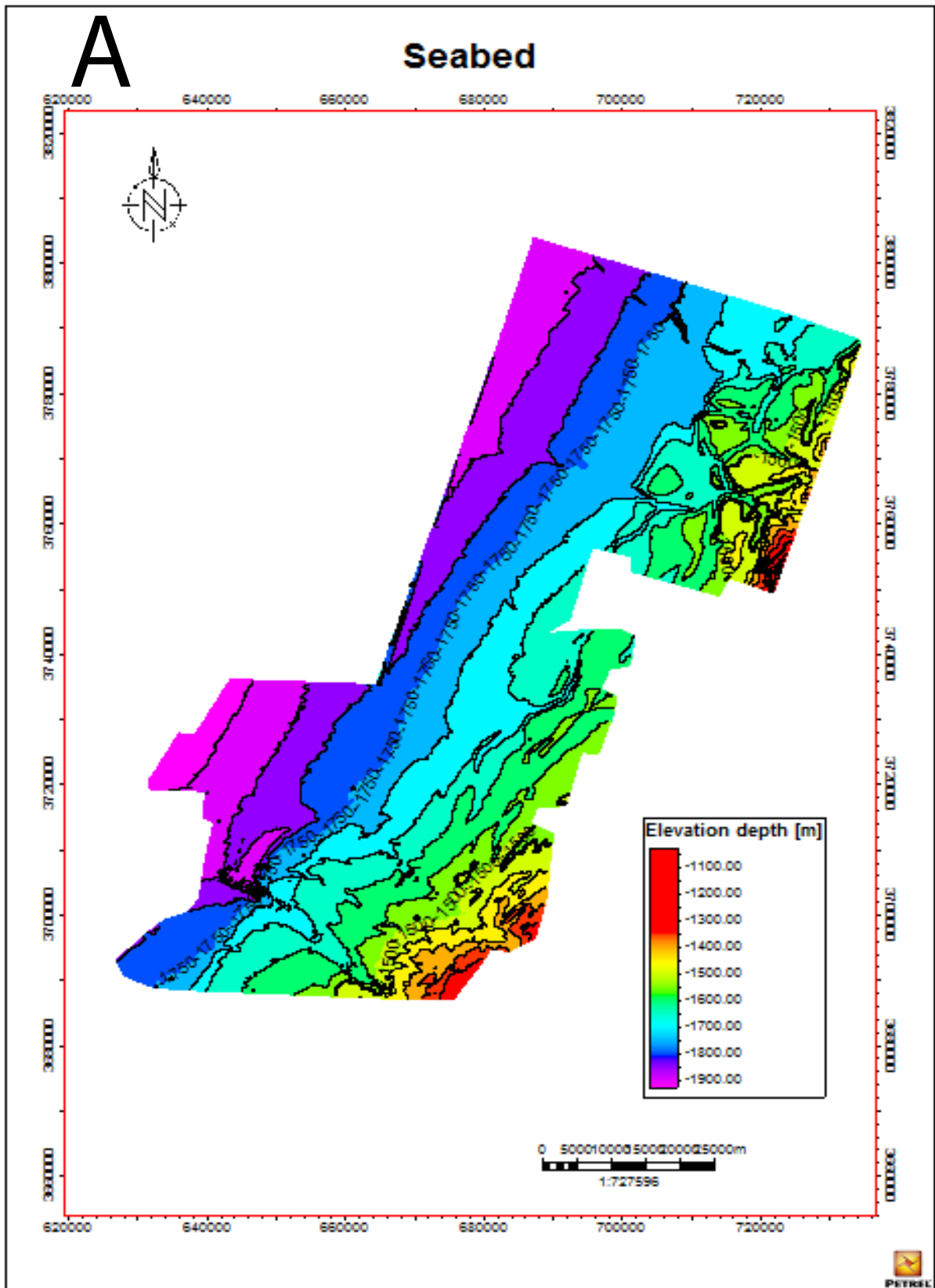


Figure 1: (A): Surface map of the seabed, horizon R9 (table 6.1).

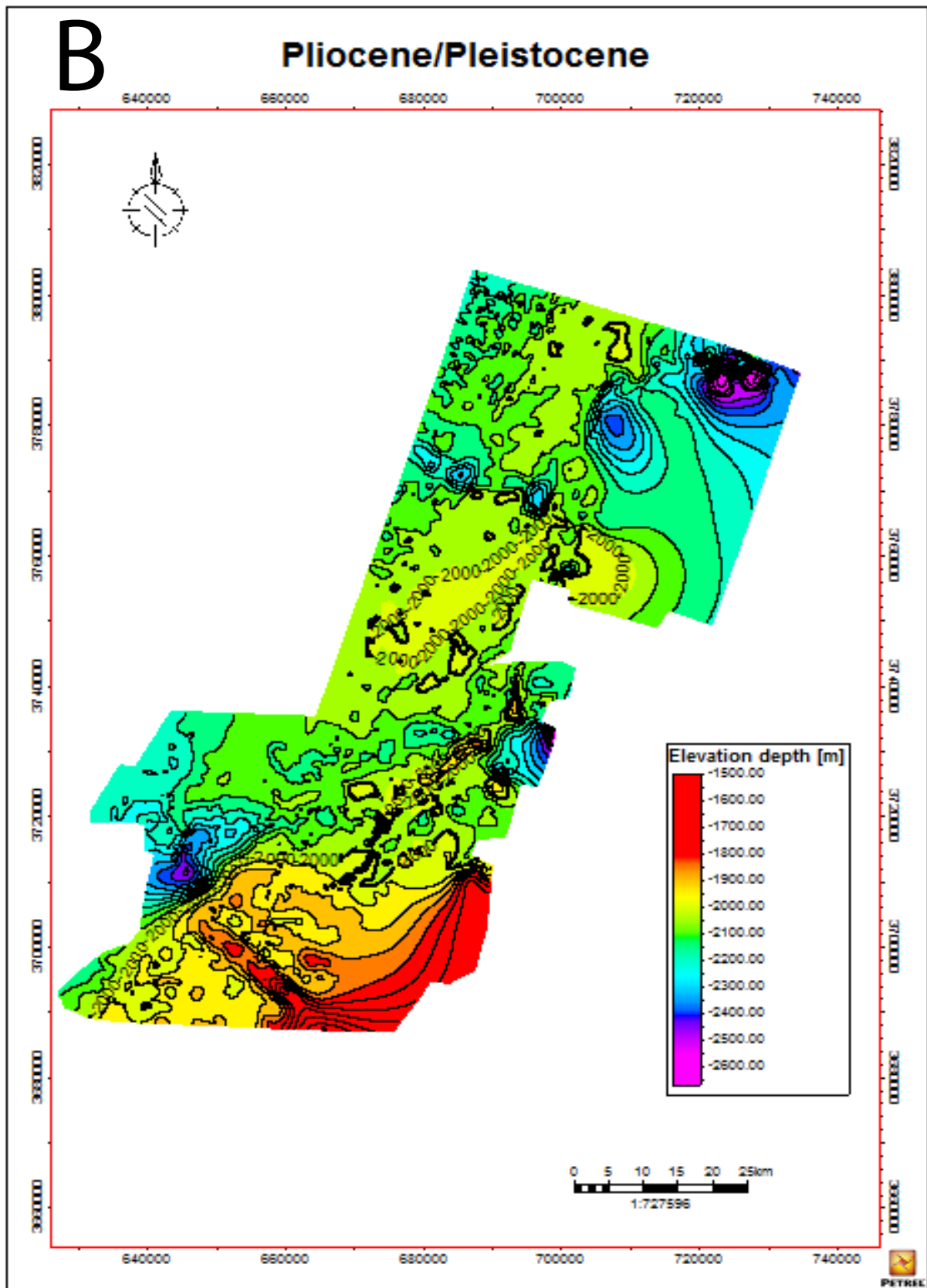


Figure 2: (B): Surface map of an interpreted horizon within the Pliocene/Pleistocene package, horizon R8 (table 6.1).

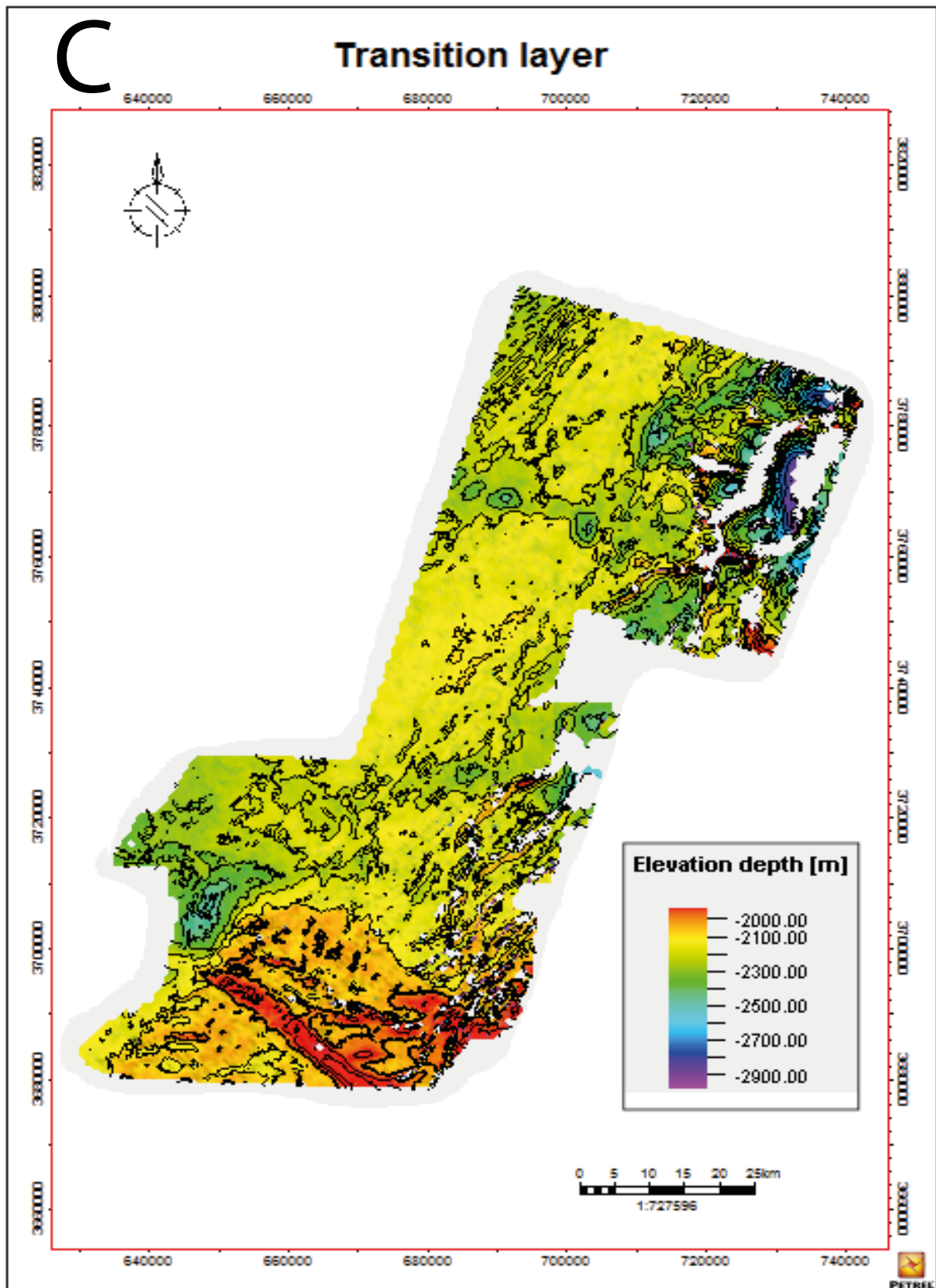


Figure 3: (C): Surface map of top Transition layer, R7 (table 6.1).

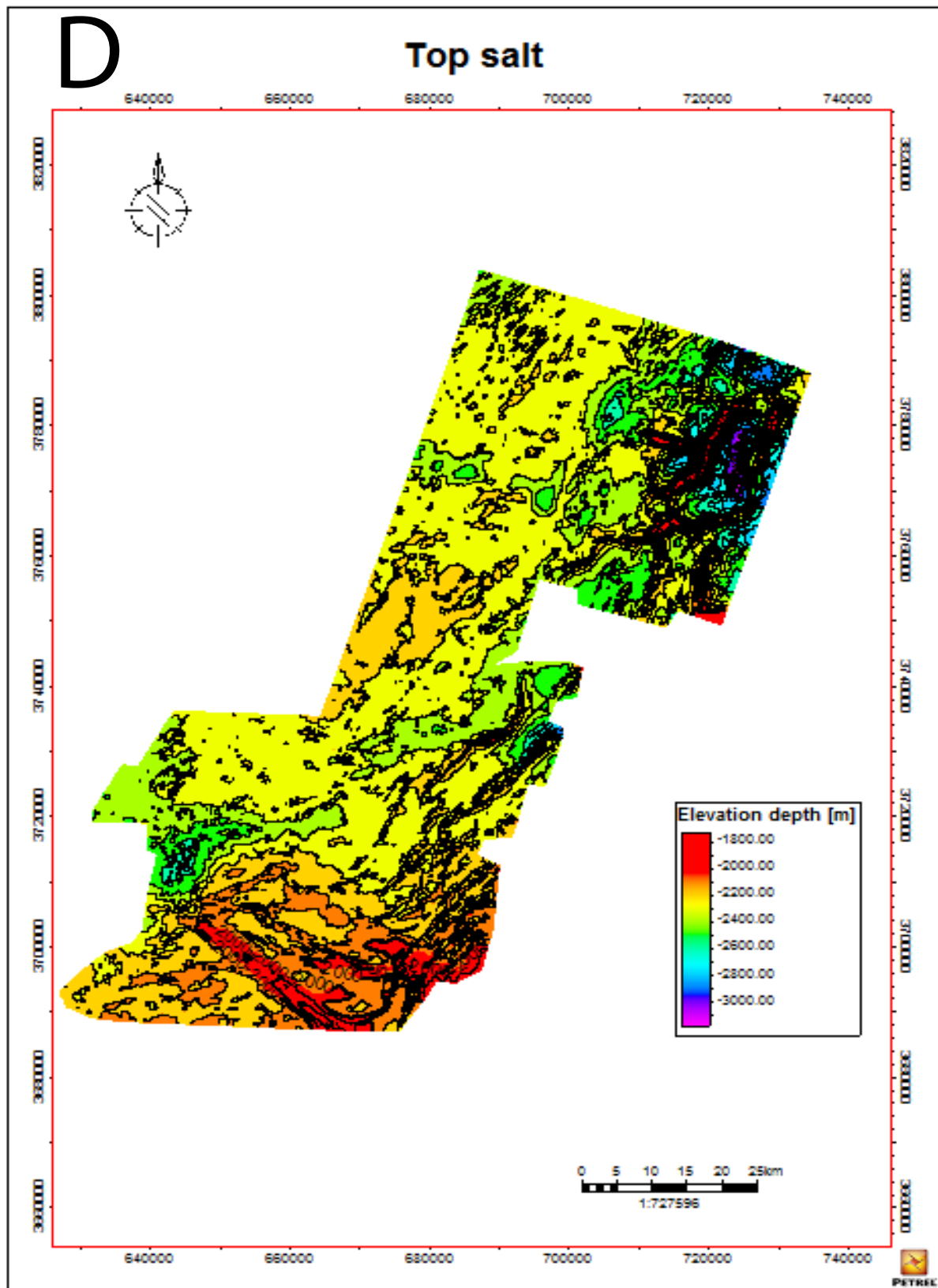


Figure 4: (D): Surface map of top Messinian evaporites, R6 (table 6.1).

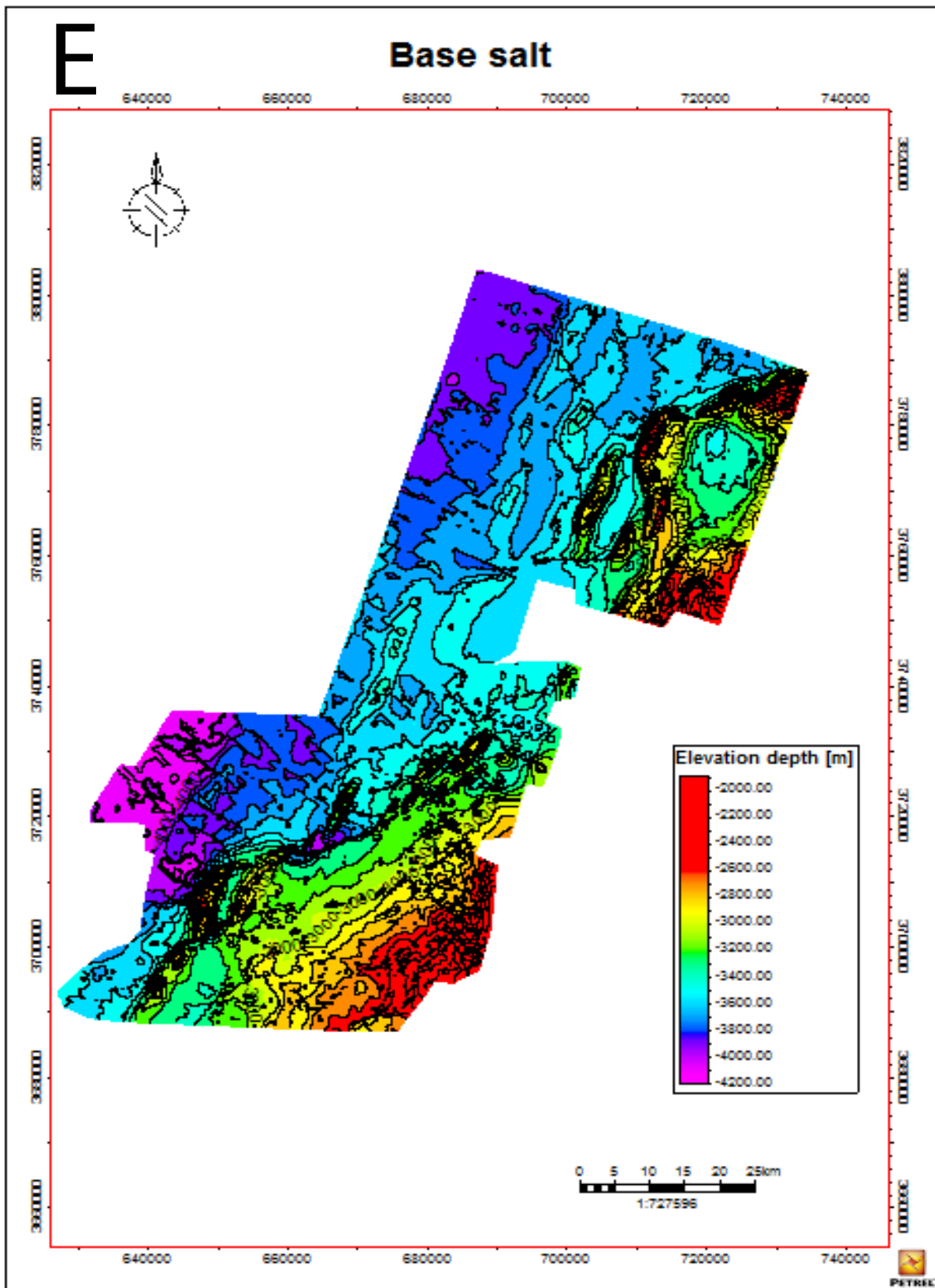


Figure 5: (E): Surface map of base Messinian evaporites, R5 (table 6.1). .

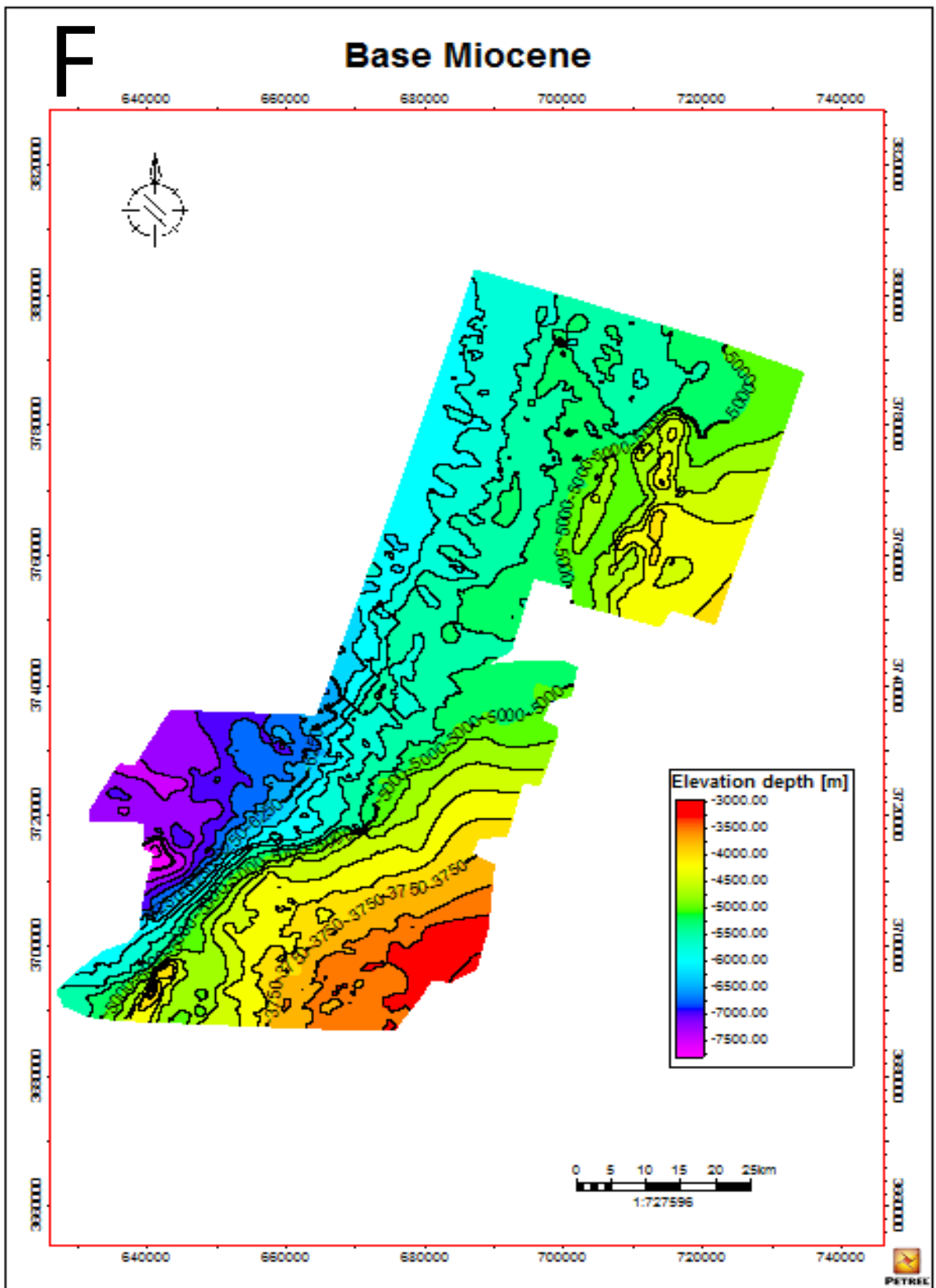


Figure 6: (F): Surface map of base Miocene, R4 (table 6.1).